Laser processing of graphene and related materials for energy storage: New horizons and prospects

Rajesh Kumar [a,b,*], Angel Pérez del Pino [c,*], Sumanta Sahoo [d], Ednan Joanni [e], Rajesh. K. Singh [f], Wai K. Tan [g], Kamal K. Kar [a], Atsunori Matsuda [b]

[a] Advanced Nanoengineering Materials Laboratory, Department of Mechanical Engineering, Indian Institute of Technology Kanpur, Kanpur 208016, UP, India

[b] Department of Electrical and Electronic Information Engineering, Toyohashi University of Technology, 1-1 Hibarigaoka, Tempaku-cho, Toyohashi, Aichi, 441-8580, Japan

[c] Institute of Materials Science of Barcelona, ICMAB-CSIC, Campus UAB, 08193 Bellaterra, Spain

[d] School of Chemical Engineering, Yeungnam University, Gyeongsan, Gyeongbuk 38541, Republic of Korea

[e] Centre for Information Technology Renato Archer (CTI), Campinas 13069-901, Brazil

[f] School of Physical and Material Sciences, Central University of Himachal Pradesh (CUHP), Kangra, Dharamshala 176215, HP, India

[g] Institute of Liberal Arts and Sciences, Toyohashi University of Technology, 1-1 Hibarigaoka, Tempaku-cho, Toyohashi, Aichi, 441-8580, Japan

---

* **Corresponding authors**
E-mail addresses: rajeshbhu1@gmail.com (R. Kumar), aperez@icmab.es (A.P. Pino)

Abstract

Laser-based methodologies for synthesis, reduction, modification and assembly of graphene-based materials are highly demanded for energy-related electrodes and devices for portable electronics. Laser technologies for graphene synthesis and modification exhibit several advantages when compared to alternative methods. They are fast, low-cost and energy saving, allowing selective heating and programmable processing, with controlled manipulation over the main experimental parameters. In this review, we summarize the most recent studies on laser-assisted synthesis of graphene-based materials, as well as their modification and application as electrodes for supercapacitor and battery applications. After a brief introduction to the physical properties of graphene and a discussion of the different types of laser processing operations, the practical uses of laser techniques for the fabrication of electrode materials are discussed in detail. Finally, the review is concluded with a brief discussion of some of the outstanding problems and possible directions for research in the area of laser-based graphene materials for energy storage devices.

Abbreviations: SCs, supercapacitors; μSCs, Micro-supercapacitors; CNTs, Carbon nanotubes; GO, Graphene oxide; rGO, Reduced graphene oxide; LrGO, Laser reduced graphene oxide; GOQDs, Graphene oxide quantum dots; GQDs, graphene quantum dots; CNTs, Carbon nanotubes; MWCNTs, Multi-walled carbon nanotubes; HOPG, Highly ordered pyrolytic graphite; MOFs, Metal organic frameworks; LCVD, Laser chemical vapor deposition; LIG, Laser-induced graphene; LSG, Laser-scribed graphene; PLD, Pulsed laser deposition; MAPLE, Matrix-assisted pulsed laser evaporation; RIMAPLE, Reactive inverse Matrix-assisted pulsed laser evaporation; LIFT, Laser-induced forward transfer; LIBT, Laser-induced backwards transfer; LIPSS, Laser induced periodic surface structures; PET, Poly(ethylene terephthalate); PVDF, Polyvinylidene fluoride; PI, Polyimide; LIP, Lithium iron phosphate

1. **Introduction**

Over the past several years, worldwide public opinion has been focused on the prevention of global warming and the promotion of renewable energy. As expected from previous experience, scientific research has closely followed global expectations [1-3]. Generally speaking, some of the main reasons for global warming are the emission of CO_2 from industries, consumption of fossil fuels in vehicles, and dumping of untreated waste in open spaces [4-7]. In order to minimize CO_2 emissions, different approaches are being pursued by different countries, such as energy substitution programs, investment in clean energy technologies, and various energy-efficiency initiatives. Clean and renewable energy sources, such as solar energy and wind power, are intrinsically intermittent. Since these energy sources cannot be activated on demand, and they may not be available when needed, they must rely on energy storage devices for achieving full time availability [8-11]. On the other hand, with the rapid growth of portable electronics and electric vehicles, the demand for high-performance energy storage devices with high energy and power densities, as well as long term cycling stability is becoming more and more pressing [12-14].

Among the electrochemical energy storage devices, supercapacitors (SCs)/ micro-supercapacitors (µSCs) and batteries have received much attention owing to their charge/discharge rates, power and energy densities, eco-friendly nature and long term cycling stability [15, 16]. In their present development stages, SCs can deliver high power densities, but their energy densities are usually not satisfactory, whereas batteries can deliver high energy densities, but normally suffer from low power densities [17, 18]. The limitations of these charge storage devices are highly dependent on the properties of their electrode materials, such as their conductivity, active specific surface area and porosity.

Recently, carbon-based materials with different structures and morphologies, obtained through various synthesis approaches, have been applied in electrodes for energy-related devices [19-22]. Among several other candidates for SC and battery electrodes, carbon materials are frequently chosen due to their low production cost, high specific surface area, wide working potential window, good chemical stability and electrical conductivity [23-25]. In hybrid electrodes, carbon materials provide a conductive framework, helping to avoid the agglomeration of metal oxides loaded on their surface [26]. Examples of carbon-based materials successfully applied in energy-related devices are carbon nanotubes (CNTs) [27, 28], carbon spheres [29, 30], carbon nanofibers [31], hollow carbon spheres [32, 33], hollow carbon nanorods [34, 35], and porous carbon [36-38].

3

Among the carbon materials, graphene has been widely studied due to its exceptional properties, such as high surface area, intrinsic mobility, Young's modulus, electrical conductivity and thermal conductivity [39-42]. Also, graphene oxide (GO), reduced graphene oxide (rGO), graphene hydrogel, graphene aerogel, graphene quantum dots (GQDs), GO quantum dots (GOQDs), and doped graphene, which are graphene derivatives, are highly demanded for electrodes, especially due to their favorable electrochemical properties, high surface area, light weight, and a wide range of electrical conductivity values [43-45]. Graphene-based materials have demonstrated enough outstanding properties at the laboratory scale to be considered crucial in future technologies, acting as either primary components or additives [46, 47]. Many applications such as environmental, structural, electrical and optoelectronic technologies, and particularly energy storage, are revealing substantial progress with the use of graphene-based materials, being close to production levels in many cases [48-51]. As expected from the variety of materials and morphologies, several methods have already been reported for synthesizing graphene and its derivatives for application in energy storage devices [52, 53]. Among the synthetic approaches, laser irradiation is one of the most powerful tools for controllably providing the designed materials and even full device electrodes in a single, fast, flexible, scalable, and energy efficient process. Furthermore, laser processing can be applied to flexible substrates, preserving their structural integrity, something which is not possible (or very difficult) when using other synthesis routes [54].

During laser processing, the material is suddenly exposed to high levels of concentrated energy. The electrons from the material that absorb the incident photons become excited, interacting through complex dynamics with the atomic lattice in a characteristic timescale. Depending on the nature of the radiation and the electronic relaxation time, the irradiated material can assume conditions out of electronic and thermodynamic equilibrium, leading to the creation of heat waves that can be localized in space and time, thus triggering homogeneous and heterogeneous reactions that can be activated by photochemical interactions (photolytic reactions) and/or photothermal mechanisms [55, 56]. In this manner, laser irradiated materials can be selectively heated to extreme temperatures, and may experience heating and cooling rates in the range of 10^6-10^{12} °C s^{-1}, which are orders of magnitude higher than the rates of conventional systems. Some emerging techniques with great promise are the laser-induced ultrafast growth and assembly of different types of functional nanomaterials [57-65] and the laser-based printing of nanomaterials, circuits and micro-devices for the fabrication of highly-

4

integrated flexible electronics [66-69]. Furthermore, laser radiation is also ideal for micro/nanofabrication of structures and devices by selective photo-induced chemical reactions, heating, melting or ablation mechanisms [70-75].

In this article, we review the state of the art regarding the application of laser technology to the synthesis and modification of graphene-based materials for use in electrodes of energy storage devices. After a brief introduction, and a summary of the thermal and optical characteristics of graphene and GO, we discuss the effects of the main laser processing parameters and the various laser processes that have been applied for synthesis and modification of graphene and related materials. In the remaining text we discuss some of the recent, most promising research on energy storage device electrodes obtained with the help of laser processing. We conclude the review with a discussion of the more pressing challenges and opportunities for laser technology in the fields of graphene processing and energy device fabrication.

The image in **Fig. 1** shows a schematic representation of the various approaches for laser synthesis and modification of graphene and related materials, as well as the main processing parameters. For a given energy storage device (supercapacitor or battery), once the fabrication technique is selected, the process is optimized by changing the laser and processing parameters. More than one type of laser processing method can be applied in the device fabrication sequence.
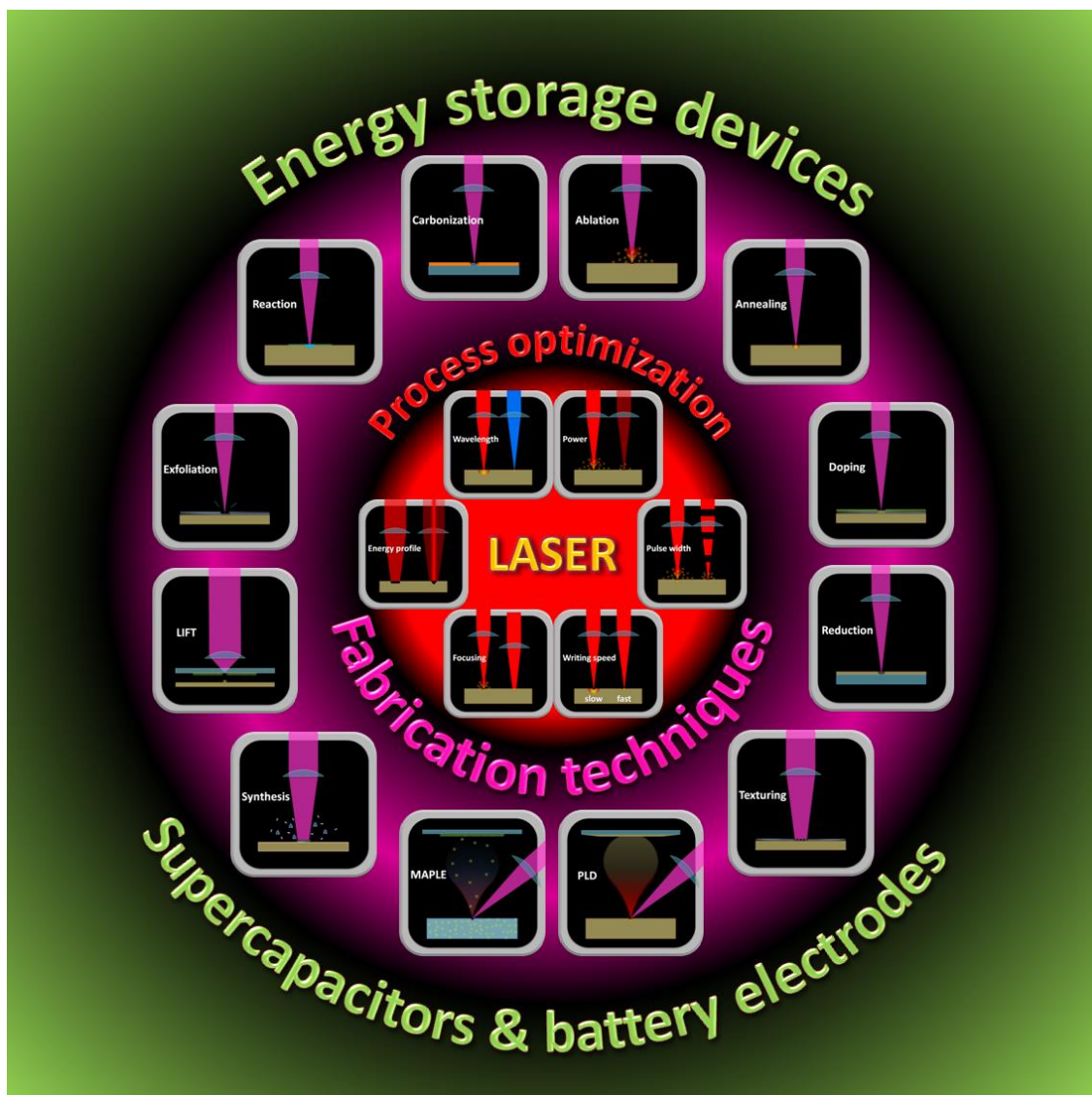
Fig. 1. Schematic representation of laser irradiation-assisted methods for synthesis and modification of graphene materials and their application as electrodes in supercapacitor devices and batteries.

2. Graphene and graphene oxide: Optical and thermal properties

Single layer graphene exhibits less than 0.1% reflectance in the visible region, increasing to approximately 2% for ten layer flakes [76, 77]. Despite its one-atom layer thickness, the optical absorption is about 2.3% over the visible spectrum, increasing proportionally to the number of layers. The absorption spectrum of graphene is actually quite smooth over a wider wavelength range (300 - 2500 nm), with an absorption peak near 270 nm from the π-π* interband transition of conjugated electrons [78]. In few-layer graphene sheets, additional absorption bands appear at lower energies, caused by Van Hove singularities in the density of states and interband coupling [79, 80]. Moderate doping of graphene with either N or B does not significantly affect its absorption spectrum, though

highly co-doped (B/N) graphene exhibits a significant red shift in the absorption bands [81]. It should be noticed that the dissociation energy of the C=C sp^2 bonds is 6.4 eV, corresponding to the wavelength of 195 nm [82]. Hence, illumination of graphene with more energetic photons may induce its extensive decomposition through photolytic processes. Carbon atoms located in structural defects, having lower dissociation energies, may undergo photoinduced chemical reactions even when irradiated with larger wavelength light. GO can be regarded as a graphene sheet decorated with a large number of disordered nanoregions with oxygen-containing functional groups (epoxide, hydroxide, carbonyl, carboxyl…), in addition to impurities (from chemical synthesis) and crystalline defects [83, 84]. Accordingly, the optical properties of GO show different features when compared to those of graphene. Smirnov *et al.* studied the photoreduction of GO during UV illumination and observed the evolution of absorption in GO films and aqueous dispersions during the reduction process [85]. The spectrum of GO reveals a monotonic increase of absorbance with photon energy, showing high absorption in the UV region. As the photoreduction of GO proceeds, an increase of absorption in the 285-400 nm wavelength range takes place, until the characteristic absorbance of graphite is reached.

The thermal properties of graphene-based materials are also remarkable. Single layer graphene displays high thermal conductivity (up to ~ 5000 WmK^{-1}), a specific heat similar to that of graphite, and a very high melting temperature of about 4500-5000 K [86-90]. The case of GO is more complex, due to its variable and disordered constitution, besides its chemical reactivity. When heated, deoxygenation processes take place, leading to the formation of different carbon structures and structural defects, depending on the particular chemical path followed [91-93]. The evolution of chemical composition and structural defects can be quantitatively studied through X-ray photoelectron and Raman spectroscopies [94, 95]. Thus, the thermal properties of GO would depend on its original composition and structural configuration. For instance, when compared to graphene, the presence of oxygen chemical groups and crystalline defects in GO significantly reduce its thermal conductivity by means of phonon scattering, though the conductivity increases with the degree of GO reduction [96-98]. It should be pointed out that the number of layers and the amount of defects markedly influence the thermophysical properties of graphene materials [99-102]. Besides, comparable thermal properties are also found in other graphitic nanocarbon materials, such as CNTs [99, 103].
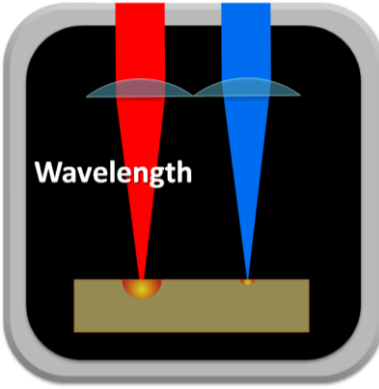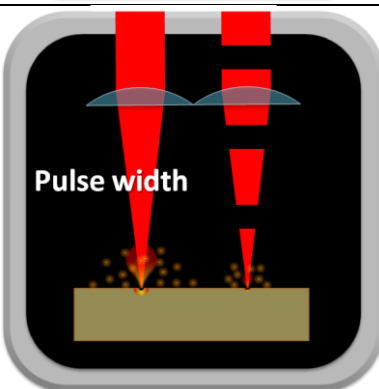
3. Laser treatments

The outcome of any laser treatment, besides being dependent on the properties of the material itself, is strongly determined by the characteristics of the laser, the optical components, the whole system setup and the immediate environment where the treatment is performed [54]. This suggests the need to control a series of experimental conditions. On the other hand, it provides a rich experimental field for synthesis and modification of materials.
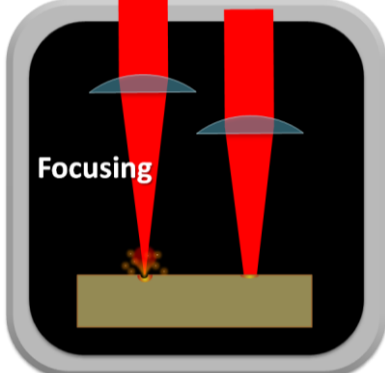
From the point of view of materials science, the laser-matter interaction, when exploited to its full potential, is an extremely attractive approach for synthesis and modification of materials. It can provide very fast, very clean and flexible processing; localized treatments with full control (over a wide range) of both the energy transferred to the material and the time elapsed in the interaction. Under the proper conditions, computer-controlled laser treatments can even be applied for direct device building, including the possibility of fast roll-to-roll processing.

3.1. Laser and processing parameters

The application of laser irradiation to the synthesis and modification of graphene and related materials has been the focus of two recent reviews [54, 104]. The processing parameters affecting the results of laser treatments have already been discussed in detail in those publications. The main variables are the laser wavelength, the laser power, the duration of the laser pulses, the fluence (energy/surface area), the energy profile of the laser beam, the degree of focusing, and the writing speed. **Table 1** summarizes the essential points, especially for the readers without previous experience with laser processing. A more detailed discussion can be found in previous study [54].

Table 1. Main experimental variables for laser processing and their effect on the final results obtained with the treatments.

Process Variable	Effects on Laser Treatment
Wavelength	The smaller the laser wavelength, the smaller the laser penetration in the material The smaller the laser wavelength, the better the beam can be focused (smaller spot size) For longer laser wavelengths, heating (thermochemical effect) is predominant, while for shorter wavelengths, bond breaking (photochemical effect) may prevail, depending on the material
Power	The higher the laser power, the larger the amount of energy transferred to the material (higher temperature) Most lasers operate at constant pulse energy, so the power is actually modified by changing pulse frequency Changing the pulse frequency of a laser beam scanning the sample also changes the spot overlap of consecutive laser pulses
Pulse width	The smaller the laser pulse width, the smaller the heat-affected zone around the treated region Determined by laser choice, since most lasers operate with nearly constant pulse widths Ultra-short pulses (in the fs range) concentrate high energy and may induce non-linear processes in the material, enabling cleaner ablation results
Energy profile	The more uniform the beam energy profile, the more uniform the result of the laser treatment applied to the material Most lasers types have a beam with a Gaussian profile, where the energy decreases towards the borders of the laser spot The energy profile can be "flattened" with pinholes or combinations of optical elements, but Gaussian profiles can also be exploited to "write" features smaller than the actual laser spot size

Focusing	Beam focusing is used for controlling the laser spot size, which determines the minimum feature size for the treatment
	The higher the degree of focusing, the higher the laser fluence (energy/spot area)
	Laser fluence is one of the most important parameters for controlling and comparing different processes
Writing speed slow fast	Writing speed has a direct effect on spot overlap. If we consider a combination of fluence and overlap, we can make an analogy with ionizing radiation and the effect of cumulative doses
	The lower the writing speed, the higher the "dose" of laser irradiation provided to a region of the material
	The laser "dose" provided during the treatment can be controlled by changing laser power or writing speed

3.2. Laser treatment of graphene and related materials

Taking into account the laser characteristics and processing parameters already discussed, many types of laser treatment operations can be performed, depending on the configuration of the system and the optical components. **Table 2** summarizes the main processes which can be carried out for synthesis and modification of materials, fabrication of components and, in some cases, even "direct writing" of working devices.

3.2.1. Treatments based on laser-activated reactions

Restricting the discussion of laser processing methods to the materials and devices in the scope of this review, a good starting point is the laser synthesis of graphene from carbon-containing substances. The highly confined nature of laser treatments allows localized graphene formation according to pre-defined patterns. The laser chemical vapor deposition (LCVD) process, based on small hydrocarbon molecules, is the most obvious example of laser-assisted graphene synthesis, although the method has also been performed using liquid and solid precursors [105-109]. The high cost and hazardous nature of some precursors are problems yet to be solved for this technology. Alternative methods based on the catalyst-assisted laser formation of graphene materials are being developed, showing new ways for avoiding such drawbacks [110, 111].

Some thermally activated chemical reactions taking place under extreme conditions can be triggered on the surface of nanocarbon materials. As an example, the growth of inorganic nanostructures on CNT and rGO surfaces by direct laser irradiation of nanocarbon mixed with other precursors has been reported, leading to the formation of hybrid materials [112-117]. The laser-induced creation of structural defects and open-ended carbon atoms has allowed the nanowelding of graphene sheets to gold metal contacts at laser fluences below the ablation threshold of graphene [118]. After subsequent thermal annealing, graphene-metal junctions with ultra-low contact resistance were obtained in a precise manner, enabling a substantial performance enhancement in suspended graphene photodetectos. Graphene has been selectively fluorinated by laser irradiation of fluoropolymer-covered graphene [119]. The fluorine radicals generated by decomposition of the polymer in the laser-treated region reacts with the sp^2-hybrized carbon, and $C-F$ bond formation leads to a dramatic increase in the resistance of graphene, while avoiding degradation of the carbon network.

Laser reduction of GO has become one of the most popular techniques for the fabrication of graphene-based materials and devices. GO can experience loss of oxygen-containing groups when exposed to laser radiation, leading to the formation of rGO [85, 120, 121]. Laser reduced GO (LrGO) can be easily obtained using different types of lasers and system setups [103, 122-125]. Excluding multiphoton absorption, GO can only be photochemically reduced by photons having energies larger than 3.2 eV, otherwise the deoxygenation reactions are triggered by photothermal mechanisms. The results of the laser-induced reduction are strongly dependent on the initial composition of GO, the characteristics of the laser radiation, and the composition and reactivity of the environment. This complex scenario leads to a great phenomenology and has generated an interesting debate over process mechanisms and reduction pathways [126]. Due to the partial restoration of the graphene network during GO reduction, the highly insulating p-type semiconductor turns into a highly conductive material [127, 128]. Enhanced structural healing has been reported in laser-reduced GO [129]. The authors observed a markedly lower electric resistivity, when compared with materials obtained by chemical and thermal routes. One area attracting particular interest in the last few years is the manufacture of flexible devices based on LrGO. Examples include various chemical, humidity and strain sensors as well as electrical circuit boards for healthcare portable electronics [130-134]. Different approaches have been reported for limiting the exposure

11

to oxygen atoms from air during LrGO synthesis, with the intent of avoiding undue combustion. Examples are the laser irradiation of GO under inert/vacuum conditions or its confinement between transparent slices [124, 135, 136]. On the other hand, there are numerous reports of laser-induced reduction of GO in air without significant carbon loss [127, 128]. Self-standing LrGO films can be fabricated by laser irradiation of GO membranes or even GO flakes contained in liquids. For instance, Shi et al. developed humidity sensors by irradiation of self-assembled GO sheets on the surface of liquids [122]. The fabricated porous LrGO films exhibited significant changes in electrical resistance with humidity.

Carbonization, the process used in the method developed by Tour and his co-workers for laser graphitization of polymers, has turned into a highly valued technique for fabrication of flexible devices based on graphene-like materials. The LIG, due to its facile, single-step, fast and cost-effective nature, has proved to be very adaptable and well suited for the fabrication of many types of devices [137]. LIG comprehends a family of 3D porous materials exhibiting high surface area, high thermal stability, and remarkable conductivity. In the first reported studies, LIG was synthesized by processing commercial films of polyimide (PI) and polyetherimide, which contain aromatic and imide repeating units, using a CO_2 infrared laser in ambient air [138, 139]. Indeed, this particular method is still used for the development of innovative materials and devices, often in combination with other techniques [140]. However, subsequent research proved that LIG could also be obtained by irradiating a great variety of materials with different types of laser sources, from IR to UV radiation. For instance, LIG has been successfully obtained by laser processing of different types of polymers, resins, as well as natural materials, such, wood, cotton fabrics, paper, and even foods and waste materials [141-144]. Of technological relevance is the fact that LIG morphology can be adjusted by choosing different laser parameters, by modifying the environment where the treatment is performed, or through changes in the structure or composition of the target material [145-149]. Porous LIG membranes have shown notable performance in a variety of applications, such as in the separation of liquid phases based on polarity, antifouling and antibacterial action in water purification, as well as Joule heating [150-152]. LIG is also revealing a great potential for application in resistive sensors. Stanford *et al*. used a 405 nm low power laser to convert PI into LIG features with micrometric resolution, enabling the fabrication of a flexible humidity sensor that could detect human breath with a response time of 250 ms [153]. Carvalho *et al*. developed electromechanical strain sensors through UV laser irradiation

of PI [144]. In this way, a low-cost arterial pulse monitor was assembled, revealing sensitive response. The use of shorter radiation wavelength allowed higher spatial resolution when compared to IR treatments, enabling device miniaturization. Yang *et al.* implemented an innovative approach for the fabrication of smart structural components with self-monitoring ability by combining 3D printing and laser carbonization technologies [154]. Structural components were fabricated through fused deposition modelling using polyetheretherketone filaments. The parts were subsequently processed by a CO_2 laser for surface patterning of sensors that were used to self-monitor the deformation (bending and stretching) of the fabricated components. Energy applications have also benefited from the introduction of LIG technology. Triboelectric nanogenerators incorporating LIG electrodes [155], and fuel cells with proton exchanging membranes using LIG loaded with platinum catalyst [156] are some of the examples of LIG in energy conversion devices. However, the most studied applications based on LIG are in the area of energy storage.

Direct functionalization of graphene (doping) is something very hard to achieve, since the material exhibits great chemical stability [157]. Nevertheless, laser treatments have been recently used for the synthesis of N-doped GQDs with enhanced optical properties [158]. In this work, graphite flakes were laser ablated while immersed in ethanol and diethylenetriamine solutions, obtaining CQDs functionalized with pyridinic, pyrrolic, and graphitic nitrogen. N-doped GQDs have also been synthesized from carbon nano-onions ablated in aqueous solutions containing ammonia, ethylenediamine and pyridine compounds [159]. In view of its versatility and low cost, the laser treatment of carbon sources in reactive environments is foreseen as a valuable methodology for obtaining a wide variety of doped graphene derivatives. As a matter of fact, doping of graphene materials is usually achieved in an easier and more convenient way as a secondary process taking place during the laser reduction of GO [83, 160]. Most studies on laser functionalization of rGO refer to nitrogen doping, since this is a good method for tuning the electron transport and electrochemical properties of graphene materials [161-164]. GO thin films or dispersed flakes irradiated with a laser in either gaseous or liquid environments with N-containing molecules undergo simultaneous reduction and N-doping [165-167]. Enhanced functionality has also been obtained by the simultaneous reduction and N-doping of GO through laser processing of films composed of mixtures of GO sheets and metal or metal oxide nanoparticles [116, 168]. In these cases, the N-rGO sheets become decorated with electronically active metal or metal oxide

nanostructures, leading to hybrid materials. Ingenious strategies have also been demonstrated for the synthesis of doped LIG designed for specific applications. Apart from the possibility to vary the dopant concentration of LIG by manipulation of the lasing parameters [138, 146], doping can also be accomplished by irradiating compositionally modified substrates or by performing the process in chemically reactive environments [147]. For instance, S-doped porous LIG has been fabricated by irradiation of polysulfone, poly(ethersulfone) and polyphenylsulfone polymers, resulting in conformal graphene embedded in the polymer substrates [169]. The obtained materials exhibited good electrocatalytic hydrogen peroxide generation, besides remarkable antifouling and antimicrobial activity. Additionally, S- and N-doped graphene patterns were laser written on different substrates by photochemical decomposition of an organic polybenzimidazole ink [170]. The use of a picosecond pulsed UV laser source reduced the heat load on the substrates, allowing the fast fabrication of highly conductive and adherent LIG tracks on glass, as well as on thermally sensitive PET substrates. The synthesis of LIG-based composites containing inorganic nanostructures that synergistically combine their functional properties represents a significant advance. Accordingly, LIG containing Ag, Pt and Au NPs has been obtained through a single-step laser processing of PI films coated with metal precursor hydrogel inks [171]. Electrochemical devices based on the resulting materials (porous 3D LIG decorated with a dense and uniform distribution of metal NPs) showed excellent performance as immunosensors. In a similar way, LIG with embedded Ag NPs was directly obtained by laser processing of $AgNO_3$–dispersed polyethersulfone polymer substrates [172]. Photoanodes composed of LIG containing CdS and PbS NPs have been obtained on ITO-glass substrates by CO_2 laser irradiation of polyethersulfone films containing metal-complexes [173]. In this case, polyethersulfone provides not only the carbon for LIG growth, but also the sulphur that reacts with Cd and Pb for creating the metal sulphide NPs.

3.2.2. Treatments based on laser ablation

Besides heating, the extreme thermodynamic conditions driven by intense laser radiation can provoke ablation processes in carbon materials [174-177]. Selective ablation provides a powerful tool for high-resolution (sub-micron scale) subtractive patterning of graphene-based layers in a rapid and versatile way [178-184]. Graphene-based films, even with micrometric thicknesses, can be laser-patterned for the fabrication of electrode structures that can be used in a wide variety of apparatus, such as microheaters, thermal sensors,

and thermostatic devices [185]. For obtaining accurate ablation, with minimal impact on the substrate or any underlying layers, femtosecond laser patterning has proved to be more appropriate than processing using longer laser pulses. This is a consequence of the reduced thermal diffusion and more efficient ablation process due to the incidence of laser energy in a restricted volume triggering photochemical processes (multiphoton absorption, direct photodissociation of atomic bonds, etc.) [186-188]. The presence of graphene wrinkles increases the ablation probability due to the concomitant reduction of electrical and thermal conductivities leading to increased energy accumulation [189]. Studies on femtosecond laser patterning of graphene electrodes for thin-film transistors showed that the quality of the patterned electrodes was enhanced by ablation in vacuum conditions due to debris reduction [190]. Femtosecond laser ablation has been adopted by Maurice *et al.* for obtaining nanogaps in monolayer graphene, opening a promising path for development of graphene-based nanogap systems for molecular electronics, memories and nanodevices [191]. Laser treatments performed under conditions slightly above the ablation threshold have been used for accurate laser-induced thinning of multilayer graphene, enabling precise control over the number of stacked sheets (up to single layers) [192, 193]. Ablation processes can also be conducted in liquid media for obtaining graphene-based materials. Bilayer and few-layer graphene nanowalls and carbon NPs have been achieved by laser ablation of graphite targets immersed in liquids such as water and dimethylformamide [194-196]. GQDs have also been synthesized by pulsed laser ablation of carbon nano-onions immersed in distilled water [197]. The obtained GQDs show smaller sizes and blue shifted absorbance and emissive properties when compared to GQDs synthesized by other methods. Interestingly, Kang et al. demonstrated that pulsed laser treatment of graphite flakes dispersed in ethanol combined with high-power sonication leads to the formation of GQDs, whereas in the absence of sonication, the laser treatment generates oxygen-rich GOQDs [198].

When the ablation process is a result of high power pulsed laser irradiation, the ejected material can be deposited in a substrate facing the irradiated target. This process, which gradually forms a thin film layer on the substrate, is fittingly named pulsed laser deposition (PLD). The ablated material exhibits high kinetic energy (up to a few keV) and its high mobility allows growing adherent films with high crystallinity. Though high vacuum is necessary, the method is theoretically simple, flexible, fast, and allows good control over morphology and thickness. The PLD growth of graphene onto different types of substrates has been accomplished by ablation of pyrolytic carbon, graphite and HOPG

targets (with or without metal catalysts) [199, 200]. Mostly, few-layer and multi-layer graphene deposits have been obtained, though single layers and bilayers have also been recently reported [201-203]. Different laser sources (excimer lasers, Nd:YAG, CO_2) have been used, and the substrate is typically maintained at RT or a few hundred degrees during deposition. One of the more interesting characteristics of the PLD method is the possibility to perform the depositions under a controlled atmosphere (pressure and composition), opening the possibility for reactive depositions. As an example, the growth of N-doped graphene thin film layers was achieved by PLD in the presence of N_2 gas during the deposition process [204]. Pyridinic and pyrrolic N-doping groups were observed in the graphene structure and the nitrogen content could be controlled by adjusting the N_2 gas pressure. Juvaid et al. have recently reported the PLD growth of wafer-scale p-type rGO with superior optical and electrical properties by UV laser ablation of glassy carbon targets in an oxidizing environment (O_2 + Ar) [205]. Uniform thin films with ultra-smooth surfaces were obtained, exhibiting high optical transmittance, low refractive index and low sheet resistance.

The matrix-assisted pulsed laser evaporation (MAPLE) is a technique for carrying out the controlled deposition of graphene materials using frozen dispersions of nanocarbon entities. The methodology is very similar to PLD, and the laser radiation can be either absorbed directly by the frozen solvent (matrix) or by the carbon nanoentities (inverse MAPLE) leading to the explosive boiling of the matrix in a rapid and energetic way. The generated vapor carries the nanoentities towards a facing substrate leading to the deposition of nanocarbon films. Thin coatings of single wall CNTs functionalized with carboxylic groups, as well as multiwall CNTs (MWCNTs) and GO sheets have been deposited in a controlled way by MAPLE [206-208]. The transferred CNTs maintained their structure, exhibiting low amount of laser-induced defects when irradiated with moderate laser fluences, whereas the GO sheets underwent reduction processes and even N-doping during the deposition in N_2 gas ambient. Furthermore, hybrid thin films constituted by rGO decorated with metal and transition metal oxide nanostructures have also been fabricated through irradiation of frozen dispersions containing GO flakes, NPs and even precursors for attaining the N-doping of rGO [116, 209-212].

Laser-induced forward transfer (LIFT) is another direct-writing technique based on ablation, where the action of a laser is used to transfer material from thin donor layers onto arbitrary substrates [213]. The donor layer must be on a transparent substrate, placed in close proximity to the receiving substrate. Solid donor films have been used since the

origins of the method [214], but the same operating principle works for liquid films and mixtures [215]. LIFT is a versatile means for direct printing of devices using functional materials. It can be seen as a nozzle-free printing technique with almost no restrictions in the particle size, composition and viscosity of the ink to be printed [216]. Depending on the material to be transferred, a sacrificial release layer may be deposited on the transparent substrate before the layer to be printed. This release layer is either a polymer with high absorption at the laser wavelength (vaporized upon irradiation) or a metal film which is locally deformed (blistered), impelling the overlying film [217]. LIFT processing has proven to be well suited for writing graphene patterns and, in some cases, even full carbon-based working devices [218-221].
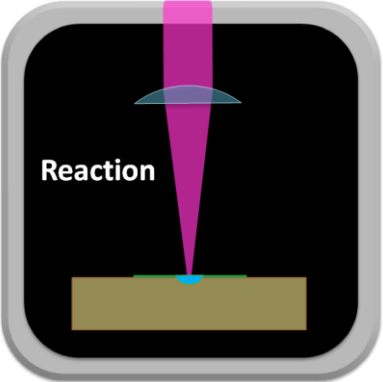
3.2.3. Other laser treatments

Laser exfoliation is an interesting alternative for obtaining few-layer graphene deposits. The technique can be performed at room temperature without the need for metal catalysts. The resulting materials display some advantages when compared to CVD-synthesized graphene, since the method is clean, fast, and the deposits are free from contamination. Qian *et al*. studied the laser exfoliation of highly ordered pyrolytic graphite (HOPG) in 1 Torr Ar using a Nd:YAG pulsed laser at different laser fluences and distances between the target and the collecting substrate [222]. Three different phases, amorphous carbon, few-layer graphene sheets and thin graphite films were deposited as the laser fluence increased, while the target-substrate distance did not have a significant effect on the results. Graphene sheets a few nanometers thick and tens of micrometers in size were obtained at intermediate fluences. Under the same processing conditions, amorphous carbon was the only product of the deposition when compressed graphite tablets were used instead of HOPG. Few-layer graphene deposits have also been obtained by performing the laser exfoliation with the graphite target immersed in water or in liquid nitrogen [223, 224]. Laser exfoliation, like other exfoliation methods, can be enhanced by previous intercalation of compounds which are easily vaporized upon heating. As an example, Carotenuto and co-workers investigated the sulfuric acid-intercalated graphite exfoliation process using a simple technique based on the continuous-wave infrared laser irradiation of graphite flakes [225]. The threshold temperature for the process was found to be about 140 °C, with the fast heating causing the sudden volatilization of the intercalate species on a time scale of the order of 0.2 s.
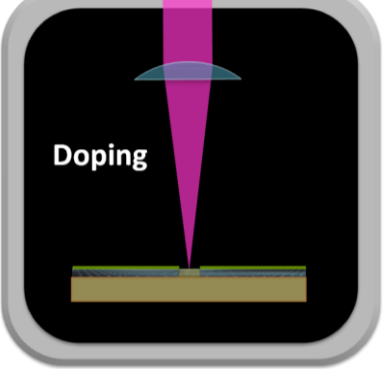
Localized laser radiation can generate very intense heating (or trigger photochemical processes) which can drive mechanisms promoting atomic mobility, creation of defects and, ultimately, the structural modification of materials. Laser texturing, one of the possible outcomes of these processes, has enabled the development of new fabrication strategies. For instance, the formation of laser induced periodic surface structures (LIPSS) in graphene under the effect of ultrafast laser irradiation has been reported by Beltaos et al. [226]. The creation of these nano-scaled "surface ripples" has been attributed to the interference between the incident femtosecond laser beam and the excited surface plasmon polariton in graphene, leading to a periodic spatial energy distribution and subsequent structural transformation of the graphene layer. In this way, high resolution patterning of graphene, exhibiting nanostructures smaller than the laser wavelength could be obtained. LIPSS has also been reported after excimer laser irradiation of polystyrene - graphene composites [227], increasing the prospects for laser structuring of complex graphene-containing materials. High-resolution patterning over large areas can be attained by two-beam laser interference. In this way, periodic patterns composed of micro/nano structures are formed where the accumulated laser energy exceeds the material conversion threshold. An application of particular interest is the simultaneous reduction and structural patterning of GO layers for the fabrication of hierarchical nanostructures over large areas, enabling anisotropic control of electrical, mechanical, and chemical properties [228-231]. As another example of texturing, graphene nanoribbons have been obtained by the unzipping of CNTs using different types of lasers [232, 233].
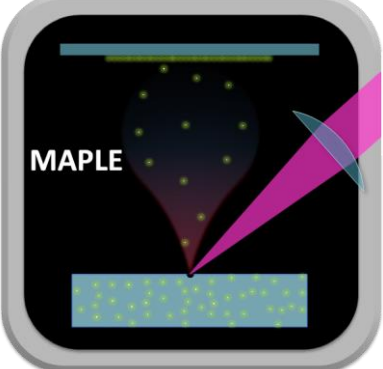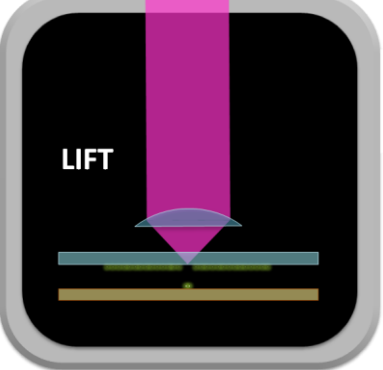
Laser annealing is a general term, comprehending fast and locally confined heat treatments which can be performed under a wide range of conditions. As an example, the process has been applied for improving the electrical and thermal conduction between graphene and metal contacts by Ermakov *et al*. [234, 235]. The enhanced contacts (to initially rough metal electrodes) were attributed to the local melting of the metal surface under laser heating, and to the increase in the actual metal–graphene contact areas. Laser annealing treatments have also been used by Bhaumik *et al*. for changing the electrical transport properties of rGO layers obtained by a modified PLD method [236]. The normally *p*-type as-fabricated rGO films were converted to *n*-type after being subjected (in air) to single pulses (20 ns) of a KrF excimer laser in the range of fluences between 0.6 and 1 J cm^{-2}. A marked decrease in the degree of wrinkling of the rGO sheets comprising the films has been observed, as well as an increase in the C/O ratio, indicating

further material reduction upon laser irradiation. The deformation of graphene and the changes in its electrical properties upon laser annealing have also been reported [237]. The benefits of laser annealing have been confirmed by the results reported by Del and co-workers in the case of graphene inks deposited by drop casting [238]. Using a continuous green laser (532 nm, 500 mW) with a power density of 55 mW cm^{-2} for 1–4 ms, the authors observed an obvious decrease in the surface roughness of the treated regions, as well as remarkable improvements in conductivity (up to four orders of magnitude), and optical transmittance. The results were attributed to the flattening of the graphene layers and the decomposition of ink residues (mainly ethyl cellulose). Laser annealing (KrF laser, H$_2$/Ar atmosphere) has also been used for removing PMMA residues remaining in graphene patterns after common substrate-transfer operations [239].

Table 2. Main types of laser treatments for synthesis and modification of graphene materials for application in energy storage devices.

Treatment	Description	Applications/Comments
Synthesis	**Synthesis** is the localized formation of graphene induced by laser irradiation of substrates in the presence of carbon or carbon-containing raw materials Can be performed with gaseous, liquid or solid precursors The synthesis, as defined, should include many instances of carbonization (or graphitization), but these have been treated as a separate operation due to the wide range of practical applications	The most relevant example is the LCVD process for growing high quality graphene films over metal catalyst-coated substrates Can be applied to the growth of films under a liquid environment Can be used (with adaptations) for direct growth of doped or decorated graphene
Reaction	**Reactions** might be activated by photochemical and/or thermochemical mechanisms upon laser irradiation The reactions may involve only solids, as in the case of a film over a substrate, or they might occur in the interface with a fluid (a powder in suspension, for example) Strictly speaking, synthesis, reduction, doping, etc. are (or at least include) reactions, but here these operations were discussed separately, due to their technological relevance	Thermally activated reactions can be used for modifying graphene and its derivatives Attachment of chemical groups for local functionalization Can be performed in liquid or gaseous media Reactions between a graphene material and its supporting substrate are also possible
Reduction	**Reduction**, in this context, is a term referring to the removal of oxygen (or oxygen-containing chemical groups) from graphene materials upon laser irradiation The laser reduction of GO is predominantly a photothermal process, well suited to IR lasers, but can also be performed with visible and UV lasers May be carried out in liquid media, including solutions	The laser reduction of GO is a very interesting process for obtaining rGO, with properties similar to graphene The process can be directly applied to device fabrication for SCs and battery electrodes Doping and decoration can be performed simultaneously with reduction Local control over the degree of GO reduction is very convenient for energy storage devices

Carbonization	**Carbonization** is the thermal decomposition of an organic material under low oxygen ambient conditions. Carbon is the only chemical element left upon complete carbonization of the material Graphite and/or graphene flakes might be the resulting structures, in which case the process has been named "graphitization" Taking advantage of the short interaction times normally used in laser irradiation, under the right set of processing parameters, the operation may be carried out in ambient conditions	The material resulting from polymer graphitization has been named "laser-induced graphene" (LIG) Laser carbonization of polymers is a very attractive method for making graphene-based flexible devices The method can be used for direct writing of electrodes for SCs and batteries Simultaneous doping and graphitization is possible, using deposited films, liquids and gases
Doping	**Doping**, in this context, is the inclusion of heteroatoms in the material structure The doping process may proceed according to a number of different pathways, but in any case the process involves bond breaking, diffusion and reaction The dopants may occupy different positions in the material structure, depending on their nature, the chemical groups replaced and the treatment conditions	Laser doping of graphene has been widely explored in several applications, including energy storage devices Simultaneous doping and reduction is a very convenient way of obtaining doped rGO Possibility of doping materials deposited over heat-sensitive substrates Decoration of doped rGO with metal or metal oxide nanoparticles can be achieved in the same process
Ablation	**Ablation** is the removal of material following the incidence of laser pulses with intensity above a minimum value The ablation threshold (more accurately expressed in terms of laser fluence) is strongly dependent on the material being treated and the laser wavelength Upon the sudden supply of concentrated energy, the surface layers are vaporized and ejected at supersonic speeds, perpendicular to the illuminated surface	This is the main mechanism for laser micromachining operations, which can be used for device fabrication Ablation can be used for sculpting bulk materials, cutting substrates, making holes, and also for selective film removal operations Controlled laser ablation can be performed on multilayer graphene for "thinning" (decreasing the number of layers)

PLD	**Pulsed laser deposition** (PLD) is a thin film deposition method which uses as source the material ejected by the laser ablation of a solid target The substrate is placed facing the target in a controlled environment (gas pressure and composition) The ionized material in the plume is condensed on the substrate, gradually building up a deposited film	The method can be used for the synthesis of graphene from carbon targets Control over the deposition atmosphere (pressure, composition) can be exploited for in-situ doping Possibility to deposit successive films from different carbon materials (by changing targets)
MAPLE	**Matrix-assisted pulsed laser evaporation** (MAPLE) is a variant of the PLD process, where the solid target is replaced by a suspension of the material to be deposited in a volatile substance kept at cryogenic temperatures The expansion of the vaporized matrix upon fast laser heating carries the material towards the substrate	The method was devised for depositing sensitive or fragile materials that would otherwise be destroyed by the laser radiation Can be used to deposit any type of layered carbon materials, including GO Can be used for making hybrid electrodes incorporating different forms of nanostructured carbon materials
LIFT	**Laser-induced forward transfer** (LIFT) is a process where the laser beam is used to cause local ablation of a film deposited on a transparent substrate, with the ejected material being deposited on another (parallel) substrate in close proximity The film working as the source for deposition (the "donor" film) is ablated by the laser illumination from the back For this reason, the substrate must be transparent at the wavelength of the laser radiation	A variation of this method, using laser-induced backwards transfer (LIBT), places the donor substrate after the (transparent) substrate that will receive the film Can be used for direct device writing on any type of substrate Can be used as a layer-by-layer additive printing technique for building 3D electrodes

Exfoliation	**Exfoliation** is a nomenclature reserved for layered materials, referring to the process of separating individual layers from the originally stacked sheets The exfoliation relies on the sudden evaporation of molecules intercalated between the layers causing their separation from the bulk This is distinct from laser thinning, which takes place by ablation of the surface layers	Laser exfoliation is used for isolating individual graphene layers (or groups of layers) from graphite The operation can be performed in air, under a controlled atmosphere, or with the material immersed in a liquid Powders can be exfoliated while suspended in a liquid/solution
Texturing	**Texturing** is a broad categorization, covering structural and morphological changes brought about by laser-treatments Shorter laser wavelengths and pulse widths are, broadly speaking, more adequate for direct texturing/structuring of surfaces Structuring can be accomplished by direct surface illumination or by carefully controlled manipulation of laser interference fringes formed in the material surface	Roughening of graphene and its derivatives for increased surface area Formation of laser-induced periodic surface structures (LIPSS) in graphene Unzipping of carbon nanotubes to obtain graphene nanoribbons Patterning of graphene materials or selective reduction of GO by exposure to laser fringes generated through interference
Annealing	**Annealing** is another wide ranging term, covering any process in which a localized thermal treatment is applied with the laser beam Depending on the material and the specific situation, possible outcomes are: structural relaxation, partial decomposition, phase change, etc. Annealing processes are also applied for changing the values of specific properties	Laser annealing can increase the conductivity of graphene and its derivatives The process can be applied after other laser operations for achieving a relaxed (closer to equilibrium) structural state Annealing can be used to improve electrical contacts between graphene and metals Annealing can be applied to remove volatile contaminants or synthetic residues

4. Laser-processing of graphene and related materials for energy storage

Currently, many researchers working in materials engineering are highly focused on the development of techniques for achieving fast, versatile, scalable and cost-effective fabrication of high performance electrochemical energy storage devices. Highly conductive, stable and large surface area graphene-based electrodes exhibit promising features for electric double layer SCs. In addition, the porous graphene structures can simultaneously act as scaffolds and electron collectors for nanomaterials undergoing faradaic charge storage. Herein we focus on the different technologies that are being developed for the laser fabrication of energy storage devices, essentially EDL and hybrid SCs, as well as batteries. The reviewed works are divided into two groups: methods based on laser-induced chemical transformation and those involving ablation processes.

4.1. Laser-induced chemical transformation

4.1.1. Supercapacitors

First of all, we must warn the reader about the different approaches reported in the literature in terms of the evaluation of the supercapacitors energy storage performance. Thereby, the capacitance values have been related to an individual electrode or, conversely, to a complete device, which can be symmetric or asymmetric. In a simple model, a SC device could be considered as two capacitors in series, each one associated to the corresponding electrode. Therefore, the total value for the SC capacitance would be equal to the reciprocal of the sum of the reciprocals of the electrodes' capacitances. As a consequence, the capacitance of the device will be lower than that of the individual electrodes. On the other hand, the capacitance is generally presented normalized in terms of mass ($F\ g^{-1}$), volume ($F\ cm^{-3}$) or area ($F\ cm^{-2}$) of the electrode/device. For proper comparisons, it has to be taken into account if the mass or volume is referred to the active material or the total material of the electrode / device (including active material, substrate, etc.). Moreover, the thickness of the active material is a capital parameter in the following cases: (i) when electrode or SC areal capacitance is provided, since the thickness (or density) will account for the loading of material per unit area; and (ii) when thin electrodes' are developed, since their functional properties cannot be linearly extrapolated to thicker electrodes due to possible changes in the microstructure configuration that may influence in the diffusion of the electrolyte ions and their interaction with the active material [X].

Despite the presence of oxygenated groups in the basal plane of GO which disrupt the π–π conjugation, making it an electrical insulator, laser processing of GO films allows easy fabrication of highly conductive rGO electrodes for electrochemical energy storage applications. Gao *et al*. have demonstrated the direct laser reduction of GO for the versatile creation of SCs by processing freestanding GO films with a CO_2 laser printer [125]. Conductive LrGO patterns were separated by non-irradiated GO gaps working as solid electrolytes, due to the porosity and large amount of trapped water imparting ionic conductance to GO. Several research groups have since adopted the laser processing SC based on the LrGO/GO/LrGO architecture, however using different materials, device configurations and laser types [136, 240-246]. Kaner and co-workers have developed pioneering work on the low-cost production of SCs by performing the laser reduction of GO films using a DVD writing technology. The resulting rGO has been named laser-scribed graphene (LSG) [247, 248]. In their method, GO/polymer films are deposited on DVD discs, which are subsequently processed in a DVD optical drive, leading to the generation of LrGO electrodes [247]. This convenient approach has enabled the fabrication of several devices, from interdigital μSCs to hybrid SCs [248-250].

High-throughput laser reduction of GO for fabrication of electrodes that can be implemented in sandwiched SCs has been achieved through CO_2 laser processing [124]. This technology allows the fabrication of complex devices, such as potassium-ion hybrid capacitors and self-charging power packs consisting of a solar cell and a laser-scribed graphene SC, showing excellent energy storage capability, energy density, and stability over thousands of charge-discharge cycles [251-253]. Often, weak adhesion may cause delamination of the rGO layers deposited on flexible polymeric substrates. An interesting strategy to overcome this limitation is the laser irradiation through the substrate, resulting in "welding" of rGO to the polymer [254, 255].

The synthesis of LrGO-based electrodes by mixing the GO flakes with other compounds or even with other types of nanostructures has also prompted the performance enhancement of energy devices. For instance, the addition of MWCNTs prevents the aggregation of rGO sheets, leading to an increase in porosity, thus enhancing ionic transport within the electrode material [256]. Similarly, the incorporation of carbon nanodots into LrGO films has been recently reported as a valuable strategy for significantly enhancing the active surface area and the conductivity of SC electrodes [257]. Wang *et al*. developed N-doped porous LrGO electrodes by picosecond laser processing of GO/urea mixed films in ambient air [258]. Through this simple method,

hierarchically structured porous LrGO materials containing pyridinic, pyrrolic, graphitic and oxidized N groups as well as structural defects were obtained. The electrodes with larger amounts of pyrrolic functionalization exhibited capacitance values up to 61 mF cm^{-2}, which is nearly three times higher than similar undoped electrodes.

Femtosecond laser sources have proved to be particularly interesting for the versatile fabrication of highly integrated energy storage systems. Shen *et al.* have demonstrated the high-resolution femtosecond laser reduction and patterning of GO films for the production of ultraminiature μSCs [259]. **Fig. 2a** shows the processing steps for fabrication of the μSC devices, starting with the deposition (and drying) of aqueous GO dispersions on SiO$_2$/Si substrates, followed by fs laser scribing of high resolution LrGO interdigitated patterns (**Figs. 2b, c**). Microdroplets of PVA-H$_2$SO$_4$ electrolyte gel are then accurately placed over the electrodes by the LIFT method using the same laser source (**Figs. 2a, d-f**). Full working devices are obtained after the gel is dried at room temperature for a few hours in order to remove extra water. In this way, high performance μSCs and even RC filter circuits containing μSCs and LGO resistors were produced in a rapid, easy and cost-effective way, avoiding cross-contamination of the electronic components by the μSC electrolyte. Femtosecond laser processing has also been used for the high-precision fabrication of Au-loaded LrGO SCs showing excellent conductivity and capacitive behaviour at high charge/discharge rates [260].
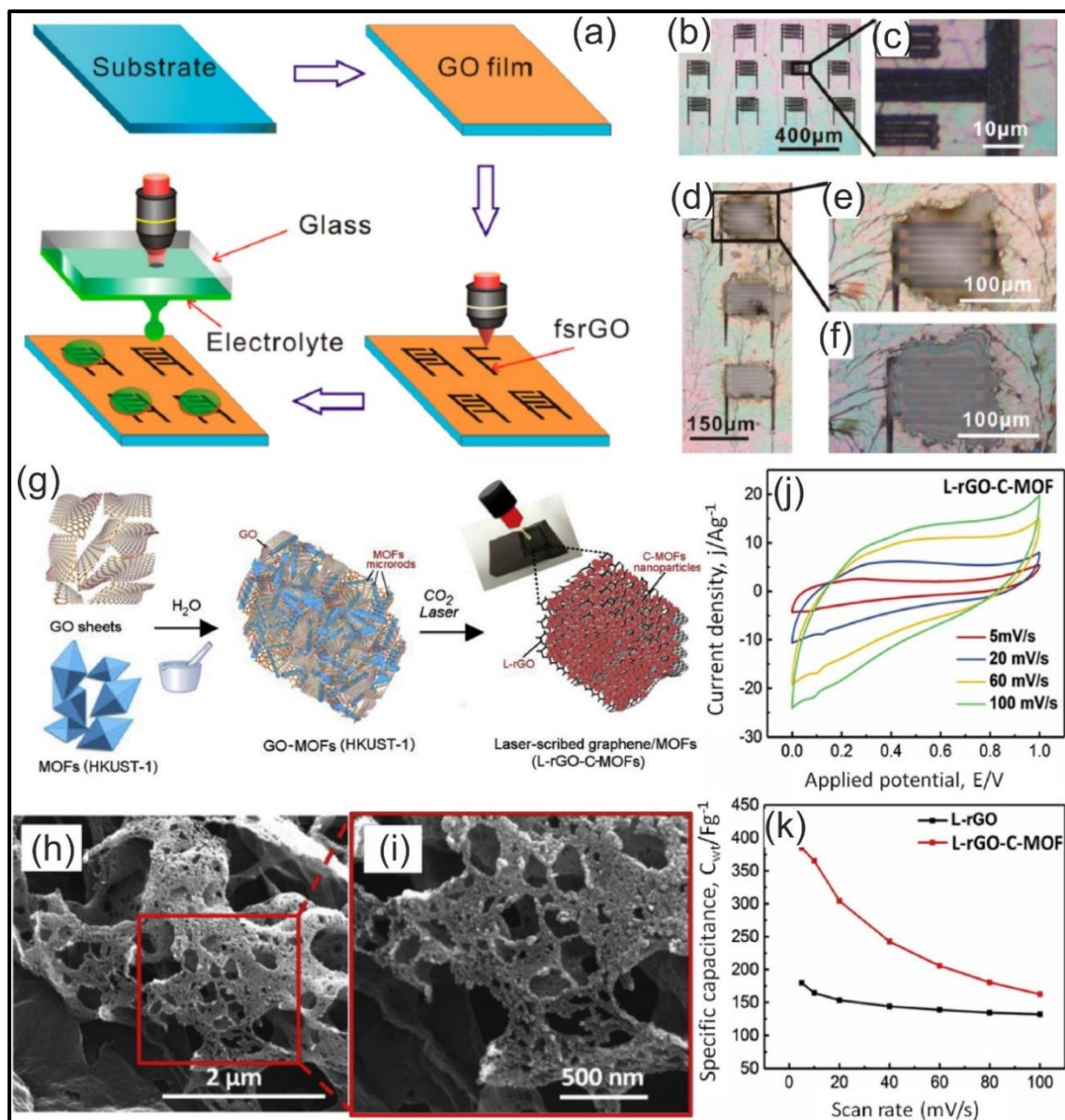
Fig. 2. (a) Schematic process for fabrication of integrated μSCs using femtosecond laser processing. (b, c) High-resolution patterned LrGO microelectrode arrays with a spacing of about 2 μm between individual fingers. (d) Electrolyte microdroplets covering the electrodes. (e) μSCs immediately after electrolyte transfer, and (f) after overnight drying. Reproduced from [259] with permission of ACS. (g) Schematic synthesis of laser reduced GO-carbonized HKUST-1 metal organic frameworks (LrGO-C-MOFs). (h, i) SEM pictures of LrGO-C-MOF composite. (j) Cyclic voltammetry of LrGO-C-MOF at different sweep rates. (k) A comparison of specific capacitances of LrGO-C-MOF and LrGO at different scan rates. Reproduced from [261] with permission of Elsevier.

The performance of electrodes for energy storage devices can be further improved by synthesizing LrGO containing electrochemically active functional groups. The coexistence of carbon electric double layers and pseudocapacitive species allows an enhancement of capacitance without a substantial loss of power delivery and cycling stability. As a recent example of this approach, Van Ngo *et al*. developed a method for

obtaining composite 3D-structured carbon electrodes by combining LrGO and carbonized HKUST-1 metalorganic framework (LrGO-C-MOF) microrods [261]. As shown in **Fig. 2g**, an aqueous dispersion of HKUST-1 and GO sheets was deposited and dried, resulting in the formation of a composite film where the HKUST-1 microrods were intercalated between GO sheets. The film was then treated with a CO_2 laser under ambient conditions, leading to the formation of a high surface area, conductive, highly porous carbon material at both micro and meso scales (**Figs. 2h, i**). The shape of the cyclic voltammetry (CV, **Fig. 2j**) and galvanostatic charge-discharge (not shown) plots revealed some features related to resistive effects. Besides EDL charge storage, the contributions of faradaic reactions were also detected, being attributed to embedded Cu_2O among the rGO sheets. The LrGO-C-MOF electrodes exhibited good capacitance (ca. 390 F g^{-1} at 5 mV s^{-1}), more than double the value for similar LrGO electrodes synthesized without MOFs (**Fig. 2k**), and a significant capacitance retention after 5000 cycles. A large number of high-performance electrode films composed of LrGO decorated with pseudocapacitive oxides, such as oxygen-deficient TiO_2, MnO_2 or RuO_2 NPs have already been produced using the laser scribing technique [112, 262, 263]. LrGO-based electrodes can be also synthesized by laser irradiation of GO liquid dispersions followed by the deposition of the resulting material as a film. Indeed, even hybrid electrodes have been developed in this way. As an example, UV pulsed laser irradiation of aqueous dispersions of GO-WO_3 NPs have been carried out for the simultaneous reduction of GO and the anchoring of nanostructured WO_3 on the rGO surfaces [264]. Subsequent deposition of the suspension by spray coating led to porous electrodes and symmetric SCs with capacitance values reaching 577 F g^{-1}.

Another approach, recently developed, comprehends the laser processing of CVD-grown graphene nanowalls electrodes immersed in aqueous solutions of metal organic precursors [X]. In this way, several types of pseudocapacitive transition metal oxide nanostructures were crystallized on the surface of the graphene flakes leading to up to three orders of magnitude increase of the electrodes' capacitance (maximum of ca. 28 F cm^{-3} at 10 mV/s) at both positive and negative voltages.

Besides graphene, other 2D layered materials, like the MXenes and the transition metal dichalcogenides (TMDs) are also attracting high interest for application in high-performance energy storage devices [265-268]. Accordingly, MoS_2 decorated LrGO electrodes and interdigitated μSCs have been synthesized by laser scribing of nanocomposite films deposited from GO-MoS_2-dimethylformamide dispersions [269].

The obtained flexible light-scribed electrodes and devices showed ca. 60 mF g^{-1} and 8 F cm^{-3} capacitances, respectively, notably higher values than those obtained with pure LrGO materials. Though the improvement of capacitance was attributed to increased surface area, the waves observed in the CV curves may indicate important pseudocapacitive contributions.

4.1.2. Battery electrodes

The incorporation of a graphene network in battery electrodes is being thoroughly investigated due to a number of practical benefits. Electrochemical performance improvements arise from (i) bigger porosity, enabling more efficient ionic transport and increasing the active surface area, (ii) enhanced structural stability through buffering of volume changes caused during ionic insertion and extraction cycles, (iii) increase in the electronic conductivity of the overall material, and (iv) synergistic effects which lead to performance improvements which are bigger than what would be expected from a mere addition of individual contributions [270-272].

Hybrid LrGO-SnO_2 anodes for Li ion batteries have been prepared by IR fibre laser conversion of binder-free mixtures of GO and stannic oxide coated on Cu substrates [273]. The electrodes, composed of layered LrGO decorated with SnO_2 NPs, revealed low sheet resistance (28 Ω sq^{-1}), high Li storage capacity and good cycling stability (700 mAh g^{-1} retained after tens of cycles at 100 mA g^{-1}). Lithium iron phosphate ($LiFePO_4$, LFP) is widely used as a cathode material in Li ion batteries. However, this material suffers from poor electronic conductivity and limited Li^+ ionic conductivity due to its olivine structure with 1D channels. Tang *et al*. have circumvented this problem by carrying out in-situ laser reduction of GO sheets added to LFP material [274]. **Fig. 3a** displays the synthesis procedure. First, a slurry composed of $LiFePO_4$ particles, GO powder, polyvinylidene fluoride (PVDF) and 1-methyl-2-pyrrolidinone solvent was coated onto an Al foil and dried. The composite film was then irradiated with a pulsed fibre laser (1064 nm wavelength), leading to total reduction of the GO sheets without damaging the LFP particles. The electrode structure consisted of a hierarchical conductive network containing large graphene-like layers covering the top of the electrode, and small LrGO pieces inserted between the LFP particles (**Figs. 3b, c**). The obtained LrGO-LFP electrodes show great enhancement of the rate capability and cycling performance when compared to electrodes composed of LFP and conductive carbon black particles.

Supercapacitive charge storage, which includes EDL and pseudocapacitive processes, is intrinsically reversible, fast and superficial, whereas battery-like materials are characterized by slow and diffusive mechanisms. However, advances in the synthesis of nanosized and hybrid materials are blurring the conceptual boundaries between supercapacitive and battery-like behaviours. Accordingly, the expression "supercapattery" has been coined for systems combining features from both types of materials [275-277]. Li et al. fabricated electrodes by CO_2 laser processing of films containing GO mixed with Co_3O_4 nanoboxes that were obtained by calcination of precipitated cobalt precursors [278]. Co_3O_4 is a material with high theoretical capacity, is abundant and cost-effective, however it suffers from limited cycling stability and low electronic conductivity. As observed in **Figs. 3d, e**, electrodes composed of hollow Co_3O_4 reveal typical faradaic peaks in the CV curves, besides higher electrochemical activity than LSG. Nevertheless, the combination of reduced GO and Co_3O_4 nanoboxes reveals synergistic effects, since the measured capacity of the composite is much higher than the sum of those of LSG and Co_3O_4 nanoboxes (about 60 mC cm^{-2} at 2 mV s^{-1}). As seen in **Fig. 3d**, the CV curve of the composite material is more rectangular-shaped, with hidden faradaic peaks, indicating the EDL contribution from LSG to the total current. Such electrodes revealed outstanding electrochemical performance, with large surface area, good ionic diffusion, fast charge transfer, ultrahigh specific capacity, low internal resistance, and notable charge-discharge stability up to thousands of cycles.
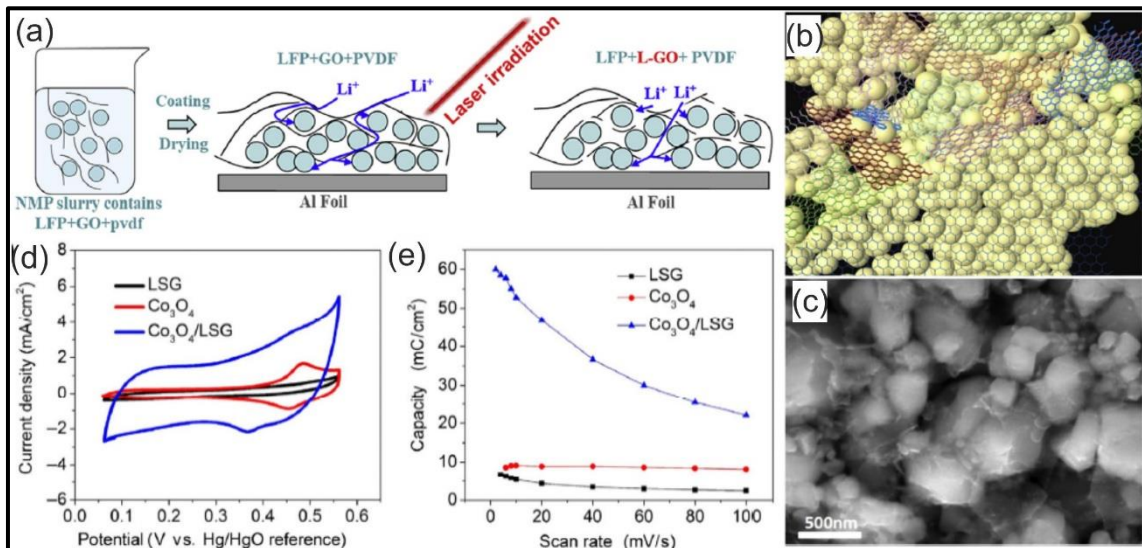

Fig. 3. (a) Schematic in-situ fabrication of LrGO-LFP electrodes, (b) Schematic structural illustration and (c) SEM picture of a hierarchical LrGO-LFP structure. Reproduced from [274] with permission of Elsevier. (d) CV plots of Co_3O_4-LSG composite, LSG, and pure Co_3O_4 at a sweep rate of 20 mV s^{-1}. (d) Comparison of areal capacity of the Co_3O_4/LSG

composite, LSG, and pure Co_3O_4 at different sweep rates. Reproduced from [253] with permission of Springer.

4.2. Laser-induced graphene

4.2.1. Flexible micro-supercapacitors

LIG material, with its conductive, highly porous and conformable structure, holds great promise for the capacitive electrochemical storage of charge, either by EDL (when pure) or by faradaic mechanisms (when combined with other compounds). Therefore, laser induced graphitization of different types of organic compounds for the low-cost and large-scale fabrication of SCs has become a hot research topic. Zhang *et al*. fabricated interdigital electrochemical SCs by processing $FeCl_3$-doped phenolic resins with an inexpensive 405 nm semiconductor laser [141]. In this work, the $FeCl_3$ dopant was added for enhancing the visible light absorption, helping to convert the phenolic resin into highly conductive and porous LIG. Flexible SCs were manufactured revealing an areal capacitance of about 1 mF cm^{-2} and excellent capacitance retention over 2000 charge-discharge cycles at a current density of 1 mA cm^{-2}. Similarly, LIG-based SCs with various in-plane geometries have been produced by 450 nm laser irradiation of PI [279]. In this way, serial/parallel arrays of flexible μSCs showing high electrochemical and cycling performance have been demonstrated. By using infrared CO_2 lasers, and by optimizing the graphenization process, Liu *et al*. succeeded in carbonizing the phenolic resins for fabrication of SCs without the aid of optical absorbers [280]. Conductive foam-like LIG electrodes have also been developed by CO_2 laser irradiation of sulfonated poly(ether-ether-ketone) films [281]. The obtained conductive porous material, containing needle-like structures, displayed a maximum capacitance of 3.4 F g^{-1} and 30 mF cm^{-2} at 3 mV s^{-1} sweep rate. Flexible solid state SCs with maximum areal capacitance of 18 mF cm^{-2} at 3 mV s^{-1} were also fabricated, showing remarkable stability upon charge-discharge cycling and repetitive bending.

Undoubtedly, technologies aiming the production of energy storage devices by using biomass or industrial waste materials hold great promise for developing sustainable fabrication approaches. Zhang et al. fabricated on-chip μSCs by CO_2 laser processing of films mainly composed of lignin material, which is a by-product from the cellulose and paper industry [282]. As displayed in **Fig. 4a**, the method consists in the laser irradiation of lignin/polyvinyl alcohol films for patterning highly porous LIG interdigitated electrodes, followed by water dissolution of the non-exposed material. Alternatively, a

thin Au coating was deposited onto the LIG patterns prior to the water dissolution step, yielding devices with areal capacitances near 10 mF cm^{-2} (**Fig. 4b**). However, their performance was degraded at elevated current densities, probably due to the Au deposited blocking part of the LIG surface macropores. Nonetheless, the Au-coated device showed excellent stability when subjected to 12000 charge/discharge cycles, with 99% capacitance retention (**Fig. 4c**). With a similar reasoning, 3D LIG electrodes containing meso- and macro-pores have been fabricated by CO_2 laser treatment using glucose as the starting material [283]. Glucose was hydrothermally transformed to carbon nanospheres, which were further graphitized to LIG leading to the formation of a conductive, well-interconnected 3D carbon framework. Symmetric SCs assembled with an organic electrolyte disclosed areal capacitance of 1 mF cm^{-2} at 100 mV s^{-1} and high rate capability, with capacitance retention of about 28% at sweep rates as high as 100 V s^{-1}. The laser graphitization of biomass and waste materials is currently attracting great attention, being responsible for the development of a variety of inexpensive SCs with increasing degree of sophistication [142, 284-287].

Tehrani *et al.* took a different approach, using LIG as a precursor for the synthesis of graphene conductive inks which were subsequently printed for manufacturing flexible SCs [288]. The method consisted in the CO_2 laser conversion of PI films to LIG powder, which was further mixed with conductive poly(3,4-ethylenedioxythiophene):polystyrene sulfonate and polyester-polyurethane composites leading to conductive ink formulations. Micro-SCs were fabricated by screen printing the ink onto flexible and intrinsically stretchable polymer substrates. As shown in **Fig. 4d**, the resulting μSCs are fully wearable devices, displaying outstanding mechanical resistance and stretchability. Moreover, the devices exhibited good electrochemical performance, with high areal capacitance (about 23 mF cm^{-2} at 5 mV s^{-1}), and significant stability over repeated stretching-releasing cycles. It is important to notice that LIG morphology strongly depends on the parent material and on the laser-writing parameters used for the graphenization process. Lamberti *et al.* obtained LIG foam electrodes with diverse compositions and nanostructural morphologies (needle, sheet, or porous-like) upon CO_2 laser processing of PI with different repetition rates and laser scan speeds (**Fig. 4e**) [146]. The structural rearrangements arise from dynamic coupling between photo-induced heating, chemical reactions kinetics and evolution of gas release during polymer decomposition. As shown in **Fig. 4f**, the needle-like material exhibited the best electrochemical performance, with larger areal capacitance (maximum of approximately 230 μF cm^{-2}), being less susceptible

to fading at higher sweep rates. This has been attributed to better access of electrolyte ions to the active surfaces. Needle-shaped LIG represents a good compromise between composition (largest amount of nitrogen groups), structural cohesion and electric conductivity.
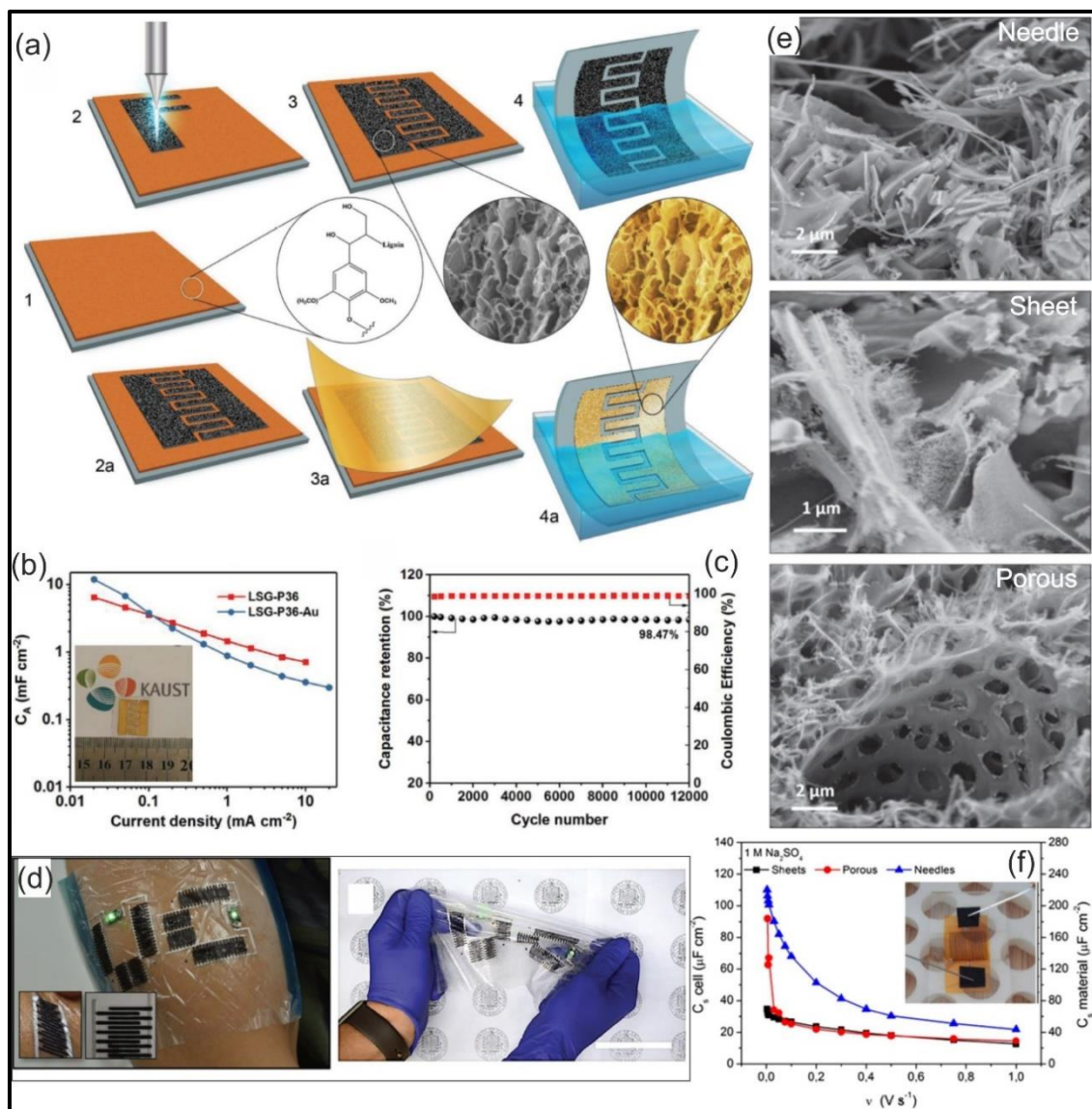
Fig. 4. (a) Schematic diagram illustrating the lignin-based laser graphitization technique: 1) Deposition of lignin/PVA film on substrate, 2) Laser processing for LIG patterned μSC electrodes, 3) Obtained LIG pattern showing a typical microstructure, 4) Water lift-off to remove unexposed lignin material. An alternative processing path with additional Au deposition is shown in images 2a-4a. (b) Areal capacitance of LIG (LSG-P36) and LIG-Au (LSG-P36-Au) μSCs versus charge–discharge current density. Inset: image of a LSG-P36-Au μSC device. (c) Charge-discharge cycling of LSG-36-Au μSCs recorded at 2 mA cm^{-2} current density. Reproduced from [282] with permission of WILEY-VCH Verlag. (d) Image showing wearable SCs printed on polyurethane foil and a demonstration of stretching performance. Reproduced from [288] with permission of WILEY-VCH Verlag. (e) SEM images of needle-, sheet- and porous-like LIG electrodes. (f) SC

capacitance calculated from cyclic voltammetry at several sweep rates. Inset: picture of a fabricated SC. Reproduced from [146] with permission of IOP.

As previously substantiated in different application fields, the compositional transformation of LIG electrodes, either by heteroatom doping or by decoration with electrochemically active nanostructures, leads to a significant enhancement of energy storage performance. For instance, Peng *et al*. demonstrated that doping of LIG with boron allows fabricating interdigitated μSCs with an effective areal capacitance of 16.5 mF cm^{-2}, which is three times higher than similar undoped LIG-based devices, with energy density increasing up to tenfold [289]. The CO_2 laser processing of H_3BO_3-PI films led to the formation of doped porous graphene structures with high effective surface area, owing to the presence of nanoscale ridges and wrinkles. Boron doping shifts the Fermi level towards the valence band, improving charge storage and transfer in the LIG structure, as well as contributing to space-charge-layer capacitance and pseudocapacitance [290-295]. Cai *et al*. recently developed boron, phosphorus and fluorine-doped LIG by 405 nm continuous-wave diode laser irradiation of PI films incorporating H_3BO_3, H_3PO_4 and $NaBF_4$ compounds, respectively [296]. Relying on XPS analyses, they concluded that the B-doped LIG contained both C–B bonds (B_4C, BC_2O) as well as B–O bonds (BCO_2 and B–O). P-doped LIG revealed similar carbon structures, exhibiting C-P, and P-O bonding, whereas F-doped LIG displayed larger porosity, with the formation of C–F bonds having a partially ionic character. All the flexible μSCs with B-doped LIG disclosed good areal capacitances (up to 65.7 mF cm^{-2} at 0.05 mA cm^{-2}), with significant stability over 50000 charge-discharge cycles. Interestingly, P- and F-doped LIG devices also revealed impressive areal capacitances (74 and 58 mF cm^{-2} at 0.05 mA cm^{-2}, respectively), though no data about cycling performance has been reported.

The synthesis of hybrid electrodes composed of LIG material with embedded pseudocapacitive nanostructures from metal oxides, sulphides or carbides is a key strategy for enhancing the charge storage performance of SCs. In this approach, the carbon source is mixed with metalorganic precursors in order to simultaneously induce the graphenization of the carbon precursor and the crystallization of the inorganic nanostructures. In a recent publication, Wang *et al*. have described the synthesis of Co_3O_4-LIG composites through the CO_2 laser irradiation of PI coated with a film of $CoCl_2$ dissolved in gelatine derived from porcine skin [297]. Highly porous structures with different morphologies were obtained, depending on the lasing parameters. Thus, a LIG morphological transition from 3D porous matrix to lamellar layers was attained with the

increase of the accumulated laser fluence. Simultaneously, the formation of Co_3O_4 nanostructures progressively evolved from the surface into the inner regions of the LIG framework, with the crystals also revealing a change of shape (from spherical to whisker-like). The highest areal capacitance for these electrodes was 22.3 mF cm^{-2}. Stretchable μSCs with charge/discharge and bending stability over 10000 cycles were obtained, showing also good performance when subjected to stretching and twisting cycles. The authors have also published similar studies in which NiO-Co_3O_4-LIG composite electrodes were fabricated by using a gelatine coating containing both $NiCl_2$ and $CoCl_2$ dissolved salts [298]. The electrodes were transferred to biodegradable waterborne polyurethane substrates with excellent stretchability. Although the authors have postulated a synergistic effect between NiO and Co_3O_4 NPs, in fact these electrodes displayed similar areal capacitances when compared to Co_3O_4-LIG.

Finally, it is worth mentioning some interesting research published by Zang *et al*. [299] in which foldable paper electronic devices were obtained by CO_2 laser processing of fibrous paper substrates soaked with gelatine-based inks containing molybdenum ions. The infrared laser radiation led to the carbonization of the paper and the simultaneous reaction of Mo^{+5} ions, forming hierarchically porous molybdenum carbide-graphene composites with remarkable electrical conductivity. In addition to sensing and piezoelectric energy harvesting applications, the pseudocapacitive Mo_3C_2-loaded graphene composites were also tested as electrodes in paper-based hybrid SCs, showing up to 14 mF cm^{-2} areal capacitance at 1 mV s^{-1}.

4.2.2. Battery electrodes

The high porosity, electrical conductivity, chemical and mechanical stability have turned LIG into a very attractive alternative for exploitation in battery electrodes. In addition to the promising features of these materials, the facile, versatile, cost-effective and large-scale synthesis of LIG-based composites could pave the way for the industrial fabrication of new generations of rechargeable batteries. Very promising systems have recently been investigated, pointing to major advances in LIG-based battery technology. Yi *et al*. studied the fabrication of LIG-based anodes for Li-metal batteries as an alternative to conventional graphite and Li metal anodes, which suffer from several technological drawbacks [300]. The authors presented a novel 3D electrode architecture consisting of a conductive copper substrate with an array of flexible PI pillars having LIG grown on the vertical pillar walls. The structure was developed by direct scribing a grid in the thick PI

films using a 532 nm laser engraving system (**Figs. 5a, b**). Li metal was then electrodeposited onto the fabricated structures, with the highly defective and porous structure of LIG providing fast Li nucleation kinetics. In this electrode system, the Cu substrate acts as a macroscopic current collector, whereas the flexible PI pillars help the release of stress during Li deposition. As shown in **Fig. 5c**, full Li-metal battery cells using $LiFePO_4$ cathodes exhibited a specific capacity of about 120 mAh g^{-1}, with very high coulombic efficiency over 250 cycles and much-extended cycle life when compared to copper anodes.

Hybrid LIG composites have also been studied in the search for enhanced battery performance, as demonstrated by Huang *et al*., who developed S- and N-doped LIG decorated with MoS_2 NPs for application as cathodes in Li-S batteries [301]. In this work, a layer of poly[2,2′-(m-phenylen)−5,5′-bibenzimidazole] dissolved in dimethyl sulfoxide and containing MoS_2 micro-particles was irradiated with a high repetition rate 10 ps pulsed UV laser source (355 nm wavelength). The energetic pulsed radiation led to ablation of the embedded MoS_2 micro-particles, forming confined plasmas which were subsequently recrystallized as NPs decorating the high surface area LIG generated from graphitization of the polymer. As shown in **Fig. 5d**, the fabricated Li-S batteries revealed a stable, high gravimetric capacity of 1150 mAh g^{-1} at 0.1 C, significantly greater than reference LIG and graphene cathodes used for comparison. A steady capacity of 445 mAh g^{-1} at the high current density of 3 C was obtained, and the initial values were recovered when the current density returned to 0.1 C. The electrochemical performance of the system was stable over 500 cycles. Zhou et al. developed hybrid anodes for Li ion batteries consisting of MnO/Mn_3O_4/N-doped-LIG materials directly bonded to a copper current collector [302]. In this work, a biomass gelatine matrix containing manganese (II) phthalocyanine was used as precursor layer, processed via CO_2 laser irradiation at room temperature. N-doped LIG frameworks decorated with MnO and Mn_3O_4 nanocrystals were obtained (**Figs. 5e, f**), displaying high porosity and a large amount of electrochemical active sites provided by MnO/Mn_3O_4 nanostructures and N-containing groups in the carbon material [303-307]. The electrodes showed a high reversible capacity of about 992 mAh g^{-1} at 0.2 A g^{-1} current density, retaining a notable rate of 365 mAh g^{-1} at 2 A g^{-1}, and a high cycling stability (ca. 700 mAh g^{-1} after 400 cycles at 0.2 A g^{-1}) when assembled in coin-type half-cells. The versatility of laser-induced graphene combined with Mn oxides has recently being highlighted in the work of Ren *et al*. They developed MnO_2-LIG cathode catalysts for Li-O_2 batteries by a four-step method

consisting in: (i) CO_2 laser processing of PI films, (ii) Oxygen plasma treatment of the obtained LIG for enhancing hydrophobicity, (iii) soaking of LIG layer in aqueous solution of $MnSO_4$, and (iv) additional laser processing for crystallization of catalytic MnO_2 nanostructures on the porous LIG [308]. The obtained MnO_2-LIG cathode catalyst displayed stable galvanostatic charge-discharge for more than 200 cycles using a cut-off capacity of 0.4 mAh cm^{-2} (over 50 cycles with 2 mAh cm^{-2}). In a similar fashion, ternary metal oxide-LIG composites have been synthesized for application as cathode catalysts in both Li–O_2 and Li–air batteries [309]. MnNiFe-LIG composites with Mn:Ni:Fe elemental ratios of 1:1:1 and 3:1:1 were synthesized by CO_2 laser processing of PI films using aqueous precursor solutions of $MnSO_4$, $Ni(NO_3)_2$, and $Fe(NO_3)_3$. Both hybrid composites behaved as efficient and durable cathode catalysts for Li–O_2 batteries. The batteries disclosed reversible cycling performance for more than 100 cycles with a cut-off capacity of 0.4 mAh cm^{-2}. The highest capacity was attained with the Mn-rich cathode, showing 26.3 mAh cm^{-2} at 2 V. Likewise, MnNiFe-LIG and CoNiFe-LIG composite cathodes with 1:1:1 and 3:1:1 atomic ratios have also been developed by the authors for Zn-Air batteries [310]. The uniform distribution of anchored ternary metal oxide NPs in a well-interconnected porous LIG matrix was achieved, without formation of large particle aggregates. Both Co- and Mn-based catalysts revealed notable activity for oxygen reduction and oxygen evolution reactions, but the Mn species provided a more balanced bi-functionality. Thus, liquid Zn-air batteries as well as flexible Zn-air battery prototypes were fabricated, showing practical applications (**Figs. 5g, h**). The batteries displayed significant stability for more than 500 cycles, despite a minor increase of the charge-discharge voltage gap over 350 h. Ren *et al*. have also researched Co_3O_4-LIG catalyst cathodes for Zn-Air and Li–O_2 batteries through the multistep method previously described, but this time soaking LIG in $Co(NO_3)_2$ solutions [311]. The obtained Co_3O_4-LIG catalysts also revealed good efficiency for oxygen reduction and oxygen evolution reactions, which are necessary for inducing faster kinetics in charge-discharge processes, increasing stability and decreasing unwanted side reactions. Accordingly, the assembled batteries exhibited low overpotentials during charge/discharge, besides stability during hundreds of cycles.

LIG has also been investigated for manufacturing electrodes for other types of metal-air batteries, besides Li- and Zn-based technologies. As a remarkable example, Zhang *et al*. have developed N-doped LIG anodes for Na-ion batteries, which are a promising alternative to avoid the dependence on scarce and expensive lithium [305]. In

this work, a single-step process for direct CO_2 laser carbonization of urea-doped PI sheets was developed for the synthesis of highly corrugated and porous 3D LIG structures, which were mainly doped with pyrrolic N, besides graphitic an pyridinic groups. The best anodes were those with the largest amount of nitrogen and lowest oxygen content, exhibiting outstanding Na-ion capacity, up to 425 mAh g^{-1} at a current density of 100 mA g^{-1}, with exceptional rate capabilities. Additionally, a capacity of 148 mAh g^{-1} at 10 A g^{-1} was obtained with excellent stability over 100 cycles. Nitrogen doping tends to enhance the surface wettability and the electrical conductivity of LIG electrodes, whereas its porosity and mechanical stability help the structure to withstand the large volume changes during charge and discharge processes, which may lead to the complete failure of conventional electrodes.
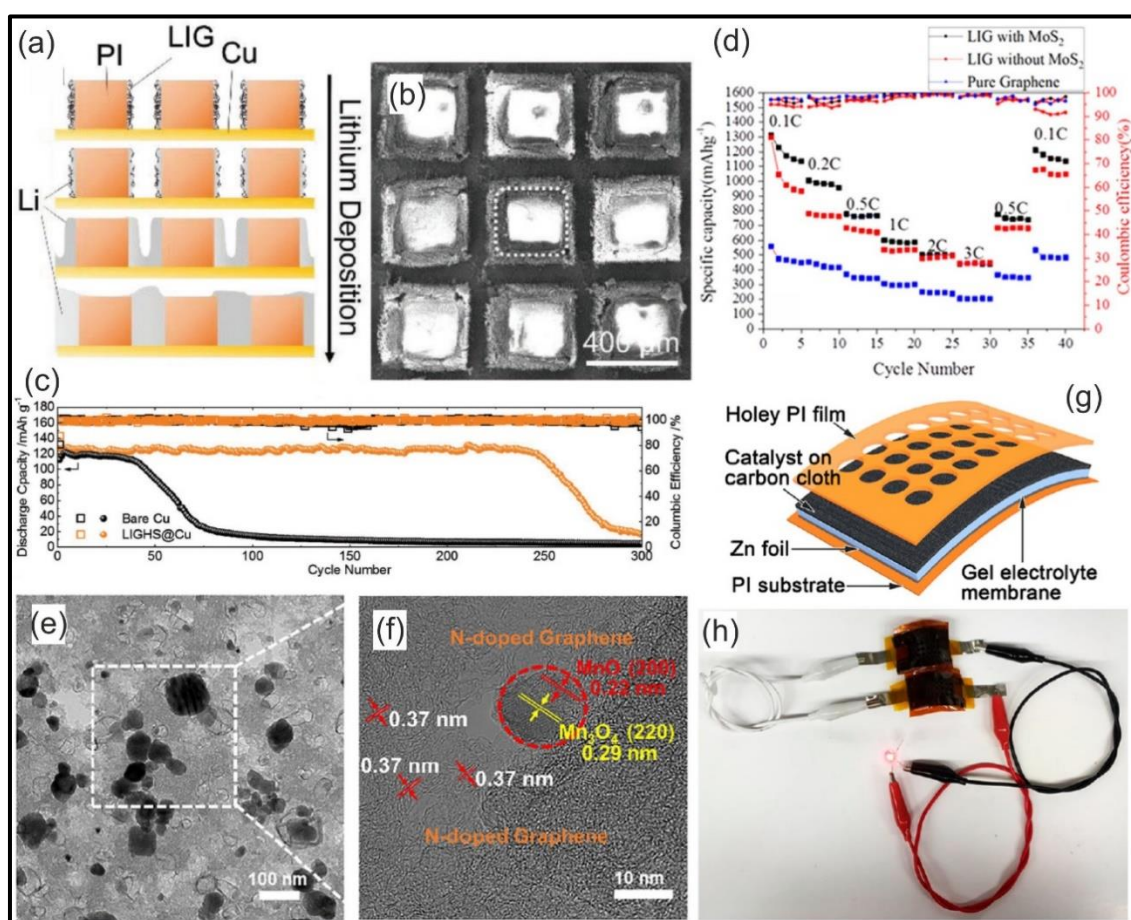

Fig. 5. (a) Diagram of the Li nucleation and growth in LIG-containing PI structures on a Cu substrate (LIGHS@Cu). (b) SEM image of LIGHS@Cu structures prior to Li electrodeposition. (c) Cyclic performance of Li-metal battery based on LFP cathode with a practical mass loading of 15 mg cm^{-2}. Reproduced from [300] with permission of Wiley-VCH Verlag. (d) Rate capacities of N/S-doped LIG with and without MoS_2 particles. Reproduced from [301] with permission of Springer Nature. (e) TEM image displaying MnO/Mn_3O_4 NPs (dark color) and the background LIG. (f) HRTEM image of few-layer graphene with different interlayer distances, as well as MnO and Mn_3O_4 with

respective 0.22 nm and, 0.29 nm interlayer distances. Reproduced from [302] with permission of Elsevier. (g) Schematic structure of a flexible Zn-air battery supported on carbon cloth in which MnNiFe-LIG acts as the air cathode and Zn plate as the anode. (h) Photograph of a LED driven by the serial connection of two flexible batteries. Reproduced from [310] with permission of ACS.

4.3. Techniques based on laser ablation

4.3.1. Flexible micro-supercapacitor devices

Although less investigated than the laser-driven direct chemical transformation methods previously described, laser-induced vaporization also enables the innovative fabrication of graphene-based energy storage devices via direct ablation and/or deposition methods. As the predominant approach, the manufacture of graphene-based SCs via high-resolution maskless laser etching is being explored for a few years with promising results [312-317]. In a remarkable work, Ye *et al*. developed the fabrication of interdigitated µSCs by direct laser ablation of multi-layered graphene films made via industry-scale CVD synthesis [318]. The method consisted in the large area CVD growth of monolayer graphene films on Cu foils which were repeatedly transferred to flexible poly(ethylene terephthalate) (PET)-Au substrates for obtaining multi-layered graphene. Afterwards, ultraviolet laser processing led to the local ablation and patterning of interdigitated electrodes with micrometric resolution (**Figs. 6a-e**). In this way, dense arrays of highly bendable ultrathin µSCs were fabricated. As observed in **Fig. 6f**, SCs assembled with PVA/H$_2$SO$_4$ hydrogel exhibited a maximum capacitance of ca. 63 µF cm^{-2} at 10 mV s^{-1}. Their capacitance increased with the number of stacked graphene layers, due to the extra contribution from the edges of the graphene monolayers. The µSCs displayed double-layer charge storage behaviour, fast ionic diffusion at extremely high sweep rates (up to 500 V s^{-1}), and remarkable stability over 20000 charge-discharge cycles at 100 V s^{-1}. Based on this fast SC technology, AC line-filtering devices, flexible integrated circuits comprising a diode bridge rectifier, a line-filter system containing fast µSCs, an array of hybrid graphene-PANI µSCs for energy harvesting, and pressure/gas sensors were all successfully fabricated. Despite the outstanding performance of the devices, one should notice that large-scale laser micromachining of CVD-grown graphene still presents important drawbacks such as the modest throughput and high costs involved.

When compared to graphene, the laser processing of GO materials provides some benefits due to the lower cost and extensive industrial production, even if the electrical conductivity of rGO is lower than CVD-grown graphene. As a notable example, Kwon *et*

al. demonstrated the laser fabrication of high quality graphene-based µSCs by photothermal CO_2 laser-assisted reduction of GO layers and subsequent photochemically-driven UV pulsed laser ablation of the resulting LrGO [319]. As a result, the laser-patterned interdigitated electrodes exhibited larger specific surface area and better capacitive properties than chemically reduced GO electrodes used as reference. Flexible SCs with different electrode configurations were also created, revealing a maximum areal capacitance of ca. 44 mF cm^{-2} at a 10 mV s^{-1} sweep rate. In a more recent work, Kamboj *et al*. have adopted a similar strategy for the development of on-chip flexible µSCs composed of highly conductive graphene foam [320]. Firstly, a layer of electrochemically reduced GO sheets deposited on PET substrates was submitted to CO_2 laser irradiation for increasing the degree of rGO reduction as well as achieving partial edge fusion interconnection between rGO sheets, which led to an enhancement of the structural and electrical properties. Interdigitated electrodes were then machined in the rGO foam via localized ablation using a near-IR (1.06 µm) laser source. Programmable laser writing allowed the fast and versatile patterning of electrodes and devices with different geometries. The fabricated µSCs revealed ca. 2.3 mF cm^{-2} of areal capacitance at 10 mA cm^{-2} current density, a working voltage of 1.2 V in aqueous solid electrolyte, as well as outstanding cycling stability over 100000 continuous charge-discharge cycles. Arrays of SC devices were also created, exhibiting a cell voltage of 10.8 V and significant capacitive performance, even when subjected to a sweep rate of 100 V s^{-1}.

Besides the laser patterning of graphene-based films for their physical isolation and definition of independent planar SC electrodes, subtractive laser fabrication methods have also been used for attaining other technological improvements. Thereby, 3D micromachining of rGO films enabled the fabrication of flexible SCs with excellent adherence to a polymeric substrate [321]. In this approach, LrGO patterns growing perpendicular to the substrate were obtained by high-repetition-rate femtosecond pulsed laser irradiation. The rGO vertical structures, sharing a common rGO basal layer, were further coated with a thin gold film and embedded into a PDMS matrix. The vertical structures fixed to the PDMS substrate operated as hooks, providing well-adhered, highly elastic and conductive rGO electrodes and fully wearable SC devices. Using a different strategy, Gao *et al*. fabricated extremely elastic multidimensional µSCs by laser cutting of full solid state macroscopic SCs [322]. Sandwiched sheet-like SC structures were assembled by chemical/calcination methods using carbon paper coated with ionic liquid-

modified rGO as electrodes and filter papers covered with carbon paste as separators. Afterwards, the SCs were patterned into several 2D and 3D designs with the help of a 355 nm ultraviolet laser. The μSCs were mechanically robust, showing no cracks after the laser cutting process. The devices exhibited good areal capacitance (27.4 mF cm^{-2}), high energy density (32.1 μWh cm^{-2}), and wide operating voltage window (0−3 V). As observed in **Figs. 6g-l**, as-fabricated 2D and 3D tensile μSCs did not show noticeable variation of their charge storage properties while enduring substantial stretching deformation. Hondred *et al*. developed highly porous graphene-based electrodes and SCs by CO_2 laser processing of films obtained from rGO inks incorporating micron sized salt crystals (as porogens) [323]. The salt crystals generated micrometric pores into the rGO during the ink drying step. Further laser irradiation simultaneously improved the welding among rGO flakes, increasing film conductivity, and etched the rGO sheets, facilitating the formation of micropores and additional edge defects, which augmented the electroactive surface area. The salt crystals were subsequently removed by washing with water, leaving a highly porous structure. Consequently, the electrodes obtained with salt-generated pores displayed enhanced double layer capacitance when compared to those obtained without salt, due to the larger surface-electrolyte contact, enabling the fabrication of SCs with higher energy density.
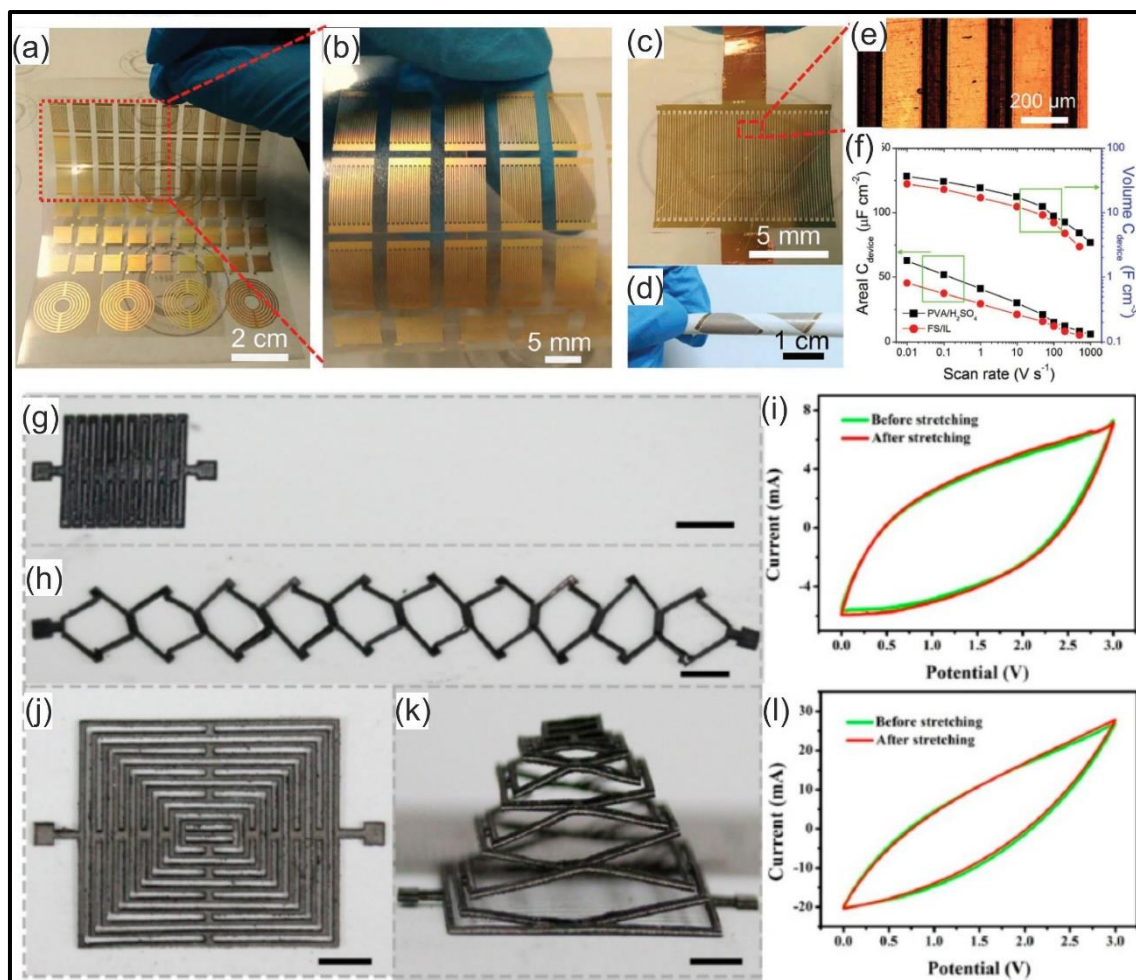
Fig. 6. (a, b) Optical images of micropatterned SC arrays with different geometries on PET substrates. Photographs of interdigital SC on (c) PET and on (d) more flexible PTFE foils. (e) Magnified optical image from (c) showing the machined electrodes. (f) Evolution of areal and volumetric capacitances with sweep rate and type of electrolyte. Reproduced from [318] with permission of WILEY-VCH Verlag. (g, h) 2D µSC before and after stretching. (i) CV curves of the 2D µSC before and after stretching. (j, k) 3D µSC before and after stretching. (f) CV curves of the 3D µSC before and after stretching. Scale bars in (g, h, j, k) correspond to 1 cm. Reproduced from [322] with permission of ACS.

4.3.2. MAPLE for supercapacitor electrodes

Laser-driven evaporation has been investigated for the deposition of graphene-based SC electrodes via the reactive inverse MAPLE technique (RIMAPLE). Inverse MAPLE of nanoentities allows their deposition through the pulsed laser irradiation of frozen dispersions. Flexible composite electrodes constituted by N-doped rGO with and without decoration by NiO nanostructures have been obtained by UV laser reactive deposition of GO flakes and NiO NPs dispersed in frozen aqueous targets containing ammonia, urea or melamine molecular compounds [324]. As depicted in **Figs. 7a, b**, the 266nm nanosecond pulsed laser radiation is absorbed by the GO flakes and NiO NPs, leading to their fast

heating up to hundreds or even thousands of degrees for GO flakes and NPs, respectively. GO flakes, whose temperature increases with the number of sheets, become reduced by both photochemical and photothermal mechanisms. In the targets containing NiO NPs, the NPs reach their melting temperature and undergo de-wetting processes. The GO and NiO nanoentities lead to the fast heating of the surrounding frozen matrix, triggering the decomposition of the N-containing molecules which react with GO, leading to N-doping, as well as sublimation and explosive boiling of water vapor which transports the nanomaterials towards the facing substrate. The end result of the laser processing is a porous coating consisting of rGO flakes with nanometre-sized NiO crystals. A maximum volumetric capacitance of 350 F cm^{-3} at 10 mV s^{-1}, corresponding to roughly 1000 F g^{-1}, was obtained using the melamine precursor (**Fig. 7c**). The electrodes containing NiO nanostructures revealed higher thicknesses (tens of μm) and robustness, but about one order of magnitude lower capacitance (up to 13 F cm^{-3}), probably due to the low active surface area of the film and the low degree of GO reduction. SCs fabricated with these electrodes revealed excellent cycling stability at high current densities (up to 50000 cycles at hundreds of A g^{-1}). In a similar work, citric acid, ascorbic acid and imidazole precursors, easily reacted with GO during laser irradiation, were used for tailoring the reduction and N-doping processes of GO during MAPLE [325]. Depending on the precursor, the rGO sheets displayed dissimilar amounts of nanoholes and furrows, besides differences in composition. The formation of nanoholes, which are important for increasing the electrochemically active surface sites, has been related to the reduction process of GO in the presence of water [326]. The imidazole precursor promoted the synthesis of N-doped rGO with the higher degree of reduction and N-doping, leading to the formation of electrodes with the largest volumetric capacitance (114 F cm^{-3} at 10 mV cm^{-1}). Symmetric and asymmetric electrochemical capacitors were fabricated, displaying good performance over 10000 charge-discharge cycles at high specific currents.

By adopting the MAPLE methodology, there is a great flexibility in the synthesis of complex compounds and the activation of coupled physical mechanisms between the reactants. In this context, the incorporation of MWCNTs in the targets allowed the deposition of GO-MWCNT-NiO composite films with increased porosity [327]. As displayed in **Figs. 7d-f**, homogeneous composites constituted by NiO-coated rGO and MMWCNTs were obtained in a simple way, leading to a substantial enhancement of capacitance (from 4 to 20 F cm^{-3} at 10 mV s^{-1} by adding just 1 wt.% of MWCNTs). Electrochemical investigations indicated that N-containing groups in rGO and MWCNTs

mainly added EDL charge storage, probably due to an increase of material porosity and edge defects, whereas redox reactions represented only a minor contribution. Due to the creation of meso-macropores that harbour NiO aggregates, the loading of MWCNTs led to an increase in the diffusion-controlled charge storage mechanisms versus capacitive ones in rGO-based electrodes. Analogous studies carried out using graphene sheets instead of GO flakes revealed comparable electrochemical performance of the graphene electrodes. Other works reported the fabrication of electrochemical energy storage electrodes composed of rGO decorated with Fe_3O_4 nanostructures as well as rGO-MWCNT-ZnO and rGO-MWCNT-CeO_x-MnO_x composites [328, 329,X]. It is worth mentioning the distinct approach adopted by Ajnsztajn *et al*. in which the fabrication of transparent supercapacitive electrodes incorporating 2D MXene nanomaterials has recently been accomplished using the resonant infrared MAPLE deposition [330]. In conclusion, the reported works indicate that, although the MAPLE technology is still in its infancy, it is a highly versatile and easy route for the fabrication of graphene-based energy storage electrodes with high innovation potential.
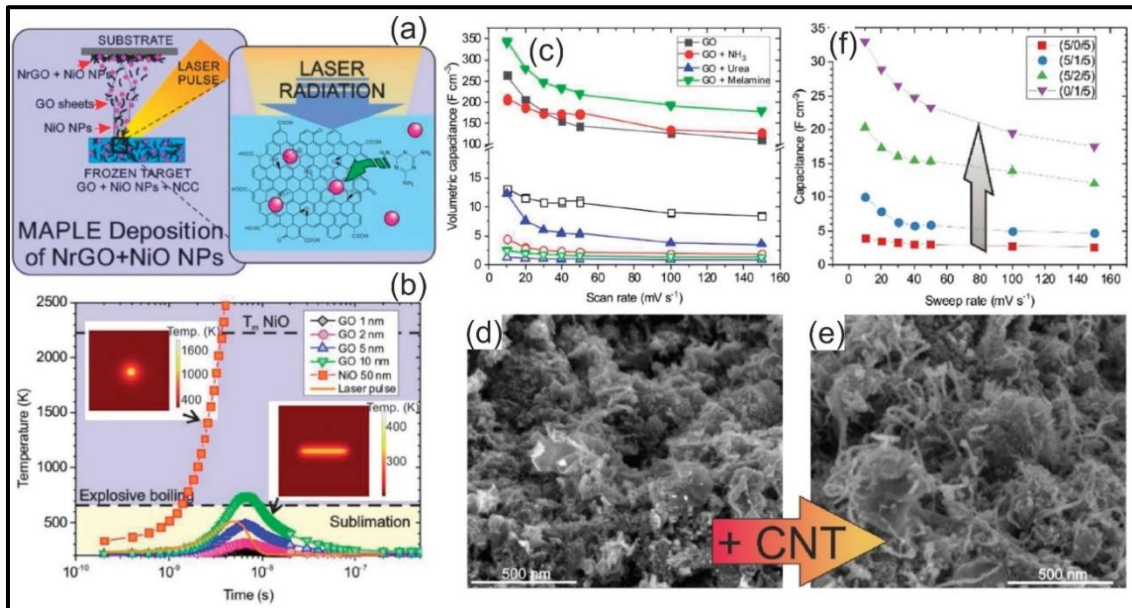

Fig. 7. (a) Schematic representation of the RIMAPLE process. (b) Simulated temperature of GO flakes and NiO NPs subjected to one UV laser pulse of 400 mJ cm^{-2}. Insets: temperature distribution maps in a 50 nm NiO NP and a 10 nm thick GO flake after 3 ns. (c) Volumetric capacitance of GO-NiO electrodes versus sweep rate. The open symbols denote the samples synthesized with NiO NPs. Reproduced from [324] with permission of RSC. High-resolution SEM images of GO–CNT–NiO samples with (d) (5/0/5) and (e) (5/1/5) relative wt.% concentrations. (f) Volumetric capacitance of GO–CNT–NiO samples obtained with different relative concentrations. Reproduced from [327] with permission of RSC.

4.3.3. LIFT and related techniques for energy storage devices

LIFT and LIBT are deposition/transfer methods which have already been studied by several groups and applied to a variety of functional devices [331-334], however their use in energy storage applications has, so far, been very restricted, and the few examples of carbon-containing LIFT electrodes for batteries have been largely concentrated in the same research group. This is actually surprising, given the large volume of research on electronic and optical devices relying on these laser transfer techniques.

In the pioneering work of Piqué and co-workers, published almost 20 years ago, the use of LIFT for the fabrication of energy storage devices has been investigated. The authors used a thick film made from a paste consisting of hydrous ruthenium oxide and 5M sulphuric acid (the electrolyte) as the donor film for their capacitors, and defined the boundaries of the device by laser micromachining [335]. Shortly after this work, they reported the fabrication of Li-ion microbatteries by LIFT [336]. This was an impressive development, since they succeeded to deposit the whole multilayer device using LIFT. A battery having a 40 µm thick $LiCoO_2$/carbon/PVDF composite cathode, and a 60 µm thick mesoporous carbon microbeads/carbon composite anode exhibited a specific capacity of 97.8 mAh/g. Slight changes to the basic characteristics of the batteries, such as composition [337] were reported in another publication, and, in another article, laser structuring of the LIFT-deposited layers [338] has been studied, with mixed results (a slight decrease in capacitance and an improvement in cyclic stability). **Fig. 8** shows a cross-sectional view of a LIFT-fabricated microbattery, both schematically (**Fig. 8a**) and in a SEM image taken from a real device (**Fig. 8b**).
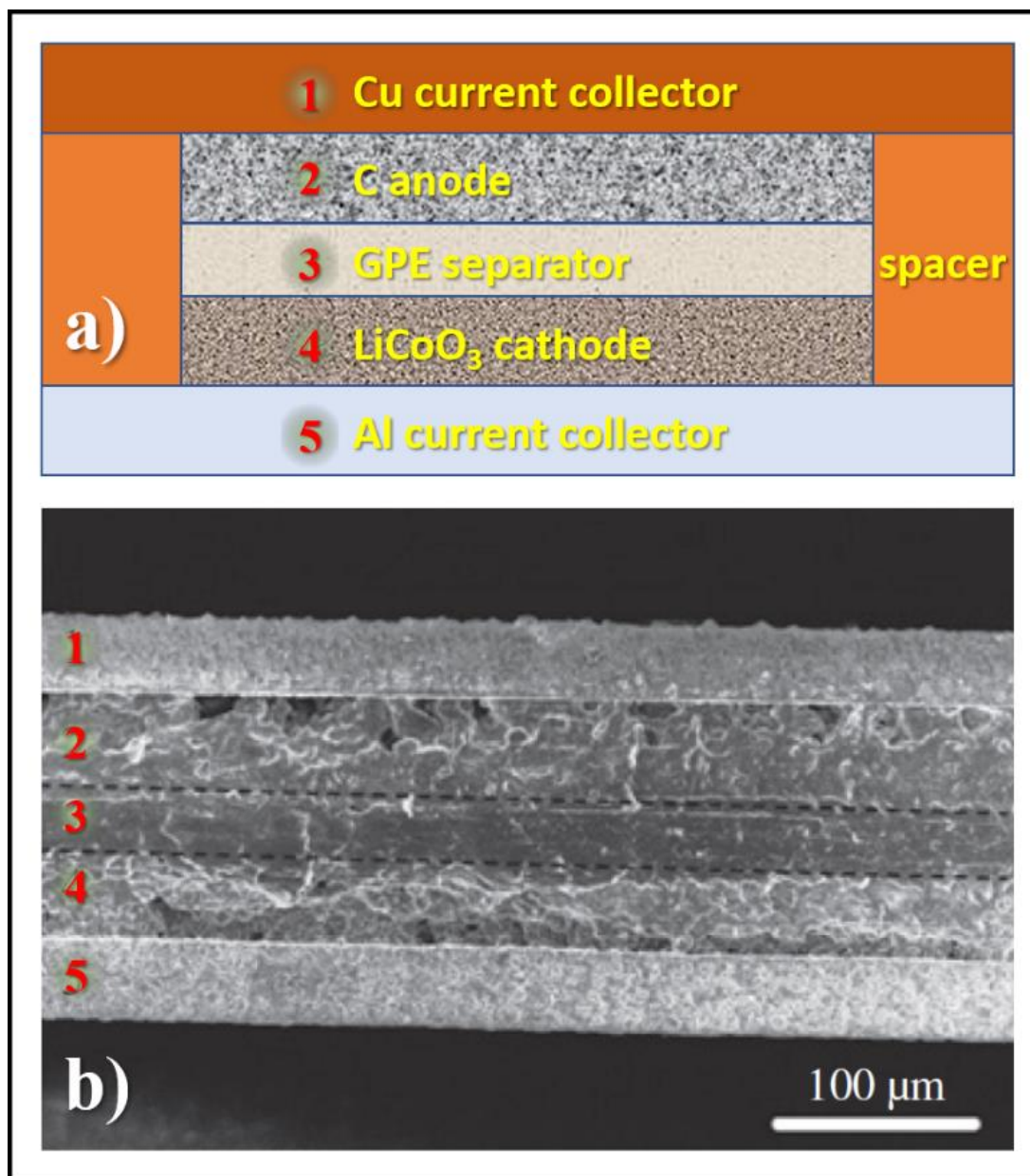
Fig. 8. (a) Schematic cross-sectional structure of a LIFT-fabricated microbattery; (b) SEM image of a real battery showing the layers corresponding to the drawing in (a). Reproduced from [337] with permission from Elsevier.

Praeger *et al.* [339] have recently demonstrated LIBT of monolayer CVD grown graphene using single femtosecond laser pulses. They used a digital micromirror device for spatial modulation of the irradiation intensity across a spot in the donor film, attenuating the laser intensity (by digital dithering) in the circle interior, while applying the full level of fluence to the perimeter of the region to be transferred. The authors have also performed graphene LIBT under reduced pressures, and in both strategies, their idea was to accomplish better detachment of the donor layer and preservation of the original shape in the receiving substrate. Carbon nanowalls [340] and carbon nanowall/SnO$_2$

hybrid materials [220] have also been deposited by Dinescu and co-workers through LIFT. In spite of the clear applicability of these carbon materials as electrochemical electrodes due to their high conductivity, large surface area, and even incorporating the pseudocapacitive tin oxide, the authors did not evaluate the performance of the resulting materials as electrodes in energy storage devices.

A new laser processing approach, which can be considered as derived from LIG, LIFT and LIBT, has been discovered and is under current development by our group. Since this review has discussed the main laser processing strategies for graphene synthesis and modification, we considered appropriate to disclose some preliminary results which should interest many researchers, since the method allows the simultaneous synthesis, modification and transfer of graphene patterns to almost any type of substrate (including flexible polymers). The method has been discovered by chance (a common occurrence which is not so commonly acknowledged), and its huge potential became immediately apparent.

During a study of the effect of laser processing conditions on the structure and properties of supercapacitors made by laser-treating polyimide sheets, we decided to enclose the polyimide films between two microscope slides, in order to avoid the pronounced wrinkling of the polymer upon laser carbonization, which was inducing changes in the laser spot size due to random defocusing episodes. By keeping the PI sheets flat, the "sandwich" setup indeed solved the problem, as expected, but this was not the only consequence. Later, when we increased the laser fluence as part of our studies, we noticed that the interdigitated supercapacitor patterns had been replicated in the upper glass slide (the one crossed by the laser). **Fig. 9a** shows a schematic drawing of the experimental configuration (a glass/PI/glass sandwich) and the simple operations used for simultaneous direct laser writing and transfer. **Fig. 9b** shows a photograph of a real sample assembly, as well as an example of the LIG electrodes sharply defined in the polyimide, with a good resolution (individual scan lines ~25μm thick). **Fig. 9c** shows an example of electrode patterns effortlessly generated and transferred to a glass slide, and a Raman spectrum with the characteristic peaks from graphene, obtained from a LIG pattern imprinted on glass. The patterns transferred using high fluence treatments exhibited extremely good adherence. They could not be erased from the glass by rubbing with the fingers, and in some cases, even by scratching with metallic tweezers. Similar results have been obtained by placing another polymer sheet (PDMS) together with the

polyimide; **Fig. 9d** shows an example of LIG patterns generated and simultaneously transferred to PDMS.

The reasons for the high adhesion of LIG to the glass and PDMS substrates have not yet been positively determined, although there are indications of glass melting at the surface in contact with the polyimide. For the PDMS, the picture is further complicated by the fact that, under the appropriate experimental conditions, the 355 nm UV laser is able to carbonize the material, even if its optical absorption is very low at this wavelength. The resulting carbon patterns in the PDMS are expected to accumulate the contributions from both LIG transfer and PDMS carbonization. The electrical resistivity of the patterns transferred to glass varies in a wide range, depending on the processing conditions. Until now, the sample with the best properties (on glass) exhibited a resistivity of $68\mu\Omega m^{-1}$, with the corresponding twin pattern in the PI displaying a value of $32~\mu\Omega m^{-1}$.
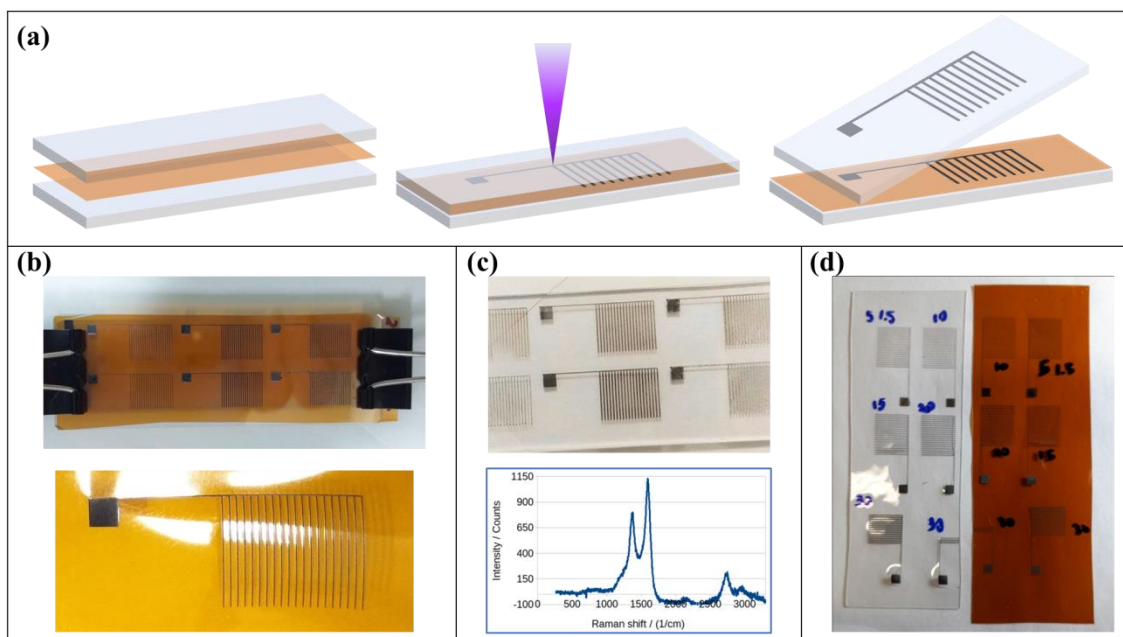

Fig. 9. (a) Illustration of the local arrangement for simultaneous LIG and LIBT of graphene patterns; (b) Photograph of a setup after writing interdigitated capacitor test patterns, with the paper clips used for keeping the layers of the "sandwich" in contact. The lower image shows an individual LIG electrode written with good resolution (lines ~25μm thick); (c) Example of LIG electrode patterns transferred to a glass slide, with the presence of graphene confirmed by the graph exhibiting characteristic Raman peaks; (d) LIG patterns written in polyimide and the corresponding replication in a PDMS sheet.

Alternative ways to decorate the laser-induced graphene patterns have already been tested with very positive results. Gold films were deposited (by sputtering) on selected regions of the polyimide foils prior to the laser processing of electrodes for biological sensors. **Fig. 10a** shows a picture of one sensor, as well as SEM images of the

resulting microstructure. One can notice uniformly distributed gold droplets (in the 5 μm - 10 μm range) embedded in a matrix of graphene sheets. In the inset picture showing a higher magnification, there is an indication that the confined environment during polymer graphitization forced the graphene sheets to assume a new, more compact configuration, different from the normal (unrestrained) "rosebud-like" morphology of LIG. Alternatively, the top glass in the sandwich can be coated with thick or thin films for simultaneous synthesis, doping/decoration and transfer. As an example of application, niobium oxide films were sputtered on the top glass slide for direct laser fabrication of flexible hybrid supercapacitors. **Fig. 10b** shows a set of supercapacitors ready for testing, and a TEM high resolution image showing the presence of Nb_2O_5 grains (~3nm) among the graphene sheets.
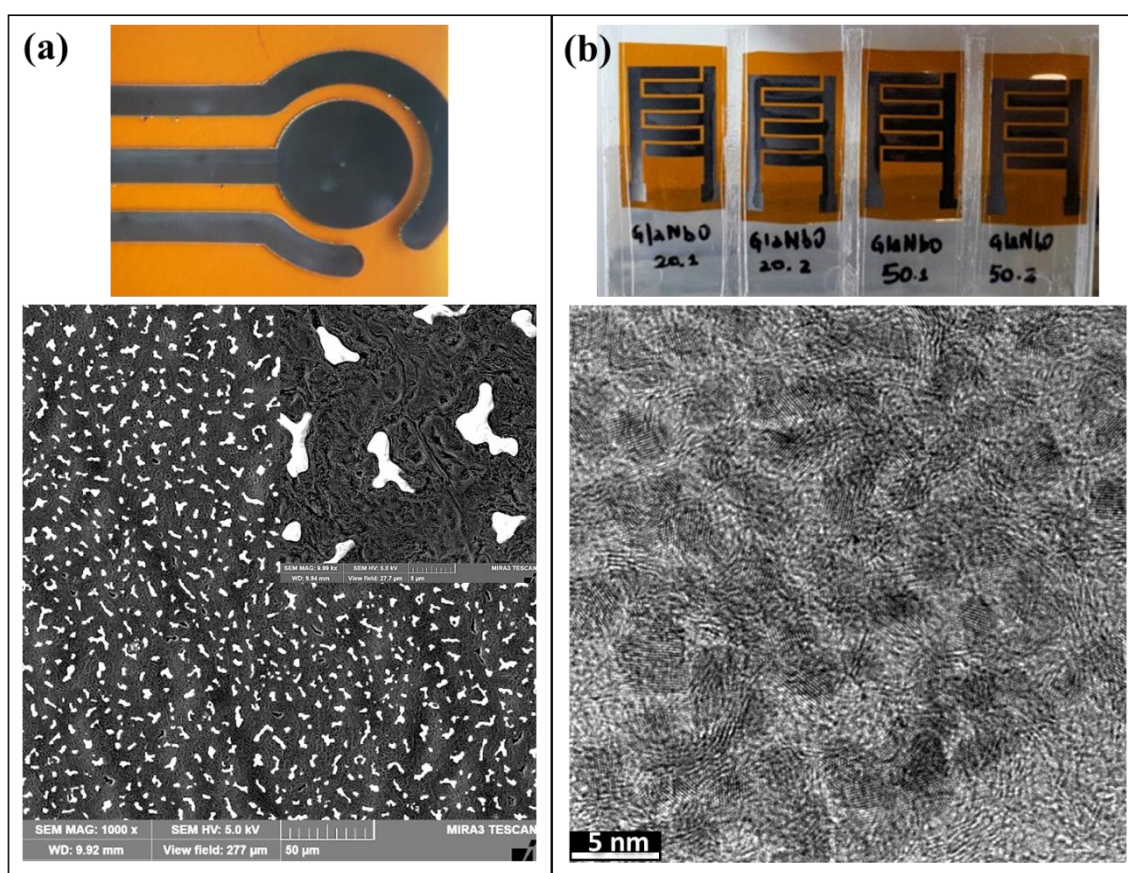

Fig. 10. (a) Biological electrochemical sensor incorporating gold particles in the active circular region, with the corresponding SEM images showing gold droplets uniformly dispersed in the graphene matrix. The morphology of LIG in a confined environment seems to consist of more densely packed graphene sheets; (b) Flexible graphene/Nb_2O_5 hybrid supercapacitors and the corresponding high resolution TEM image showing the nanometric scaled oxide grains mixed with the graphene sheets.

At this early stage in the research, there are still some outstanding practical problems that need to be solved (or, at least, circumvented). The more troublesome is the

generation of liquid by-products during the carbonization process. Due to the confined environment, the liquid may gradually accumulate, interfering in the cooling rate of the treated material and in the optical path of the laser (due to bubble formation). Depending on the processing conditions, the thickness of the polyimide layer and the design and dimensions of the laser-treated device, the writing/transfer processes might not be affected, with very good final results. On the other hand, for extremely unfavourable conditions, the written device may be riddled with defective regions due to the irregular attachment of the graphene flakes upon separation of the sandwich.

Forward transfer of the graphene patterns to the underlying glass has also been successfully accomplished, using higher fluences and thinner PI sheets. The method is very straightforward, opening the possibility for simultaneous synthesis, doping/decoration and transfer of graphene patterns to arbitrary substrates at room temperature and pressure. The extreme local conditions during the confined induction of graphitization can probably help chemical reactions, doping, and the intercalation of compounds in the multilayer graphene sheets.

Most researchers use CO_2 laser cutters/engravers for photothermal LIG processing. This is probably the main reason for the technique to remain undiscovered until now, since the long infrared wavelengths cannot cross soda-lime-silica (or borosilicate) glass slides. In our experiments we used a frequency tripled $NdYVO_4$ laser (355 nm), but the method could most probably be performed with other visible, near infrared or near UV lasers.

5. Conclusions and outlook

In summary, the current review article provided an outline of the recent progress in laser-based synthesis and modification of graphene and related materials, discussing the most important techniques applied to energy storage devices. For the fabrication of graphene-based electronics, laser processing is highly beneficial due to the short reaction times, area-selective modification, and generation of high-quality (impurity-free) graphene materials at low thermal budgets. For graphene patterning, laser ablation is arguably the most favourable route, but direct laser writing (graphitization) of flexible substrates is very attractive for future application purposes. Moreover, laser-irradiation assisted reduction of GO, as well as rGO doping, are also quite popular for the development of flexible electronics.

Laser-based techniques have been widely applied for developing sensing devices, actuators, flexible optoelectronic devices as well as integrated smart devices. For a summary of additional research on laser processing of graphene and related materials (not covered in the main text), the reader can refer to the table in the supplementary information. It is important to mention that apart from energy storage, the successful conversion of carbon-based natural resources into graphene materials through laser processing has accelerated the progress of bio-compatible electronics.

Laser-based technologies exhibit some unique characteristics which make them uniquely suited for the fabrication of graphene-based energy storage devices:

1. Fast processing: Laser thinning of graphene layers, precise local cutting and material removal, selective heteroatom-doping, and synthesis of high-purity graphene materials, all of these operations can be performed within extremely short times.

2. Impurity-free: For the construction of 3D porous graphene nano-architectures, laser processing is more favourable than the wet-chemical synthetic routes, as well as high-temperature growth processes.

3. Local heating: The ability of the laser techniques to induce site-specific thermal effects is exceedingly beneficial for tailoring the structural features of graphene without negatively affecting heat-sensitive substrates

4. Multiple effects: Laser methods allow more than one operation to be performed during a single processing step. Thus synthesis, deposition, patterning, reduction, doping, etc. are some of the technologically relevant processes that can be induced to take place simultaneously, for faster and cheaper fabrication of energy storage devices.

In spite of the rapid progress of laser technologies for processing of graphene materials, a few challenges should still be properly addressed for the widespread commercialization of graphene-based devices. Some of the most pressing issues are:

1. Direct laser writing of graphene (as in LIG) can be successfully achieved only in a very few types of substrates (normally polymers with six-membered rings in their basic structure). As a whole, this processing technique suffers from low fabrication efficiency. In this regard, more research (and practical demonstrations) on parallel processing methods would be highly desirable for achieving viable, wide scale production of graphene devices.

2. Although numerous investigations using different laser technologies have already been carried out, the exact mechanisms for accurate property tuning of graphene

materials through laser processing have not yet been clearly understood. Even if the good results already reported indicate some directions, or general trends.

3. The results of some of the laser processing techniques are highly sensitive to small changes in the processing parameters (narrow "processing windows"). From a commercial point of view, these techniques should be optimized for achieving a more robust fabrication which would ensure higher yields.

4. For many of the practical energy storage applications, the capacitance of μSCs based on laser-induced graphene should be further enhanced. The combination of graphene materials with pseudocapacitive materials and other forms of carbon nanostructures still needs more research, especially focusing on building specific architectures which are more favourable for high performance device operation.

5. Some key issues related to the laser processing of graphene, like the recovery of the sp^2 network in GO, the synthesis of less defective laser-induced graphene, etc. are still not fully understood, and therefore, they cannot be satisfactorily controlled.

6. The relationship between the characteristics of the laser irradiation and the functionalization of graphene has not yet been systematically investigated. This knowledge will be beneficial for linking structure-property relations to the variables of laser processing.

Regarding the possible directions for future research: Laser-based additive manufacturing methods (laser stereolithography, laser sintering, laser melting) have been increasingly applied to the fabrication of functional devices, including SCs and batteries. 3D printing associated with laser carbonization has a huge potential for fabrication of functional polymer parts, including sensors or other electronic components. Microfluidics and lab-on-a-chip devices are some of the additively manufactured products which could also benefit from the inclusion of easily fabricated conductive carbon electrodes and even fully-functional electrical and electronic devices.

Maybe some more research effort should be shifted towards the application of laser-driven deposition approaches, such as LIFT and LIBT. These direct-writing (or transfer) techniques have already been adequately studied (especially LIFT), and used for depositing carbon materials (including graphene by LIBT). They have also been applied to electronic devices, including batteries. However, the storage devices based on graphene materials are still a wide open field for both techniques. With the possibility of sequentially depositing different solids and liquids, and in some cases, even building hybrid 3D electrodes incorporating higher amounts of pseudocapacitive materials, these

techniques should provide ample ground for experimentation and development of charge storage devices.

We finish this survey with a reminder about the importance of properly describing laser-based treatments. Unfortunately, some researchers (especially those using CO_2 laser engraving or cutting machines) are still oblivious to the negative aspects of reporting their experiments using terms which are borrowed from traditional printing practices. Although they might be conveying an accurate description of the parameters, as they appear in the machine display, the conditions are not defined in a physically meaningful way, and can only be replicated by using the same type of equipment. This is a serious problem, but it is not the only detrimental aspect, since researchers should always plan their experiments taking into consideration the light-matter interactions, and these are actually ruled by the variables described at the beginning of this review (laser power, wavelength, pulse width and repetition rate, spot size and writing speed). The results should, accordingly, be analysed taking into consideration parameters such as the fluence of radiation and the degree of laser spot overlap as the beam is scanned on the material, for example. Reviewers of research articles describing laser-based work could also play a bigger role, remembering the authors that the adequate reporting of laser treatment conditions is an essential step for keeping the pace of ongoing advances in the laser processing of graphene and its derivatives.

Although the laser-based approaches are quite new in the processing of graphene materials, when compared to other methods, we anticipate the technology to become invaluable for the fabrication of advanced devices in the near future.

Acknowledgements

References

[1] Liang K, Li L, Yang Y. Inorganic Porous Films for Renewable Energy Storage. ACS Energy Letters. 2017;2:373-90.

[2] Yu G, Hu L, Vosgueritchian M, Wang H, Xie X, McDonough JR, et al. Solution-Processed Graphene/MnO2 Nanostructured Textiles for High-Performance Electrochemical Capacitors. Nano Letters. 2011;11:2905-11.

[3] Afzal S, Sengupta D, Sarkar A, El-Halwagi M, and, Elbashir N. Optimization Approach to the Reduction of CO2 Emissions for Syngas Production Involving Dry Reforming. ACS Sustainable Chemistry & Engineering. 2018;6:7532-44.

[4] Günther A, Barthelmes A, Huth V, Joosten H, Jurasinski G, Koebsch F, et al. Prompt rewetting of drained peatlands reduces climate warming despite methane emissions. Nature Communications. 2020;11.

[5] Adedoyin F, Ozturk I, Abubakar I, Kumeka T, Folarin O, Bekun FV. Structural breaks in CO2 emissions: Are they caused by climate change protests or other factors? Journal of Environmental Management. 2020;266:110628.

[6] Fan J, Hong H, Jin H. Life cycle global warming impact of CO2 capture by in-situ gasification chemical looping combustion using ilmenite oxygen carriers. Journal of Cleaner Production. 2019;234:568-78.

[7] Soutter ARB, Mõttus R. "Global warming" versus "climate change": A replication on the association between political self-identification, question wording, and environmental beliefs. Journal of Environmental Psychology. 2020;69:101413.

[8] Li C, Zhang Q, E S, Li T, Zhu Z, He B, et al. An ultra-high endurance and high-performance quasi-solid-state fiber-shaped Zn–Ag2O battery to harvest wind energy. Journal of Materials Chemistry A. 2019;7:2034-40.

[9] Gao T, Liao J, Wang J, Qiu Y, Yang Q, Zhang M, et al. Highly oriented BaTiO3 film self-assembled using an interfacial strategy and its application as a flexible piezoelectric generator for wind energy harvesting. Journal of Materials Chemistry A. 2015;3:9965-71.

[10] Prabhu K, Chandiran AK. Solar energy storage in a Cs2AgBiBr6 halide double perovskite photoelectrochemical cell. Chemical Communications. 2020;56:7329-32.

[11] Lin Y, Feng H, Chen R, Zhang B, An L. One-dimensional TiO2 nanotube array photoanode for a microfluidic all-vanadium photoelectrochemical cell for solar energy storage. Catalysis Science & Technology. 2020;10:4352-61.

[12] Hossain MS, Pandey AK, Rahim NA, Selvaraj J, Tyagi VV, Islam MM. Self-cleaning assisted photovoltaic system with thermal energy storage: Design and performance evaluation. Solar Energy. 2020;206:487-98.

[13] Li M, Addad A, Roussel P, Szunerits S, Boukherroub R. High performance flexible hybrid supercapacitors based on nickel hydroxide deposited on copper oxide supported by copper foam for a sunlight-powered rechargeable energy storage system. Journal of Colloid and Interface Science. 2020;579:520-30.

[14] Zhang Y, Liu J, Li S-L, Su Z-M, Lan Y-Q. Polyoxometalate-based materials for sustainable and clean energy conversion and storage. EnergyChem. 2019;1:100021.

[15] Park SH, Goodall G, Kim WS. Perspective on 3D-designed micro-supercapacitors. Materials & Design. 2020;193:108797.

[16] Wang X, Yushin G. Chemical vapor deposition and atomic layer deposition for advanced lithium ion batteries and supercapacitors. Energy & Environmental Science. 2015;8:1889-904.

[17] Kumar R, Sahoo S, Joanni E, Singh RK, Yadav RM, Verma RK, et al. A review on synthesis of graphene, h-BN and MoS2 for energy storage applications: Recent progress and perspectives. Nano Research. 2019;12:2655-94.

[18] Noori A, El-Kady MF, Rahmanifar MS, Kaner RB, Mousavi MF. Towards establishing standard performance metrics for batteries, supercapacitors and beyond. Chemical Society Reviews. 2019;48:1272-341.

[19] Kumar N S, Grekov D, Pré P, Alappat BJ. Microwave mode of heating in the preparation of porous carbon materials for adsorption and energy storage applications – An overview. Renewable and Sustainable Energy Reviews. 2020;124:109743.

[20] Shanmuga Priya M, Divya P, Rajalakshmi R. A review status on characterization and electrochemical behaviour of biomass derived carbon materials for energy storage supercapacitors. Sustainable Chemistry and Pharmacy. 2020;16:100243.

[21] Thomas P, Lai CW, Bin Johan MR. Recent developments in biomass-derived carbon as a potential sustainable material for super-capacitor-based energy storage and environmental applications. Journal of Analytical and Applied Pyrolysis. 2019;140:54-85.

[22] Wang J, Zhang X, Li Z, Ma Y, Ma L. Recent progress of biomass-derived carbon materials for supercapacitors. Journal of Power Sources. 2020;451:227794.

[23] Zhao X, Chen H, Kong F, Zhang Y, Wang S, Liu S, et al. Fabrication, characteristics and applications of carbon materials with different morphologies and porous structures produced from wood liquefaction: A review. Chemical Engineering Journal. 2019;364:226-43.

[24] Yuan K, Hu T, Xu Y, Graf R, Brunklaus G, Forster M, et al. Engineering the Morphology of Carbon Materials: 2D Porous Carbon Nanosheets for High-Performance Supercapacitors. ChemElectroChem. 2016;3:822-8.

[25] Hursán D, Samu AA, Janovák L, Artyushkova K, Asset T, Atanassov P, et al. Morphological Attributes Govern Carbon Dioxide Reduction on N-Doped Carbon Electrodes. Joule. 2019;3:1719-33.

[26] Samdani KJ, Kim SH, Park JH, Hong SH, Lee KT. Morphology-controlled synthesis of Co3O4 composites with bio-inspired carbons as high-performance supercapacitor electrode materials. Journal of Industrial and Engineering Chemistry. 2019;74:96-102.

[27] Kumar R, Singh RK, Tiwari VS, Yadav A, Savu R, Vaz AR, et al. Enhanced magnetic performance of iron oxide nanoparticles anchored pristine/ N-doped multi-walled carbon nanotubes by microwave-assisted approach. Journal of Alloys and Compounds. 2017;695:1793-801.

[28] Kumar R, Singh RK, Tiwari RS. Growth analysis and high-yield synthesis of aligned-stacked branched nitrogen-doped carbon nanotubes using sesame oil as a natural botanical hydrocarbon precursor. Materials & Design. 2016;94:166-75.

[29] Xu M, Yu Q, Liu Z, Lv J, Lian S, Hu B, et al. Tailoring porous carbon spheres for supercapacitors. Nanoscale. 2018;10:21604-16.

[30] Ye J, Zang J, Tian Z, Zheng M, Dong Q. Sulfur and nitrogen co-doped hollow carbon spheres for sodium-ion batteries with superior cyclic and rate performance. Journal of Materials Chemistry A. 2016;4:13223-7.

[31] Peng S, Li L, Kong Yoong Lee J, Tian L, Srinivasan M, Adams S, et al. Electrospun carbon nanofibers and their hybrid composites as advanced materials for energy conversion and storage. Nano Energy. 2016;22:361-95.

[32] Liu Y, Jiang G, Huang Z, Lu Q, Yu B, Evariste U, et al. Decoration of Hollow Mesoporous Carbon Spheres by NiCo2S4 Nanoparticles as Electrode Materials for Asymmetric Supercapacitors. ACS Applied Energy Materials. 2019;2:8079-89.

[33] Ding J, Zhang H, Zhou H, Feng J, Zheng X, Zhong C, et al. Sulfur-Grafted Hollow Carbon Spheres for Potassium-Ion Battery Anodes. Advanced Materials. 2019;31:1900429.

[34] Fu X, Liu L, Yu Y, Lv H, Zhang Y, Hou S, et al. Hollow carbon spheres/hollow carbon nanorods composites as electrode materials for supercapacitor. Journal of the Taiwan Institute of Chemical Engineers. 2019;101:244-50.

[35] Wang X, Wang S, Shen K, He S, Hou X, Chen F. Phosphorus-doped porous hollow carbon nanorods for high-performance sodium-based dual-ion batteries. Journal of Materials Chemistry A. 2020;8:4007-16.

[36] Li Z, Guo D, Liu Y, Wang H, Wang L. Recent advances and challenges in biomass-derived porous carbon nanomaterials for supercapacitors. Chemical Engineering Journal. 2020;397:125418.

[37] Liu P, Wang Y, Liu J. Biomass-derived porous carbon materials for advanced lithium sulfur batteries. Journal of Energy Chemistry. 2019;34:171-85.

[38] Benzigar MR, Talapaneni SN, Joseph S, Ramadass K, Singh G, Scaranto J, et al. Recent advances in functionalized micro and mesoporous carbon materials: synthesis and applications. Chemical Society Reviews. 2018;47:2680-721.

[39] Geim AK, Novoselov KS. The rise of graphene. Nature Materials. 2007;6:183-91.

[40] Kumar R, Joanni E, Singh RK, Singh DP, Moshkalev SA. Recent advances in the synthesis and modification of carbon-based 2D materials for application in energy conversion and storage. Progress in Energy and Combustion Science. 2018;67:115-57.

[41] Singh RK, Kumar R, Singh DP. Graphene oxide: strategies for synthesis, reduction and frontier applications. RSC Advances. 2016;6:64993-5011.

[42] Nardecchia S, Carriazo D, Ferrer ML, Gutiérrez MC, del Monte F. Three dimensional macroporous architectures and aerogels built of carbon nanotubes and/or graphene: synthesis and applications. Chemical Society Reviews. 2013;42:794-830.

[43] Kumar R, Sahoo S, Joanni E, Singh RK, Maegawa K, Tan WK, et al. Heteroatom doped graphene engineering for energy storage and conversion. Materials Today. 2020.

[44] Kumar R, Sahoo S, Joanni E, Singh RK, Tan WK, Kar KK, et al. Recent progress in the synthesis of graphene and derived materials for next generation electrodes of high performance lithium ion batteries. Progress in Energy and Combustion Science. 2019;75:100786.

[45] Ambrosi A, Chua CK, Latiff NM, Loo AH, Wong CHA, Eng AYS, et al. Graphene and its electrochemistry – an update. Chemical Society Reviews. 2016;45:2458-93.

[46] Reiss T, Hjelt K, Ferrari AC. Graphene is on track to deliver on its promises. Nature Nanotechnology. 2019;14:907-10.

[47] Ferrari AC, Bonaccorso F, Fal'ko V, Novoselov KS, Roche S, Bøggild P, et al. Science and technology roadmap for graphene, related two-dimensional crystals, and hybrid systems. Nanoscale. 2015;7:4598-810.

[48] Novoselov KS, Fal′ko VI, Colombo L, Gellert PR, Schwab MG, Kim K. A roadmap for graphene. Nature. 2012;490:192-200.

[49] Shivananju BN, Yu W, Liu Y, Zhang Y, Lin B, Li S, et al. The Roadmap of Graphene-Based Optical Biochemical Sensors. Advanced Functional Materials. 2017;27:1603918.

[50] Huo P, Zhao P, Wang Y, Liu B, Yin G, Dong M. A Roadmap for Achieving Sustainable Energy Conversion and Storage: Graphene-Based Composites Used Both as an Electrocatalyst for Oxygen Reduction Reactions and an Electrode Material for a Supercapacitor. Energies. 2018;11:167.

[51] Tsang CHA, Huang H, Xuan J, Wang H, Leung DYC. Graphene materials in green energy applications: Recent development and future perspective. Renewable and Sustainable Energy Reviews. 2020;120:109656.

[52] Solís-Fernández P, Bissett M, Ago H. Synthesis, structure and applications of graphene-based 2D heterostructures. Chemical Society Reviews. 2017;46:4572-613.

[53] Kumar R, Singh RK, Singh DP. Natural and waste hydrocarbon precursors for the synthesis of carbon based nanomaterials: Graphene and CNTs. Renewable and Sustainable Energy Reviews. 2016;58:976-1006.

[54] Kumar R, Singh RK, Singh DP, Joanni E, Yadav RM, Moshkalev SA. Laser-assisted synthesis, reduction and micro-patterning of graphene: Recent progress and applications. Coordination Chemistry Reviews. 2017;342:34-79.

[55] Gamaly EG. The physics of ultra-short laser interaction with solids at non-relativistic intensities. Physics Reports. 2011;508:91-243.

[56] Bauerle D. Laser Processing and Chemistry. Forth ed. Heilderberg: Springer; 2011.

[57] Huang X, Guo Q, Yang D, Xiao X, Liu X, Xia Z, et al. Reversible 3D laser printing of perovskite quantum dots inside a transparent medium. Nature Photonics. 2020;14:82-8.

[58] Liu H, Liu Y, Guo W, Zhou X, Lin L, Peng P. Laser assisted ink-printing of copper oxide nanoplates for memory device. Materials Letters. 2020;261:127097.

[59] Jin HM, Lee SH, Kim JY, Son S-W, Kim BH, Lee HK, et al. Laser Writing Block Copolymer Self-Assembly on Graphene Light-Absorbing Layer. ACS Nano. 2016;10:3435-42.

[60] Kabashin AV, Singh A, Swihart MT, Zavestovskaya IN, Prasad PN. Laser-Processed Nanosilicon: A Multifunctional Nanomaterial for Energy and Healthcare. ACS Nano. 2019;13:9841-67.

[61] Esqueda-Barrón Y, Herrera M, Camacho-López S. ZnO synthesized in air by fs laser irradiation on metallic Zn thin films. Applied Surface Science. 2018;439:681-8.

[62] Queraltó A, Pérez del Pino A, de la Mata M, Arbiol J, Tristany M, Obradors X, et al. Ultrafast Epitaxial Growth Kinetics in Functional Oxide Thin Films Grown by Pulsed Laser Annealing of Chemical Solutions. Chemistry of Materials. 2016;28:6136-45.

[63] Palneedi H, Park JH, Maurya D, Peddigari M, Hwang G-T, Annapureddy V, et al. Laser Irradiation of Metal Oxide Films and Nanostructures: Applications and Advances. Advanced Materials. 2018;30:1705148.

[64] Sun X, Ehrhardt M, Lotnyk A, Lorenz P, Thelander E, Gerlach JW, et al. Crystallization of Ge2Sb2Te5 thin films by nano- and femtosecond single laser pulse irradiation. Scientific Reports. 2016;6:28246.

[65] Lee J, Seok JY, Son S, Yang M, Kang B. High-energy, flexible micro-supercapacitors by one-step laser fabrication of a self-generated nanoporous metal/oxide electrode. Journal of Materials Chemistry A. 2017;5:24585-93.

[66] Wang G, Zhang Y, Yang H, Wang W, Dai Y-Z, Niu L-G, et al. Fast-response humidity sensor based on laser printing for respiration monitoring. RSC Advances. 2020;10:8910-6.

[67] Kaidarova A, Alsharif N, Oliveira BNM, Marengo M, Geraldi NR, Duarte CM, et al. Laser-Printed, Flexible Graphene Pressure Sensors. Global Challenges. 2020;4:2000001.

[68] Huang G-W, Feng Q-P, Xiao H-M, Li N, Fu S-Y. Rapid Laser Printing of Paper-Based Multilayer Circuits. ACS Nano. 2016;10:8895-903.

[69] Li Q, Grojo D, Alloncle A-P, Chichkov B, Delaporte P. Digital laser micro- and nanoprinting. Nanophotonics. 2018;8:27-44.

[70] Yu Y, Bai S, Wang S, Hu A. Ultra-Short Pulsed Laser Manufacturing and Surface Processing of Microdevices. Engineering. 2018;4:779-86.

[71] Wang X, Xu B, Chen Y, Ma C, Huang Y. Fabrication of micro/nano-hierarchical structures for droplet manipulation via velocity-controlled picosecond laser surface texturing. Optics and Lasers in Engineering. 2019;122:319-27.

[72] Xiong W, Zhou Y, Hou W, Jiang L, Mahjouri-Samani M, Park J, et al. Laser-based micro/nanofabrication in one, two and three dimensions. Frontiers of Optoelectronics. 2015;8:351-78.

[73] Reyes-Contreras A, Camacho-López M, Camacho-López S, Olea-Mejía O, Esparza-García A, Bañuelos-Muñetón JG, et al. Laser-induced periodic surface structures on bismuth thin films with ns laser pulses below ablation threshold. Opt Mater Express. 2017;7:1777-86.

[74] Yang L, Wei J, Ma Z, Song P, Ma J, Zhao Y, et al. The Fabrication of Micro/Nano Structures by Laser Machining. Nanomaterials (Basel, Switzerland). 2019;9.

[75] Heiskanen S, Geng Z, Mastomäki J, Maasilta IJ. Nanofabrication on 2D and 3D Topography via Positive-Tone Direct-Write Laser Lithography. Advanced Engineering Materials. 2020;22:1901290.

[76] Casiraghi C, Hartschuh A, Lidorikis E, Qian H, Harutyunyan H, Gokus T, et al. Rayleigh Imaging of Graphene and Graphene Layers. Nano Letters. 2007;7:2711-7.

[77] Nair RR, Blake P, Grigorenko AN, Novoselov KS, Booth TJ, Stauber T, et al. Fine Structure Constant Defines Visual Transparency of Graphene. Science. 2008;320:1308-.

[78] Djurišić AB, Li EH. Optical properties of graphite. Journal of Applied Physics. 1999;85:7404-10.

[79] Wang F, Zhang Y, Tian C, Girit C, Zettl A, Crommie M, et al. Gate-Variable Optical Transitions in Graphene. Science. 2008;320:206-9.

[80] Mak KF, Shan J, Heinz TF. Electronic Structure of Few-Layer Graphene: Experimental Demonstration of Strong Dependence on Stacking Sequence. Physical Review Letters. 2010;104:176404.

[81] Rani P, Dubey GS, Jindal VK. DFT study of optical properties of pure and doped graphene. Physica E: Low-dimensional Systems and Nanostructures. 2014;62:28-35.

[82] Vogel A, Venugopalan V. Mechanisms of Pulsed Laser Ablation of Biological Tissues. Chemical Reviews. 2003;103:577-644.

[83] Dreyer DR, Park S, Bielawski CW, Ruoff RS. The chemistry of graphene oxide. Chemical Society Reviews. 2010;39:228-40.

[84] Erickson K, Erni R, Lee Z, Alem N, Gannett W, Zettl A. Determination of the Local Chemical Structure of Graphene Oxide and Reduced Graphene Oxide. Advanced Materials. 2010;22:4467-72.

[85] Smirnov VA, Arbuzov AA, Shul'ga YM, Baskakov SA, Martynenko VM, Muradyan VE, et al. Photoreduction of graphite oxide. High Energy Chemistry. 2011;45:57-61.

[86] Pop E, Varshney V, Roy AK. Thermal properties of graphene: Fundamentals and applications. MRS Bulletin. 2012;37:1273-81.

[87] Balandin AA, Ghosh S, Bao W, Calizo I, Teweldebrhan D, Miao F, et al. Superior Thermal Conductivity of Single-Layer Graphene. Nano Letters. 2008;8:902-7.

[88] Ganz E, Ganz AB, Yang L-M, Dornfeld M. The initial stages of melting of graphene between 4000 K and 6000 K. Physical Chemistry Chemical Physics. 2017;19:3756-62.

[89] Zakharchenko KV, Fasolino A, Los JH, Katsnelson MI. Melting of graphene: from two to one dimension. Journal of Physics: Condensed Matter. 2011;23:202202.

[90] Los JH, Zakharchenko KV, Katsnelson MI, Fasolino A. Melting temperature of graphene. Physical Review B. 2015;91:045415.

[91] Larciprete R, Fabris S, Sun T, Lacovig P, Baraldi A, Lizzit S. Dual Path Mechanism in the Thermal Reduction of Graphene Oxide. Journal of the American Chemical Society. 2011;133:17315-21.

[92] Dave SH, Gong C, Robertson AW, Warner JH, Grossman JC. Chemistry and Structure of Graphene Oxide via Direct Imaging. ACS Nano. 2016;10:7515-22.

[93] Lazauskas A, Baltrusaitis J, Grigaliūnas V, Guobienė A, Prosyčevas I, Narmontas P, et al. Thermally-driven structural changes of graphene oxide multilayer films deposited on glass substrate. Superlattices and Microstructures. 2014;75:461-7.

[94] Ganguly A, Sharma S, Papakonstantinou P, Hamilton J. Probing the Thermal Deoxygenation of Graphene Oxide Using High-Resolution In Situ X-ray-Based Spectroscopies. The Journal of Physical Chemistry C. 2011;115:17009-19.

[95] Ferrari AC, Basko DM. Raman spectroscopy as a versatile tool for studying the properties of graphene. Nature Nanotechnology. 2013;8:235-46.

[96] Yang Y, Cao J, Wei N, Meng D, Wang L, Ren G, et al. Thermal Conductivity of Defective Graphene Oxide: A Molecular Dynamic Study. Molecules (Basel, Switzerland). 2019;24.

[97] Mu X, Wu X, Zhang T, Go DB, Luo T. Thermal Transport in Graphene Oxide – From Ballistic Extreme to Amorphous Limit. Scientific Reports. 2014;4:3909.

[98] Kim CB, Lee J, Cho J, Goh M. Thermal conductivity enhancement of reduced graphene oxide via chemical defect healing for efficient heat dissipation. Carbon. 2018;139:386-92.

[99] Balandin AA. Thermal properties of graphene and nanostructured carbon materials. Nature Materials. 2011;10:569-81.

[100] Hao F, Fang D, Xu Z. Mechanical and thermal transport properties of graphene with defects. Applied Physics Letters. 2011;99:041901.

[101] Ghosh S, Bao W, Nika DL, Subrina S, Pokatilov EP, Lau CN, et al. Dimensional crossover of thermal transport in few-layer graphene. Nature Materials. 2010;9:555-8.

[102] Zhong W-R, Zhang M-P, Ai B-Q, Zheng D-Q. Chirality and thickness-dependent thermal conductivity of few-layer graphene: A molecular dynamics study. Applied Physics Letters. 2011;98:113107.

[103] Huang X, Wang J, Eres G, Wang X. Thermophysical properties of multi-wall carbon nanotube bundles at elevated temperatures up to 830K. Carbon. 2011;49:1680-91.

[104] You R, Liu Y-Q, Hao Y-L, Han D-D, Zhang Y-L, You Z. Laser Fabrication of Graphene-Based Flexible Electronics. Advanced Materials. 2020;32:1901981.

[105] Fauzi F. Direct Laser Writing of Graphene on Nickel and Platinum. 2017.

[106] Park JB, Xiong W, Gao Y, Qian M, Xie ZQ, Mitchell M, et al. Fast growth of graphene patterns by laser direct writing. Applied Physics Letters. 2011;98:123109.

[107] Kumar P. Laser flash synthesis of graphene and its inorganic analogues: An innovative breakthrough with immense promise. RSC Advances. 2013;3:11987-2002.

[108] Zhou YS, Xiong W, Park J, Qian M, Mahjouri-Samani M, Gao Y, et al. Laser-assisted nanofabrication of carbon nanostructures. Journal of Laser Applications. 2012;24:042007.

[109] Tu R, Liang Y, Zhang C, Li J, Zhang S, Yang M, et al. Fast synthesis of high-quality large-area graphene by laser CVD. Applied Surface Science. 2018;445:204-10.

[110] Peng P, Li L, He P, Zhu Y, Fu J, Huang Y, et al. One-step selective laser patterning of copper/graphene flexible electrodes. Nanotechnology. 2019;30:185301.

[111] Sha J, Li Y, Villegas Salvatierra R, Wang T, Dong P, Ji Y, et al. Three-Dimensional Printed Graphene Foams. ACS Nano. 2017;11:6860-7.

[112] Chen Y, Xu J, Yang Y, Zhao Y, Yang W, He X, et al. Enhanced electrochemical performance of laser scribed graphene films decorated with manganese dioxide nanoparticles. Journal of Materials Science: Materials in Electronics. 2016;27:2564-73.

[113] Sandoval S, Kepić D, Pérez del Pino Á, György E, Gómez A, Pfannmoeller M, et al. Selective Laser-Assisted Synthesis of Tubular van der Waals Heterostructures of Single-Layered PbI2 within Carbon Nanotubes Exhibiting Carrier Photogeneration. ACS Nano. 2018;12:6648-56.

[114] Pérez del Pino A, György E, Alshaikh I, Pantoja-Suárez F, Andújar JL, Pascual E, et al. Laser-driven coating of vertically aligned carbon nanotubes with manganese oxide from metal organic precursors for energy storage. Nanotechnology. 2017;28:395405.

[115] Pérez del Pino A, Gyorgy E, Hussain S, Andújar JL, Pascual E, Amade R, et al. Laser-induced nanostructuration of vertically aligned carbon nanotubes coated with nickel oxide nanoparticles. Journal of Materials Science. 2017;52:4002-15.

[116] György E, del Pino AP, Datcu A, Duta L, Logofatu C, Iordache I, et al. Titanium oxide – reduced graphene oxide – silver composite layers synthesized by laser technique: Wetting and electrical properties. Ceramics International. 2016;42:16191-7.

[117] Pérez del Pino A, György E, Logofatu C, Puigmartí-Luis J, Gao W. Laser-induced chemical transformation of graphene oxide–iron oxide nanoparticles composites deposited on polymer substrates. Carbon. 2015;93:373-83.

[118] Keramatnejad K, Zhou YS, Li DW, Golgir HR, Huang X, Zhou QM, et al. Laser-Assisted Nanowelding of Graphene to Metals: An Optical Approach toward Ultralow Contact Resistance. Advanced Materials Interfaces. 2017;4:1700294.

[119] Lee WH, Suk JW, Chou H, Lee J, Hao Y, Wu Y, et al. Selective-Area Fluorination of Graphene with Fluoropolymer and Laser Irradiation. Nano Letters. 2012;12:2374-8.

[120] Matsumoto Y, Koinuma M, Ida S, Hayami S, Taniguchi T, Hatakeyama K, et al. Photoreaction of Graphene Oxide Nanosheets in Water. The Journal of Physical Chemistry C. 2011;115:19280-6.

[121] Hou W-C, Chowdhury I, Goodwin DG, Henderson WM, Fairbrother DH, Bouchard D, et al. Photochemical Transformation of Graphene Oxide in Sunlight. Environmental Science & Technology. 2015;49:3435-43.

[122] Shi HH, Jang S, Naguib HE. Freestanding Laser-Assisted Reduced Graphene Oxide Microribbon Textile Electrode Fabricated on a Liquid Surface for Supercapacitors and Breath Sensors. ACS Applied Materials & Interfaces. 2019;11:27183-91.

[123] Zhang Y, Guo L, Wei S, He Y, Xia H, Chen Q, et al. Direct imprinting of microcircuits on graphene oxides film by femtosecond laser reduction. Nano Today. 2010;5:15-20.

[124] Tran TX, Choi H, Che CH, Sul JH, Kim IG, Lee S-M, et al. Laser-Induced Reduction of Graphene Oxide by Intensity-Modulated Line Beam for Supercapacitor Applications. ACS Applied Materials & Interfaces. 2018;10:39777-84.

[125] Gao W, Singh N, Song L, Liu Z, Reddy ALM, Ci L, et al. Direct laser writing of micro-supercapacitors on hydrated graphite oxide films. Nature Nanotechnology. 2011;6:496-500.

[126] Wan Z, Streed EW, Lobino M, Wang S, Sang RT, Cole IS, et al. Laser-Reduced Graphene: Synthesis, Properties, and Applications. Advanced Materials Technologies. 2018;3:1700315.

[127] Wan Z, Wang S, Haylock B, Kaur J, Tanner P, Thiel D, et al. Tuning the sub-processes in laser reduction of graphene oxide by adjusting the power and scanning speed of laser. Carbon. 2019;141:83-91.

[128] Yang C-R, Tseng S-F, Chen Y-T. Laser-induced reduction of graphene oxide powders by high pulsed ultraviolet laser irradiations. Applied Surface Science. 2018;444:578-83.

[129] Antonelou A, Sygellou L, Vrettos K, Georgakilas V, Yannopoulos SN. Efficient defect healing and ultralow sheet resistance of laser-assisted reduced graphene oxide at ambient conditions. Carbon. 2018;139:492-9.

[130] Park R, Kim H, Lone S, Jeon S, Kwon YW, Shin B, et al. One-Step Laser Patterned Highly Uniform Reduced Graphene Oxide Thin Films for Circuit-Enabled Tattoo and Flexible Humidity Sensor Application. Sensors (Basel, Switzerland). 2018;18.

[131] Giacomelli C, Álvarez-Diduk R, Testolin A, Merkoçi A. Selective stamping of laser scribed rGO nanofilms: from sensing to multiple applications. 2D Materials. 2020;7:024006.

[132] Cai J, Lv C, Watanabe A. Laser Direct Writing and Selective Metallization of Metallic Circuits for Integrated Wireless Devices. ACS Applied Materials & Interfaces. 2018;10:915-24.

[133] Mao L, Gong T, Ai Q, Hong Y, Guo J, He Y, et al. Morphologically modulated laser-patterned reduced graphene oxide strain sensors for human fatigue recognition. Smart Materials and Structures. 2019;29:015009.

[134] Strong V, Dubin S, El-Kady MF, Lech A, Wang Y, Weiller BH, et al. Patterning and Electronic Tuning of Laser Scribed Graphene for Flexible All-Carbon Devices. ACS Nano. 2012;6:1395-403.

[135] Torrisi L, Cutroneo M, Silipigni L, Fazio M, Torrisi A. Effects of the Laser Irradiation on Graphene Oxide Foils in Vacuum and Air. Physics of the Solid State. 2019;61:1327-31.

[136] Chuquitarqui A, Cotet LC, Baia M, György E, Magyari K, Barbu-Tudoran L, et al. New fabrication method for producing reduced graphene oxide flexible electrodes by using a low-power visible laser diode engraving system. Nanotechnology. 2020;31:325402.

[137] Ye R, James DK, Tour JM. Laser-Induced Graphene: From Discovery to Translation. Advanced Materials. 2019;31:1803621.

[138] Lin J, Peng Z, Liu Y, Ruiz-Zepeda F, Ye R, Samuel ELG, et al. Laser-induced porous graphene films from commercial polymers. Nature Communications. 2014;5:5714.

[139] Luo S, Hoang PT, Liu T. Direct laser writing for creating porous graphitic structures and their use for flexible and highly sensitive sensor and sensor arrays. Carbon. 2016;96:522-31.

[140] Ruan X, Luo J, Wang R, Yao Y, Guan J, Liu T. Microcontact Printing with Laser Direct Writing Carbonization for Facile Fabrication of Carbon-Based Ultrathin Disk Arrays and Ordered Holey Films. Small. 2019;15:1902819.

[141] Zhang Z, Song M, Hao J, Wu K, Li C, Hu C. Visible light laser-induced graphene from phenolic resin: A new approach for directly writing graphene-based electrochemical devices on various substrates. Carbon. 2018;127:287-96.

[142] Ye R, Chyan Y, Zhang J, Li Y, Han X, Kittrell C, et al. Laser-Induced Graphene Formation on Wood. Advanced Materials. 2017;29:1702211.

[143] Chyan Y, Ye R, Li Y, Singh SP, Arnusch CJ, Tour JM. Laser-Induced Graphene by Multiple Lasing: Toward Electronics on Cloth, Paper, and Food. ACS Nano. 2018;12:2176-83.

[144] Carvalho AF, Fernandes AJS, Leitão C, Deuermeier J, Marques AC, Martins R, et al. Laser-Induced Graphene Strain Sensors Produced by Ultraviolet Irradiation of Polyimide. Advanced Functional Materials. 2018;28:1805271.

[145] Duy LX, Peng Z, Li Y, Zhang J, Ji Y, Tour JM. Laser-induced graphene fibers. Carbon. 2018;126:472-9.

[146] Lamberti A, Perrucci F, Caprioli M, Serrapede M, Fontana M, Bianco S, et al. New insights on laser-induced graphene electrodes for flexible supercapacitors: tunable morphology and physical properties. Nanotechnology. 2017;28:174002.

[147] Li Y, Luong DX, Zhang J, Tarkunde YR, Kittrell C, Sargunaraj F, et al. Laser-Induced Graphene in Controlled Atmospheres: From Superhydrophilic to Superhydrophobic Surfaces. Advanced Materials. 2017;29:1700496.

[148] Tiliakos A, Ceaus C, Iordache SM, Vasile E, Stamatin I. Morphic transitions of nanocarbons via laser pyrolysis of polyimide films. Journal of Analytical and Applied Pyrolysis. 2016;121:275-86.

[149] Tan KW, Jung B, Werner JG, Rhoades ER, Thompson MO, Wiesner U. Transient laser heating induced hierarchical porous structures from block copolymer–directed self-assembly. Science. 2015;349:54-8.

[150] Singh SP, Li Y, Be'er A, Oren Y, Tour JM, Arnusch CJ. Laser-Induced Graphene Layers and Electrodes Prevents Microbial Fouling and Exerts Antimicrobial Action. ACS Applied Materials & Interfaces. 2017;9:18238-47.

[151] Luong DX, Yang K, Yoon J, Singh SP, Wang T, Arnusch CJ, et al. Laser-Induced Graphene Composites as Multifunctional Surfaces. ACS Nano. 2019;13:2579-86.

[152] Bayati M, Peng H, Deng H, Lin J, Fidalgo de Cortalezzi M. Laser induced graphene /ceramic membrane composite: Preparation and characterization. Journal of Membrane Science. 2020;595:117537.

[153] Stanford MG, Zhang C, Fowlkes JD, Hoffman A, Ivanov IN, Rack PD, et al. High-Resolution Laser-Induced Graphene. Flexible Electronics beyond the Visible Limit. ACS Applied Materials & Interfaces. 2020;12:10902-7.

[154] Yang W, Zhao W, Li Q, Li H, Wang Y, Li Y, et al. Fabrication of Smart Components by 3D Printing and Laser-Scribing Technologies. ACS Applied Materials & Interfaces. 2020;12:3928-35.

[155] Dong K, Peng X, Wang ZL. Fiber/Fabric-Based Piezoelectric and Triboelectric Nanogenerators for Flexible/Stretchable and Wearable Electronics and Artificial Intelligence. Advanced Materials. 2020;32:1902549.

[156] Tiliakos A, Trefilov AMI, Tanasă E, Balan A, Stamatin I. Laser-induced graphene as the microporous layer in proton exchange membrane fuel cells. Applied Surface Science. 2020;504:144096.

[157] Loh KP, Bao Q, Ang PK, Yang J. The chemistry of graphene. Journal of Materials Chemistry. 2010;20:2277-89.

[158] Kang S, Jeong YK, Ryu JH, Son Y, Kim WR, Lee B, et al. Pulsed laser ablation based synthetic route for nitrogen-doped graphene quantum dots using graphite flakes. Applied Surface Science. 2020;506:144998.

[159] Calabro RL, Yang D-S, Kim DY. Controlled Nitrogen Doping of Graphene Quantum Dots through Laser Ablation in Aqueous Solutions for Photoluminescence and Electrocatalytic Applications. ACS Applied Nano Materials. 2019;2:6948-59.

[160] Yeh T-F, Chen S-J, Yeh C-S, Teng H. Tuning the Electronic Structure of Graphite Oxide through Ammonia Treatment for Photocatalytic Generation of H2 and O2 from Water Splitting. The Journal of Physical Chemistry C. 2013;117:6516-24.

[161] Hulicova-Jurcakova D, Seredych M, Lu GQ, Bandosz TJ. Combined Effect of Nitrogen- and Oxygen-Containing Functional Groups of Microporous Activated Carbon on its Electrochemical Performance in Supercapacitors. Advanced Functional Materials. 2009;19:438-47.

[162] Seredych M, Hulicova-Jurcakova D, Lu GQ, Bandosz TJ. Surface functional groups of carbons and the effects of their chemical character, density and accessibility to ions on electrochemical performance. Carbon. 2008;46:1475-88.

[163] Su F, Poh CK, Chen JS, Xu G, Wang D, Li Q, et al. Nitrogen-containing microporous carbon nanospheres with improved capacitive properties. Energy & Environmental Science. 2011;4:717-24.

[164] Lin T, Chen I-W, Liu F, Yang C, Bi H, Xu F, et al. Nitrogen-doped mesoporous carbon of extraordinary capacitance for electrochemical energy storage. Science. 2015;350:1508-13.

[165] Kepić D, Sandoval S, Pino ÁPd, György E, Cabana L, Ballesteros B, et al. Nanosecond Laser-Assisted Nitrogen Doping of Graphene Oxide Dispersions. ChemPhysChem. 2017;18:935-41.

[166] Pérez del Pino A, González-Campo A, Giraldo S, Peral J, György E, Logofatu C, et al. Synthesis of graphene-based photocatalysts for water splitting by laser-induced doping with ionic liquids. Carbon. 2018;130:48-58.

[167] Pérez del Pino A, György E, Cotet C, Baia L, Logofatu C. Laser-induced chemical transformation of free-standing graphene oxide membranes in liquid and gas ammonia environments. RSC Advances. 2016;6:50034-42.

[168] Datcu A, Duta L, Pérez del Pino A, Logofatu C, Luculescu C, Duta A, et al. One-step preparation of nitrogen doped titanium oxide/Au/reduced graphene oxide composite thin films for photocatalytic applications. RSC Advances. 2015;5:49771-9.

[169] Singh SP, Li Y, Zhang J, Tour JM, Arnusch CJ. Sulfur-Doped Laser-Induced Porous Graphene Derived from Polysulfone-Class Polymers and Membranes. ACS Nano. 2018;12:289-97.

[170] Huang Y, Zeng L, Liu C, Zeng D, Liu Z, Liu X, et al. Laser Direct Writing of Heteroatom (N and S)-Doped Graphene from a Polybenzimidazole Ink Donor on Polyethylene Terephthalate Polymer and Glass Substrates. Small. 2018;14:1803143.

[171] You Z, Qiu Q, Chen H, Feng Y, Wang X, Wang Y, et al. Laser-induced noble metal nanoparticle-graphene composites enabled flexible biosensor for pathogen detection. Biosensors & bioelectronics. 2020;150:111896.

[172] Gupta A, Holoidovsky L, Thamaraiselvan C, Thakur AK, Singh SP, Meijler MM, et al. Silver-doped laser-induced graphene for potent surface antibacterial activity and anti-biofilm action. Chemical Communications. 2019;55:6890-3.

[173] Ge L, Hong Q, Li H, Liu C, Li F. Direct-Laser-Writing of Metal Sulfide-Graphene Nanocomposite Photoelectrode toward Sensitive Photoelectrochemical Sensing. Advanced Functional Materials. 2019;29:1904000.

[174] Wu X, Yin H, Li Q. Ablation and Patterning of Carbon Nanotube Film by Femtosecond Laser Irradiation. Applied Sciences. 2019;9:3045.

[175] Vasquez A, Samolis P, Zeng J, Sander MY. Micro-structuring, ablation, and defect generation in graphene with femtosecond pulses. OSA Continuum. 2019;2:2925-34.

[176] Liu Z-B, Li L, Xu Y-F, Liang J-J, Zhao X, Chen S-Q, et al. Direct patterning on reduced graphene oxide nanosheets using femtosecond laser pulses. Journal of Optics. 2011;13:085601.

[177] Kiisk V, Kahro T, Kozlova J, Matisen L, Alles H. Nanosecond laser treatment of graphene. Applied Surface Science. 2013;276:133-7.

[178] Kovalchuk NG, Niherysh KA, Felsharuk AV, Svito IA, Tamulevičius T, Tamulevičius S, et al. Direct patterning of nitrogen-doped chemical vapor deposited graphene-based microstructures for charge carrier measurements employing femtosecond laser ablation. Journal of Physics D: Applied Physics. 2019;52:30LT01.

[179] Pérez-Mas AM, Álvarez P, Campos N, Gómez D, Menéndez R. Graphene patterning by nanosecond laser ablation: the effect of the substrate interaction with graphene. Journal of Physics D: Applied Physics. 2016;49:305301.

[180] Rodriguez RD, Murastov GV, Lipovka A, Fatkullin MI, Nozdrina O, Pavlov SK, et al. High-power laser-patterning graphene oxide: A new approach to making arbitrarily-shaped self-aligned electrodes. Carbon. 2019;151:148-55.

[181] Sahin R, Simsek E, Akturk S. Nanoscale patterning of graphene through femtosecond laser ablation. Applied Physics Letters. 2014;104:053118.

[182] Zhou Y, Bao Q, Varghese B, Tang LAL, Tan CK, Sow C-H, et al. Microstructuring of Graphene Oxide Nanosheets Using Direct Laser Writing. Advanced Materials. 2010;22:67-71.

[183] Park JB, Yoo J-H, Grigoropoulos CP. Multi-scale graphene patterns on arbitrary substrates via laser-assisted transfer-printing process. Applied Physics Letters. 2012;101:043110.

[184] Lin L, Li J, Li W, Yogeesh MN, Shi J, Peng X, et al. Optothermoplasmonic Nanolithography for On-Demand Patterning of 2D Materials. Advanced Functional Materials. 2018;28:1803990.

[185] Tseng S-F, Cheng P-Y, Hsiao W-T, Chen M-F, Chung C-K, Wang P-H. High-performance graphene-based heaters fabricated using maskless ultraviolet laser patterning. The International Journal of Advanced Manufacturing Technology. 2019;102:3011-20.

[186] Bobrinetskiy I, Emelianov A, Nasibulin A, Komarov I, Otero N, Romero PM. Photophysical and photochemical effects in ultrafast laser patterning of CVD graphene. Journal of Physics D: Applied Physics. 2016;49:41LT01.

[187] Yoo J-H, Kim E, Hwang DJ. Femtosecond laser patterning, synthesis, defect formation, and structural modification of atomic layered materials. MRS Bulletin. 2016;41:1002-8.

[188] Mendoza ME, Ferreira EHM, Kuznetsov A, Achete CA, Aumanen J, Myllyperkiö P, et al. Revealing lattice disorder, oxygen incorporation and pore formation in laser induced two-photon oxidized graphene. Carbon. 2019;143:720-7.

[189] Gil-Villalba A, Meyer R, Giust R, Rapp L, Billet C, Courvoisier F. Single shot femtosecond laser nano-ablation of CVD monolayer graphene. Scientific Reports. 2018;8:14601.

[190] Kasischke M, Subaşı E, Bock C, Pham D-V, Gurevich EL, Kunze U, et al. Femtosecond laser patterning of graphene electrodes for thin-film transistors. Applied Surface Science. 2019;478:299-303.

[191] Maurice A, Bodelot L, Tay BK, Lebental B. Controlled, Low-Temperature Nanogap Propagation in Graphene Using Femtosecond Laser Patterning. Small. 2018;14:1801348.

[192] Lin Z, Ye X, Han J, Chen Q, Fan P, Zhang H, et al. Precise Control of the Number of Layers of Graphene by Picosecond Laser Thinning. Scientific Reports. 2015;5:11662.

[193] Han GH, Chae SJ, Kim ES, Güneş F, Lee IH, Lee SW, et al. Laser Thinning for Monolayer Graphene Formation: Heat Sink and Interference Effect. ACS Nano. 2011;5:263-8.

[194] Pramanik A, Karmakar S, Kumbhakar P, Biswas S, Sarkar R, Kumbhakar P. Synthesis of bilayer graphene nanosheets by pulsed laser ablation in liquid and observation of its tunable nonlinearity. Applied Surface Science. 2020;499:143902.

[195] Compagnini G, Sinatra M, Russo P, Messina GC, Puglisi O, Scalese S. Deposition of few layer graphene nanowalls at the electrodes during electric field-assisted laser ablation of carbon in water. Carbon. 2012;50:2362-5.

[196] Thongpool V, Phunpueok A, Piriyawong V, Limsuwan S, Limsuwan P. Pulsed Laser Ablation of Graphite Target in Dimethyformamide. Energy Procedia. 2013;34:610-6.

[197] Calabro RL, Yang D-S, Kim DY. Liquid-phase laser ablation synthesis of graphene quantum dots from carbon nano-onions: Comparison with chemical oxidation. Journal of Colloid and Interface Science. 2018;527:132-40.

[198] Kang S, Jeong YK, Jung KH, Son Y, Choi S-C, An GS, et al. Simple preparation of graphene quantum dots with controllable surface states from graphite. RSC Advances. 2019;9:38447-53.

[199] Bleu Y, Bourquard F, Tite T, Loir A-S, Maddi C, Donnet C, et al. Review of Graphene Growth From a Solid Carbon Source by Pulsed Laser Deposition (PLD). Frontiers in Chemistry. 2018;6.

[200] Larki F, Kameli P, Nikmanesh H, Jafari M, Salamati H. The influence of external magnetic field on the pulsed laser deposition growth of graphene on nickel substrate at room temperature. Diamond and Related Materials. 2019;93:233-40.

[201] Wang J, Fan L, Wang X, Xiao T, Peng L, Wang X, et al. Pulsed laser deposition of monolayer and bilayer graphene. Applied Surface Science. 2019;494:651-8.

[202] Bleu Y, Bourquard F, Gartiser V, Loir A-S, Caja-Munoz B, Avila J, et al. Graphene synthesis on SiO2 using pulsed laser deposition with bilayer predominance. Materials Chemistry and Physics. 2019;238:121905.

[203] Wang J, Wang X, Yu J, Xiao T, Peng L, Fan L, et al. Tailoring the Grain Size of Bi-Layer Graphene by Pulsed Laser Deposition. Nanomaterials (Basel, Switzerland). 2018;8:885.

[204] Ren P, Pu E, Liu D, Wang Y, Xiang B, Ren X. Fabrication of nitrogen-doped graphenes by pulsed laser deposition and improved chemical enhancement for Raman spectroscopy. Materials Letters. 2017;204:65-8.

[205] Juvaid MM, Sarkar S, Gogoi PK, Ghosh S, Annamalai M, Lin Y-C, et al. Direct Growth of Wafer-Scale, Transparent, p-Type Reduced-Graphene-Oxide-like Thin Films by Pulsed Laser Deposition. ACS Nano. 2020;14:3290-8.

[206] Pérez del Pino Á, György E, Cabana L, Ballesteros B, Tobias G. Deposition of functionalized single wall carbon nanotubes through matrix assisted pulsed laser evaporation. Carbon. 2012;50:4450-8.

[207] György E, Pérez del Pino Á, Roqueta J, Ballesteros B, Cabana L, Tobias G. Effect of laser radiation on multi-wall carbon nanotubes: study of shell structure and immobilization process. Journal of Nanoparticle Research. 2013;15:1852.

[208] Pino ÁPd, György E, Logofatu C, Duta A. Study of the deposition of graphene oxide by matrix-assisted pulsed laser evaporation. Journal of Physics D: Applied Physics. 2013;46:505309.

[209] O'Malley SM, Tomko J, Pino APd, Logofatu C, György E. Resonant Infrared and Ultraviolet Matrix-Assisted Pulsed Laser Evaporation of Titanium Oxide/Graphene Oxide Composites: A Comparative Study. The Journal of Physical Chemistry C. 2014;118:27911-9.

[210] Queraltó A, Pérez del Pino Á, Logofatu C, Calota A, Amade R, Alshaikh I, et al. MAPLE synthesis of reduced graphene oxide/silver nanocomposite electrodes: Influence of target composition and gas ambience. Journal of Alloys and Compounds. 2017;726:1003-13.

[211] György E, Logofatu C, Pérez del Pino Á, Datcu A, Pascu O, Ivan R. Enhanced UV- and visible-light driven photocatalytic performances and recycling properties of graphene oxide/ZnO hybrid layers. Ceramics International. 2018;44:1826-35.

[212] Ivan R, Popescu C, del Pino AP, Yousef I, Logofatu C, György E. Laser-induced synthesis and photocatalytic properties of hybrid organic–inorganic composite layers. Journal of Materials Science. 2019;54:3927-41.

[213] Fernández-Pradas JM, Serra P. Laser-Induced Forward Transfer: A Method for Printing Functional Inks. Crystals. 2020;10:651.

[214] Bohandy J, Kim BF, Adrian FJ. Metal deposition from a supported metal film using an excimer laser. Journal of Applied Physics. 1986;60:1538-9.

[215] Fernández-Pradas JM, Sopeña P, González-Torres S, Arrese J, Cirera A, Serra P. Laser-induced forward transfer for printed electronics applications. Applied Physics A. 2018;124:214.

[216] Papazoglou S, Zergioti I. Laser Induced Forward Transfer (LIFT) of nano-micro patterns for sensor applications. Microelectronic Engineering. 2017;182:25-34.

[217] Fardel R, Nagel M, Nüesch F, Lippert T, Wokaun A. Laser forward transfer using a sacrificial layer: Influence of the material properties. Applied Surface Science. 2007;254:1322-6.

[218] Papazoglou S, Raptis YS, Chatzandroulis S, Zergioti I. A study on the pulsed laser printing of liquid-phase exfoliated graphene for organic electronics. Applied Physics A. 2014;117:301-6.

[219] Komlenok MS, Pivovarov PA, Dezhkina MA, Rybin MG, Savin SS, Obraztsova ED, et al. Printing of Crumpled CVD Graphene via Blister-Based Laser-Induced Forward Transfer. Nanomaterials. 2020;10:1103.

[220] Palla-Papavlu A, Filipescu M, Vizireanu S, Vogt L, Antohe S, Dinescu M, et al. Laser-induced forward transfer of hybrid carbon nanostructures. Applied Surface Science. 2016;374:312-7.

[221] Smits ECP, Walter A, Leeuw DMd, Asadi K. Laser induced forward transfer of graphene. Applied Physics Letters. 2017;111:173101.

[222] Qian M, Zhou YS, Gao Y, Park JB, Feng T, Huang SM, et al. Formation of graphene sheets through laser exfoliation of highly ordered pyrolytic graphite. Applied Physics Letters. 2011;98:173108.

[223] Qian M, Zhou YS, Gao Y, Feng T, Sun Z, Jiang L, et al. Production of few-layer graphene through liquid-phase pulsed laser exfoliation of highly ordered pyrolytic graphite. Applied Surface Science. 2012;258:9092-5.

[224] Mortazavi SZ, Parvin P, Reyhani A. Fabrication of graphene based on Q-switched Nd:YAG laser ablation of graphite target in liquid nitrogen. Laser Physics Letters. 2012;9:547-52.

[225] Carotenuto G, Longo A, Nicolais L, De Nicola S, Pugliese E, Ciofini M, et al. Laser-Induced Thermal Expansion of H2SO4-Intercalated Graphite Lattice. The Journal of Physical Chemistry C. 2015;119:15942-7.

[226] Beltaos A, Kovačević AG, Matković A, Ralević U, Savić-Šević S, Jovanović D, et al. Femtosecond laser induced periodic surface structures on multi-layer graphene. Journal of Applied Physics. 2014;116:204306.

[227] Fajstavr D, Neznalová K, Švorčík V, Slepička P. LIPSS Structures Induced on Graphene-Polystyrene Composite. Materials. 2019;12:3460.

[228] Guo L, Jiang H-B, Shao R-Q, Zhang Y-L, Xie S-Y, Wang J-N, et al. Two-beam-laser interference mediated reduction, patterning and nanostructuring of graphene oxide for the production of a flexible humidity sensing device. Carbon. 2012;50:1667-73.

[229] Jiang H-B, Liu Y-Q, Zhang Y-L, Liu Y, Fu X-Y, Han D-D, et al. Reed Leaf-Inspired Graphene Films with Anisotropic Superhydrophobicity. ACS Applied Materials & Interfaces. 2018;10:18416-25.

[230] Jiang HB, Liu Y, Liu J, Li SY, Song YY, Han DD, et al. Moisture-Responsive Graphene Actuators Prepared by Two-Beam Laser Interference of Graphene Oxide Paper. Front Chem. 2019;7:464.

[231] Guo L, Hao Y-W, Li P-L, Song J-F, Yang R-Z, Fu X-Y, et al. Improved NO2 Gas Sensing Properties of Graphene Oxide Reduced by Two-beam-laser Interference. Scientific Reports. 2018;8:4918.

[232] Van HH, Badura K, Zhang M. Laser-induced transformation of freestanding carbon nanotubes into graphene nanoribbons. RSC Advances. 2015;5:44183-91.

[233] Kumar P, Panchakarla LS, Rao CNR. Laser-induced unzipping of carbon nanotubes to yield graphene nanoribbons. Nanoscale. 2011;3:2127-9.

[234] Ermakov VA, Alaferdov AV, Vaz AR, Baranov AV, Moshkalev SA. Nonlocal laser annealing to improve thermal contacts between multi-layer graphene and metals. Nanotechnology. 2013;24:155301.

[235] Moshkalev SA, Ermakov VA, Vaz AR, Alaferdov AV, Savu R, Silveira JV, et al. Formation of reliable electrical and thermal contacts between graphene and metal electrodes by laser annealing. Microelectronic Engineering. 2014;121:55-8.

[236] Bhaumik A, Narayan J. Conversion of p to n-type reduced graphene oxide by laser annealing at room temperature and pressure. Journal of Applied Physics. 2017;121:125303.

[237] Coleman C, Erasmus R, Bhattacharyya S. Nanoscale deformations in graphene by laser annealing. Applied Physics Letters. 2016;109:253102.

[238] Del SK, Bornemann R, Bablich A, Schäfer-Eberwein H, Li J, Kowald T, et al. Optimizing the optical and electrical properties of graphene ink thin films by laser-annealing. 2D Materials. 2015;2:011003.

[239] Hwang HJ, Lee Y, Cho C, Lee BH. Facile process to clean PMMA residue on graphene using KrF laser annealing. AIP Advances. 2018;8:105326.

[240] Pan Q, Tong N, He N, Liu Y, Shim E, Pourdeyhimi B, et al. Electrospun Mat of Poly(vinyl alcohol)/Graphene Oxide for Superior Electrolyte Performance. ACS Applied Materials & Interfaces. 2018;10:7927-34.

[241] Kumar R, Savu R, Joanni E, Vaz AR, Canesqui MA, Singh RK, et al. Fabrication of interdigitated micro-supercapacitor devices by direct laser writing onto ultra-thin, flexible and free-standing graphite oxide films. RSC Advances. 2016;6:84769-76.

[242] Wang G, Babaahmadi V, He N, Liu Y, Pan Q, Montazer M, et al. Wearable supercapacitors on polyethylene terephthalate fabrics with good wash fastness and high flexibility. Journal of Power Sources. 2017;367:34-41.

[243] Kumar R, Joanni E, Singh RK, da Silva E, Savu R, Kubota LT, et al. Direct laser writing of micro-supercapacitors on thick graphite oxide films and their electrochemical properties in different liquid inorganic electrolytes. J Colloid Interface Sci. 2017;507:271-8.

[244] Shao C, Xu T, Gao J, Liang Y, Zhao Y, Qu L. Flexible and integrated supercapacitor with tunable energy storage. Nanoscale. 2017;9:12324-9.

[245] Kumar R, Joanni E, Savu R, Pereira MS, Singh RK, Constantino CJL, et al. Fabrication and electrochemical evaluation of micro-supercapacitors prepared by direct laser writing on free-standing graphite oxide paper. Energy. 2019;179:676-84.

[246] Ladrón-de-Guevara A, Boscá A, Pedrós J, Climent-Pascual E, de Andrés A, Calle F, et al. Reduced graphene oxide/polyaniline electrochemical supercapacitors fabricated by laser. Applied Surface Science. 2019;467-468:691-7.

[247] El-Kady MF, Kaner RB. Scalable fabrication of high-power graphene micro-supercapacitors for flexible and on-chip energy storage. Nature Communications. 2013;4:1475.

[248] El-Kady MF, Strong V, Dubin S, Kaner RB. Laser Scribing of High-Performance and Flexible Graphene-Based Electrochemical Capacitors. Science. 2012;335:1326-30.

[249] Lee S-H, Kim JH, Yoon J-R. Laser Scribed Graphene Cathode for Next Generation of High Performance Hybrid Supercapacitors. Scientific Reports. 2018;8:8179.

[250] Velasco A, Ryu YK, Boscá A, Ladrón-de-Guevara A, Hunt E, Zuo J, et al. Recent trends in graphene supercapacitors: from large area to microsupercapacitors. Sustainable Energy & Fuels. 2021;5:1235-54.

[251] Thekkekara LV, Gu M. Large-scale waterproof and stretchable textile-integrated laser- printed graphene energy storages. Scientific Reports. 2019;9:11822.

[252] Moussa M, Al-Bataineh SA, Losic D, Dubal DP. Engineering of high-performance potassium-ion capacitors using polyaniline-derived N-doped carbon nanotubes anode and laser scribed graphene oxide cathode. Applied Materials Today. 2019;16:425-34.

[253] Liu H, Li M, Kaner RB, Chen S, Pei Q. Monolithically Integrated Self-Charging Power Pack Consisting of a Silicon Nanowire Array/Conductive Polymer Hybrid Solar Cell and a Laser-Scribed Graphene Supercapacitor. ACS Appl Mater Interfaces. 2018;10:15609-15.

[254] Oh J-S, Kim S-H, Hwang T, Kwon H-Y, Lee TH, Bae A-H, et al. Laser-Assisted Simultaneous Patterning and Transferring of Graphene. The Journal of Physical Chemistry C. 2013;117:663-8.

[255] Choi H, Nguyen PT, In JB. Laser transmission welding and surface modification of graphene film for flexible supercapacitor applications. Applied Surface Science. 2019;483:481-8.

[256] Mao X, Xu J, He X, Yang W, Yang Y, Xu L, et al. All-solid-state flexible microsupercapacitors based on reduced graphene oxide/multi-walled carbon nanotube composite electrodes. Applied Surface Science. 2018;435:1228-36.

[257] Strauss V, Muni M, Borenstein A, Badamdorj B, Heil T, Kowal MD, et al. Patching laser-reduced graphene oxide with carbon nanodots. Nanoscale. 2019;11:12712-9.

[258] Wang F, Dong X, Wang K, Duan W, Gao M, Zhai Z, et al. Laser-induced nitrogen-doped hierarchically porous graphene for advanced electrochemical energy storage. Carbon. 2019;150:396-407.

[259] Shen D, Zou G, Liu L, Zhao W, Wu A, Duley WW, et al. Scalable High-Performance Ultraminiature Graphene Micro-Supercapacitors by a Hybrid Technique Combining Direct Writing and Controllable Microdroplet Transfer. ACS Applied Materials & Interfaces. 2018;10:5404-12.

[260] Li RZ, Peng R, Kihm KD, Bai S, Bridges D, Tumuluri U, et al. High-rate in-plane micro-supercapacitors scribed onto photo paper using in situ femtolaser-reduced graphene oxide/Au nanoparticle microelectrodes. Energy & Environmental Science. 2016;9:1458-67.

[261] Van Ngo T, Moussa M, Tung TT, Coghlan C, Losic D. Hybridization of MOFs and graphene: A new strategy for the synthesis of porous 3D carbon composites for high performing supercapacitors. Electrochimica Acta. 2020;329:135104.

[262] Yang S, Li Y, Sun J, Cao B. Laser induced oxygen-deficient TiO2/graphene hybrid for high-performance supercapacitor. Journal of Power Sources. 2019;431:220-5.

[263] Hwang JY, El-Kady MF, Wang Y, Wang L, Shao Y, Marsh K, et al. Direct preparation and processing of graphene/RuO2 nanocomposite electrodes for high-performance capacitive energy storage. Nano Energy. 2015;18:57-70.

[264] Ibrahim YO, Gondal MA, Alaswad A, Moqbel RA, Hassan M, Cevik E, et al. Laser-induced anchoring of WO3 nanoparticles on reduced graphene oxide sheets for photocatalytic water decontamination and energy storage. Ceramics International. 2020;46:444-51.

[265] Pang J, Mendes RG, Bachmatiuk A, Zhao L, Ta HQ, Gemming T, et al. Applications of 2D MXenes in energy conversion and storage systems. Chemical Society Reviews. 2019;48:72-133.

[266] Tang H, Hu Q, Zheng M, Chi Y, Qin X, Pang H, et al. MXene–2D layered electrode materials for energy storage. Progress in Natural Science: Materials International. 2018;28:133-47.

[267] Anasori B, Lukatskaya MR, Gogotsi Y. 2D metal carbides and nitrides (MXenes) for energy storage. Nature Reviews Materials. 2017;2:16098.

[268] Han Y, Ge Y, Chao Y, Wang C, Wallace GG. Recent progress in 2D materials for flexible supercapacitors. Journal of Energy Chemistry. 2018;27:57-72.

[269] Khameneh Asl S, Namdar Habashi M, Kianvash A, Alipour A, Mohini S, Asgharzadeh H. Fabrication of Graphene/MoS2 Nanocomposite for Flexible Energy Storage. Journal of Nanostructures. 2019;9:21-8.

[270] Raccichini R, Varzi A, Passerini S, Scrosati B. The role of graphene for electrochemical energy storage. Nature Materials. 2015;14:271-9.

[271] Fan X, Chen X, Dai L. 3D graphene based materials for energy storage. Current Opinion in Colloid & Interface Science. 2015;20:429-38.

[272] Georgakilas V, Tiwari JN, Kemp KC, Perman JA, Bourlinos AB, Kim KS, et al. Noncovalent Functionalization of Graphene and Graphene Oxide for Energy Materials, Biosensing, Catalytic, and Biomedical Applications. Chemical Reviews. 2016;116:5464-519.

[273] Lu X, Wu G, Xiong Q, Qin H, Wang W, Luo F. Fabrication of binder-free graphene-SnO2 electrodes by laser introduced conversion of precursors for lithium secondary batteries. Applied Surface Science. 2017;406:265-73.

[274] Tang J, Zhong X, Li H, Li Y, Pan F, Xu B. In-situ and selectively laser reduced graphene oxide sheets as excellent conductive additive for high rate capability LiFePO4 lithium ion batteries. Journal of Power Sources. 2019;412:677-82.

[275] Yu L, Chen GZ. Redox electrode materials for supercapatteries. Journal of Power Sources. 2016;326:604-12.

[276] Chen GZ. Supercapacitor and supercapattery as emerging electrochemical energy stores. International Materials Reviews. 2017;62:173-202.

[277] Yu L, Chen GZ. Supercapatteries as High-Performance Electrochemical Energy Storage Devices. Electrochemical Energy Reviews. 2020;3:271-85.

[278] Li M, El-Kady MF, Hwang JY, Kowal MD, Marsh K, Wang H, et al. Embedding hollow Co3O4 nanoboxes into a three-dimensional macroporous graphene framework for high-performance energy storage devices. Nano Research. 2018;11:2836-46.

[279] Shi X, Zhou F, Peng J, Wu Ra, Wu Z-S, Bao X. One-Step Scalable Fabrication of Graphene-Integrated Micro-Supercapacitors with Remarkable Flexibility and Exceptional Performance Uniformity. Advanced Functional Materials. 2019;29:1902860.

[280] Liu J, Zhang L, Yang C, Tao S. Preparation of multifunctional porous carbon electrodes through direct laser writing on a phenolic resin film. Journal of Materials Chemistry A. 2019;7:21168-75.

[281] Lamberti A, Serrapede M, Ferraro G, Fontana M, Perrucci F, Bianco S, et al. All-SPEEK flexible supercapacitor exploiting laser-induced graphenization. 2D Materials. 2017;4:035012.

[282] Zhang W, Lei Y, Ming F, Jiang Q, Costa PMFJ, Alshareef HN. Lignin Laser Lithography: A Direct-Write Method for Fabricating 3D Graphene Electrodes for Microsupercapacitors. Advanced Energy Materials. 2018;8:1801840.

[283] Zhang W, Lei Y, Jiang Q, Ming F, Costa PMFJ, Alshareef HN. 3D Laser Scribed Graphene Derived from Carbon Nanospheres: An Ultrahigh-Power Electrode for Supercapacitors. Small Methods. 2019;3:1900005.

[284] Mahmood F, Zhang C, Xie Y, Stalla D, Lin J, Wan C. Transforming lignin into porous graphene via direct laser writing for solid-state supercapacitors. RSC Advances. 2019;9:22713-20.

[285] Hawes GF, Yilman D, Noremberg BS, Pope MA. Supercapacitors Fabricated via Laser-Induced Carbonization of Biomass-Derived Poly(furfuryl alcohol)/Graphene Oxide Composites. ACS Applied Nano Materials. 2019;2:6312-24.

[286] Le T-SD, Park S, An J, Lee PS, Kim Y-J. Ultrafast Laser Pulses Enable One-Step Graphene Patterning on Woods and Leaves for Green Electronics. Advanced Functional Materials. 2019;29:1902771.

[287] Wang S, Yu Y, Luo S, Cheng X, Feng G, Zhang Y, et al. All-solid-state supercapacitors from natural lignin-based composite film by laser direct writing. Applied Physics Letters. 2019;115:083904.

[288] Tehrani F, Beltrán-Gastélum M, Sheth K, Karajic A, Yin L, Kumar R, et al. Laser-Induced Graphene Composites for Printed, Stretchable, and Wearable Electronics. Advanced Materials Technologies. 2019;4:1900162.

[289] Peng Z, Ye R, Mann JA, Zakhidov D, Li Y, Smalley PR, et al. Flexible Boron-Doped Laser-Induced Graphene Microsupercapacitors. ACS Nano. 2015;9:5868-75.

[290] Zuo Z, Jiang Z, Manthiram A. Porous B-doped graphene inspired by Fried-Ice for supercapacitors and metal-free catalysts. Journal of Materials Chemistry A. 2013;1:13476-83.

[291] Han J, Zhang LL, Lee S, Oh J, Lee K-S, Potts JR, et al. Generation of B-Doped Graphene Nanoplatelets Using a Solution Process and Their Supercapacitor Applications. ACS Nano. 2013;7:19-26.

[292] Niu L, Li Z, Hong W, Sun J, Wang Z, Ma L, et al. Pyrolytic synthesis of boron-doped graphene and its application as electrode material for supercapacitors. Electrochimica Acta. 2013;108:666-73.

[293] Wang D-W, Li F, Chen Z-G, Lu GQ, Cheng H-M. Synthesis and Electrochemical Property of Boron-Doped Mesoporous Carbon in Supercapacitor. Chemistry of Materials. 2008;20:7195-200.

[294] Shiraishi S, Kibe M, Yokoyama T, Kurihara H, Patel N, Oya A, et al. Electric double layer capacitance of multi-walled carbon nanotubes and B-doping effect. Applied Physics A. 2006;82:585-91.

[295] Kwon T, Nishihara H, Itoi H, Yang Q-H, Kyotani T. Enhancement Mechanism of Electrochemical Capacitance in Nitrogen-/Boron-Doped Carbons with Uniform Straight Nanochannels. Langmuir. 2009;25:11961-8.

[296] Cai J, Lv C, Hu C, Luo J, Liu S, Song J, et al. Laser direct writing of heteroatom-doped porous carbon for high-performance micro-supercapacitors. Energy Storage Materials. 2020;25:404-15.

[297] Wang W, Lu L, Xie Y, Mei X, Tang Y, Wu W, et al. Tailoring the surface morphology and nanoparticle distribution of laser-induced graphene/Co3O4 for high-performance flexible microsupercapacitors. Applied Surface Science. 2020;504:144487.

[298] Wang W, Lu L, Xie Y, Yuan W, Wan Z, Tang Y, et al. A Highly Stretchable Microsupercapacitor Using Laser-Induced Graphene/NiO/Co3O4 Electrodes on a Biodegradable Waterborne Polyurethane Substrate. Advanced Materials Technologies. 2020;5:1900903.

[299] Zang X, Shen C, Chu Y, Li B, Wei M, Zhong J, et al. Laser-Induced Molybdenum Carbide–Graphene Composites for 3D Foldable Paper Electronics. Advanced Materials. 2018;30:1800062.

[300] Yi J, Chen J, Yang Z, Dai Y, Li W, Cui J, et al. Facile Patterning of Laser-Induced Graphene with Tailored Li Nucleation Kinetics for Stable Lithium-Metal Batteries. Advanced Energy Materials. 2019;9:1901796.

[301] Huang Y, Field R, Chen Q, Peng Y, Walczak MS, Zhao H, et al. Laser induced molybdenum sulphide loading on doped graphene cathode for highly stable lithium sulphur battery. Communications Chemistry. 2019;2:138.

[302] Zhou C, Zhang K, Hong M, Yang Y, Hu N, Su Y, et al. Laser-induced MnO/Mn3O4/N-doped-graphene hybrid as binder-free anodes for lithium ion batteries. Chemical Engineering Journal. 2020;385:123720.

[303] Jiang Y, Yue J-L, Guo Q, Xia Q, Zhou C, Feng T, et al. Highly Porous Mn3O4 Micro/Nanocuboids with In Situ Coated Carbon as Advanced Anode Material for Lithium-Ion Batteries. Small. 2018;14:1704296.

[304] Zou Y, Zhang W, Chen N, Chen S, Xu W, Cai R, et al. Generating Oxygen Vacancies in MnO Hexagonal Sheets for Ultralong Life Lithium Storage with High Capacity. ACS Nano. 2019;13:2062-71.

[305] Zhang F, Alhajji E, Lei Y, Kurra N, Alshareef HN. Highly Doped 3D Graphene Na-Ion Battery Anode by Laser Scribing Polyimide Films in Nitrogen Ambient. Advanced Energy Materials. 2018;8:1800353.

[306] Chu Y, Guo L, Xi B, Feng Z, Wu F, Lin Y, et al. Embedding MnO@Mn3O4 Nanoparticles in an N-Doped-Carbon Framework Derived from Mn-Organic Clusters for Efficient Lithium Storage. Advanced Materials. 2018;30:1704244.

[307] Xiao Y-C, Xu C-Y, Sun X-Y, Pei Y, Wang P-P, Ma F-X, et al. Constructing yolk-shell MnO@C nanodiscs through a carbothermal reduction process for highly stable lithium storage. Chemical Engineering Journal. 2018;336:427-35.

[308] Ren M, Zhang J, Zhang C, Stanford MG, Chyan Y, Yao Y, et al. Quasi-Solid-State Li–O2 Batteries with Laser-Induced Graphene Cathode Catalysts. ACS Applied Energy Materials. 2020;3:1702-9.

[309] Ren M, Zhang J, Fan M, Ajayan PM, Tour JM. Li-Breathing Air Batteries Catalyzed by MnNiFe/Laser-Induced Graphene Catalysts. Advanced Materials Interfaces. 2019;6:1901035.

[310] Ren M, Zhang J, Tour JM. Laser-Induced Graphene Hybrid Catalysts for Rechargeable Zn-Air Batteries. ACS Applied Energy Materials. 2019;2:1460-8.

[311] Ren M, Zhang J, Tour JM. Laser-induced graphene synthesis of Co3O4 in graphene for oxygen electrocatalysis and metal-air batteries. Carbon. 2018;139:880-7.

[312] Djuric SM, Kitic G, Dubourg G, Gajic R, Tomasevic-Ilic T, Minic V, et al. Miniature graphene-based supercapacitors fabricated by laser ablation. Microelectronic Engineering. 2017;182:1-7.

[313] Liu Y, Weng B, Xu Q, Hou Y, Zhao C, Beirne S, et al. Facile Fabrication of Flexible Microsupercapacitor with High Energy Density. Advanced Materials Technologies. 2016;1:1600166.

[314] Yun X, Xiong Z, Tu L, Bai L, Wang X. Hierarchical porous graphene film: An ideal material for laser-carving fabrication of flexible micro-supercapacitors with high specific capacitance. Carbon. 2017;125:308-17.

[315] Wu M, Li Y, Yao B, Chen J, Li C, Shi G. A high-performance current collector-free flexible in-plane micro-supercapacitor based on a highly conductive reduced graphene oxide film. Journal of Materials Chemistry A. 2016;4:16213-8.

[316] Xie B, Wang Y, Lai W, Lin W, Lin Z, Zhang Z, et al. Laser-processed graphene based micro-supercapacitors for ultrathin, rollable, compact and designable energy storage components. Nano Energy. 2016;26:276-85.

[317] Shao Y, Li J, Li Y, Wang H, Zhang Q, Kaner RB. Flexible quasi-solid-state planar micro-supercapacitor based on cellular graphene films. Materials Horizons. 2017;4:1145-50.

[318] Ye J, Tan H, Wu S, Ni K, Pan F, Liu J, et al. Direct Laser Writing of Graphene Made from Chemical Vapor Deposition for Flexible, Integratable Micro-Supercapacitors with Ultrahigh Power Output. Advanced Materials. 2018;30:1801384.

[319] Kwon S, Yoon Y, Ahn J, Lim H, Kim G, Kim J-H, et al. Facile laser fabrication of high quality graphene-based microsupercapacitors with large capacitance. Carbon. 2018;137:136-45.

[320] Kamboj N, Purkait T, Das M, Sarkar S, Hazra KS, Dey RS. Ultralong cycle life and outstanding capacitive performance of a 10.8 V metal free micro-supercapacitor with highly conducting and robust laser-irradiated graphene for an integrated storage device. Energy & Environmental Science. 2019;12:2507-17.

[321] Park S, Lee H, Kim Y-J, Lee PS. Fully laser-patterned stretchable microsupercapacitors integrated with soft electronic circuit components. NPG Asia Materials. 2018;10:959-69.

[322] Gao J, Shao C, Shao S, Bai C, Khalil UR, Zhao Y, et al. Laser-Assisted Multiscale Fabrication of Configuration-Editable Supercapacitors with High Energy Density. ACS Nano. 2019;13:7463-70.

[323] Hondred JA, Medintz IL, Claussen JC. Enhanced electrochemical biosensor and supercapacitor with 3D porous architectured graphene via salt impregnated inkjet maskless lithography. Nanoscale Horizons. 2019;4:735-46.

[324] Pérez del Pino Á, Martínez Villarroya A, Chuquitarqui A, Logofatu C, Tonti D, György E. Reactive laser synthesis of nitrogen-doped hybrid graphene-based electrodes for energy storage. Journal of Materials Chemistry A. 2018;6:16074-86.

[325] Pérez del Pino Á, Ramadan MA, Garcia Lebière P, Ivan R, Logofatu C, Yousef I, et al. Fabrication of graphene-based electrochemical capacitors through reactive inverse matrix assisted pulsed laser evaporation. Applied Surface Science. 2019;484:245-56.

[326] Acik M, Mattevi C, Gong C, Lee G, Cho K, Chhowalla M, et al. The Role of Intercalated Water in Multilayered Graphene Oxide. ACS Nano. 2010;4:5861-8.

[327] Pérez del Pino Á, Rodríguez López M, Ramadan MA, García Lebière P, Logofatu C, Martínez-Rovira I, et al. Enhancement of the supercapacitive properties of laser deposited graphene-based electrodes through carbon nanotube loading and nitrogen doping. Physical Chemistry Chemical Physics. 2019;21:25175-86.

[328] Queraltó A, del Pino AP, Logofatu C, Datcu A, Amade R, Bertran-Serra E, et al. Reduced graphene oxide/iron oxide nanohybrid flexible electrodes grown by laser-based technique for energy storage applications. Ceramics International. 2018;44:20409-16.

[329] Ivan R, Popescu C, Pérez del Pino A, Logofatu C, György E. Carbon-based nanomaterials and ZnO ternary compound layers grown by laser technique for environmental and energy storage applications. Applied Surface Science. 2020;509:145359.

[330] Ajnsztajn A, Ferguson S, Thostenson JO, Ngaboyamahina E, Parker CB, Glass JT, et al. Transparent MXene-Polymer Supercapacitive Film Deposited Using RIR-MAPLE. Crystals. 2020;10:152.

[331] Bian J, Zhou L, Wan X, Zhu C, Yang B, Huang Y. Laser Transfer, Printing, and Assembly Techniques for Flexible Electronics. Advanced Electronic Materials. 2019;5:1800900.

[332] Wang X, Zhang J, Mei X, Xu B, Miao J. Laser fabrication of fully printed graphene oxide microsensor. Optics and Lasers in Engineering. 2021;140:106520.

[333] Sopeña P, Arrese J, González-Torres S, Fernández-Pradas JM, Cirera A, Serra P. Low-Cost Fabrication of Printed Electronics Devices through Continuous Wave Laser-Induced Forward Transfer. ACS Applied Materials & Interfaces. 2017;9:29412-7.

[334] Auyeung RCY, Kim H, Mathews S, Piqué A. Spatially modulated laser pulses for printing electronics. Appl Opt. 2015;54:F70-F7.

[335] Arnold CB, Wartena RC, Swider-Lyons KE, Pique A. Direct-Write Planar Microultracapacitors by Laser Engineering. Journal of The Electrochemical Society. 2003;150:A571.

[336] Wartena R, Curtright AE, Arnold CB, Piqué A, Swider-Lyons KE. Li-ion microbatteries generated by a laser direct-write method. Journal of Power Sources. 2004;126:193-202.

[337] Kim H, Auyeung RCY, Piqué A. Laser-printed thick-film electrodes for solid-state rechargeable Li-ion microbatteries. Journal of Power Sources. 2007;165:413-9.

[338] Kim H, Proell J, Kohler R, Pfleging W, Piqué A. Laser-Printed and Processed LiCoO 2 CathodeThick Films for Li-Ion Microbatteries. Journal of Laser Micro Nanoengineering. 2012;7:320-5.

[339] Praeger M, Papazoglou S, Pesquera A, Zurutuza A, Levi A, Naveh D, et al. Laser-induced backward transfer of monolayer graphene. Applied Surface Science. 2020;533:147488.

[340] Constantinescu C, Vizireanu S, Ion V, Aldica G, Stoica SD, Lazea-Stoyanova A, et al. Laser-induced forward transfer of carbon nanowalls for soft electrodes fabrication. Applied Surface Science. 2016;374:49-55.